ANALYSIS OF NEUROPATHOGENESIS ASSOCIATED WITH SIMIAN IMMUNODEFICIENCY VIRUS INFECTION THROUGH DIFFERENTIAL GENE EXPRESSION STUDIES

by

Mimi Ghosh

BS, Salem-Teikyo University, 1995

MS, Salem-Teikyo University, 1999

Submitted to the Graduate Faculty of

Graduate School of Public Health in partial fulfillment

of the requirements for the degree of

Doctor of Philosophy

University of Pittsburgh

2005

UNIVERSITY OF PITTSBURGH

Graduate School of Public Health

This dissertation was presented

by

Mimi Ghosh

It was defended on

April 18, 2005

and approved by

Dissertation Advisor
Todd A. Reinhart, Sc.D.
Associate Professor, Department of Infectious Diseases and Microbiology
Graduate School of Public Health
University of Pittsburgh

Committee Member
Phalguni Gupta, Ph.D.
Professor, Department of Infectious Diseases and Microbiology
Graduate School of Public Health
University of Pittsburgh

Committee Member
Clayton Wiley, M.D, Ph.D
Professor, Department of Pathology
School of Medicine
University of Pittsburgh

Committee Member
David G. Peters, PhD.
Lecturer, Department of Pharmacology and Therapeutics
University of Liverpool

Todd A. Reinhart, Sc.D

ANALYSIS OF NEUROPATHOGENESIS ASSOCIATED WITH SIMIAN IMMUNODEFICIENCY VIRUS INFECTION THROUGH DIFFERENTIAL GENE EXPRESSION STUDIES

Mimi Ghosh, PhD

University of Pittsburgh, 2005

Approximately 25-30% of people infected with human immunodeficiency virus 1 (HIV-1) develop HIV-associated encephalitis and HIV-associated dementia. The underlying mechanisms leading to HIV encephalitis remain unclear. In an attempt to understand the molecular events that lead to encephalitis and subsequent dementia, I focused on identifying differentially expressed genes in the central nervous system (CNS) using SIV infected rhesus macaques as an experimental model system by using methods serial analysis of gene expression (SAGE), and microarray hybridization. I studied two different brain regions, caudate and globus pallidus, in non-infected, acutely infected, and mildly encephalitic animals. Since my analysis of macaque SAGE data utilized existing human nucleotide sequence databases, identification of the genes from which the SAGE tags were obtained proved to be challenging. I successfully identified the genes from which two of the tags were obtained. These were major histocompatibility complex class I (MHCI), differentially expressed during disease and neurogranin (Nrg), differentially expressed in caudate relative to globus pallidus. The differential expression of these two genes was confirmed by real-time RT-PCR and *in situ* hybridization techniques. I further characterized the localization of MHCI in the CNS tissue and found that whereas in non-infected tissues, endothelial cells were the major cell types expressing MHCI mRNA, during acute infection and mild encephalitis, when local virus replication was low or absent, all CNS cell types could

express this mRNA. In addition, I observed upregulation of interferon-stimulated genes (ISGs), MxA, OAS2, and G1P3, both in the CNS and in the periphery that could be potential surrogate markers for SIV infection. Since encephalitis is observed only at end-stage disease, traditional thinking has been that the CNS remains relatively unaffected until later stages of infection. Our findings indicate that immune activation within the CNS might occur early in infection and persist in a chronic manner thereby causing continuous damage, which might affect the development of end-stage encephalitis and dementia. Therefore, early, potent, suppression of systemic viral replication could potentially inhibit the development of virus-mediated neuropathology later on. Such an approach would be of important public heath significance.

TABLE OF CONTENTS

LIST OF TABLES

LIST OF FIGURES

Acknowledgements

I would like to thank Dr. Todd Reinhart for his support, encouragement, and scientific direction over the past few years. I would also like to thank my committee members Drs Phalguni Gupta, Clayton Wiley, David Peters for their time and effort towards the completion of this dissertation. In particular, I would like to thank Dr. Gupta for always having an answer and a word of advice regarding both scientific and non-scientific issues.

I would like to extend my appreciations to my co-workers and friends who provided scientific support as well as made it a pleasure to come to work everyday. These people are Dr. Todd Schaffer, Dr. Craig Fuller, Beth Fallert, Melanie Pfeifer, Amarendra Pegu, and Yu-Jen Tung. I could not have gone through the last six years without them.

I would also like to thank my friends outside the lab for their tremendous belief in me. Thank you to Dr. Anna Noller, Dr. Betsy Schauer, Urvi Parikh, and Dr. Tahir Malik for being there for me in good times and bad.

Finally I would like to thank my parents for their love and constant encouragement. All my accomplishments to date have been achieved as a result of their unconditional support.

List of Abbreviations

AcSIV	Acute infection SIV
AIDS	Acquired Immunodeficiency Syndrome
Ax LN	Axillary lymph node
B2M	B2 microglobulin
BG	Basal ganglia
BBB	Blood brain barrier
bp	base pair
CA	Caudate
CNS	Central nervous system
CSF	Cerebrospinal fluid
Cyt C	Cytochrome C
dpi	days post infection
EAA	Excitatory amino acids
FC	Frontal cortex
Fkn	Fractalkine
GLGI	Generation of longer cDNA fragments from SAGE tags for gene identification
G1P3	Interferon alpha inducible protein/ 6-16
GP	Globus pallidus
HAART	Highly active antiretroviral therapy
HAD	HIV associated dementia
HIV	Human Immunodeficiency Virus
HIVE	HIV associated encephalitis
HSP70	Heat shock protein 70
IHC	Immunohistochemistry
IFIT1	Interferon induced protein tetratricopeptide repeats 1
IFIT2	Interferon induced protein tetratricopeptide repeats 2
IFI27	Interferon alpha inducible protein 27
IFNα	Interferon alpha
IFNβ	Interferon beta
IFNγ	Interferon gamma
IL-1β	Interleukin 1 beta
IL-2	Interleukin 2
IL-6	Interleukin 6
IL-12	Interleukin 12
ISG	Interferon stimulated gene
ISH	In situ hybridization
MF	Macrophage
Mgl	Microglia
MHCI	Major histocompatibility complex I
MHCII	Major histocompatibility complex II

mSIVE	Mild SIV encephalitis
MO	Monocyte
MMP	Matrix metalloproteinase
MNGC	Multinucleated giant cell
MxA	Myxovirus influenzae resistance 1
MxB	Myxovirus influenzae resistance 2
NO	Nitric oxide
nt	Nucleotide
Nrg	Neurogranin
OAS2	Oligoadenylate synthetase 2
OASL	Oligoadenylate synthetase like
OxPhos	Oxidative phosphorylation
PAF	Platelet activating factor
PBMC	Peripheral blood mononuclear cells
PCR	Polymerase chain reaction
RACE	Rapid amplification of cDNA ends
RAST-PCR	Rapid analysis of unknown SAGE tags
RT-PCR	Reverse transcription polymerase chain reaction
SAGE	Serial analysis of gene expression
SCID	Severe combined immunodeficiency system
SIV	Simian Immunodeficiency virus
SIVE	SIV associated encephalitis
TLR	Toll-like receptor
TNFα	Tumor necrosis factor alpha
UI	Uninfected

I.   Introduction

HIV is the causative agent for acquired immunodeficiency syndrome (AIDS). Since the HIV epidemic began in the 1980s, over 60 million people worldwide have been infected and over 20 million have died. Currently, throughout the world, greater than 14,000 people are newly infected every day and greater than 8,000 people die daily of complications related to HIV infection [1]. No vaccine or fully efficacious treatment exists for HIV-infection and AIDS and many aspects of the mechanisms by which this virus causes disease are still poorly understood. Obtaining a better understanding of the pathogenesis of HIV infection will be important for the development of vaccines and treatments.

A.   HIV: Epidemiology, transmission, and disease progression

1. Epidemiology and distribution

As of December 2004, 39.4 million people were living with HIV world-wide out of which 25 million infections are localized in Sub-Saharan Africa [2]. Whereas access to treatments in North America has reduced the number of HIV infected people in that region to approximately 1 million, the number of daily infections continues to rise in the developing world particularly in South Eastern Asia (currently at 7 million) [2].

Based on its genomic sequence and pathogenic potential, the HIV virus can be divided into two distinct subtypes. HIV-1 is the predominant type found throughout the world, whereas HIV-2 is primarily found in the African continent. Of these, HIV-1 is the better-studied subtype

and has been grouped into M (for "main") and O (for "outgroup"). The M group is responsible for the majority of infections worldwide whereas the O group is relatively rare and found in Cameroon, Gabon, and France [3]. Group M can be divided into eight different clades (A-H), which are unevenly distributed world-wide [4]. For example, clade B is predominant in North America and Europe, clade C in India, and clade E in China and Thailand. The effects of these sequence differences on transmission and disease are not clear and remain an area of intense study.

2. Primate lentiviruses and the origins of HIV

Retroviruses comprise a diverse group of enveloped RNA viruses. This group of viruses is unique in their replicative strategy, which includes reverse transcription of the virion RNA into linear double-stranded DNA and the subsequent integration of this DNA into the genome of the cell[3]. All retroviruses contain three major coding domains, *gag*, coding for viral matrix, capsid and nucleoprotein; *pol*, coding for the reverse transcriptase and integrase enzymes; and *env*, coding for the viral envelope protein. An additional, smaller, coding domain present in all retroviruses is *pro*, which encodes the virion protease. Complex retroviruses encode additional proteins that might or might not be essential for viral replication. HIV is a lentivirus distinguished from other retroviruses by morphology and the presence of auxiliary genes such as *tat or rev* [3].

Primate lentiviruses can be divided into five distinct groups based on their genomic sequences. These groups are HIV-1/SIVcpz (chimpanzees), HIV-2/SIVsmm (sooty mangabey monkeys), SIVmac (macaque monkeys), SIVagm (African green monkeys), SIVmnd (mandrill monkeys), and SIVsyk (sykes monkeys) [3]. There is evidence that some monkey species have

been natural hosts for their cognate strains of SIV for long periods of time. For example, African green monkeys infected with SIVagm develop a lifelong persistent infection with no overt symptoms of disease [5]. However, in the case of rhesus macaques, SIV infection does results in an AIDS-like disease [6] making it an appropriate model to study HIV infection of humans. HIV-2 is believed to have arisen by cross species transmission from mangabey monkeys as the natural habitat of these monkeys and the region of endemic HIV-2 infection coincide well [5,6]. The origins of HIV-1 are less clear. Infection studies and phylogenetic analyses point toward a close relationship with SIVcpz [7]. It is theorized that the virus has been entering the human population from an animal reservoir for a long time, through the butchering of monkeys, for example. With the modern age of globalization, world travel, and urbanization of populations in developing countries, the virus was introduced into the developed world. Once there, it was easy for it to spread extensively through the population by drug-related needle use and unsafe sexual practices.

3. Transmission

HIV can be transmitted by direct homosexual or heterosexual contact, by blood or blood products, and from mother to child *in utero*, during birth, or via breast milk [3]. The likely targets for initial viral infection are antigen-presenting cells of the mucosa, specifically dendritic cells. Infected cells are then transported to the lymphoid tissue where the virus comes into contact with susceptible CD4 cells and establishes infection. Subsequent bursts of viremia spreads the virus to other parts of the body [8]. HIV infects CD4 T cells and macrophages (MF) utilizing CD4 as a receptor for binding and entry. In addition it requires a chemokine receptor as co-receptor and the two main coreceptors are CCR5 (for macrophage tropic virus) and CXCR4 (for T cell tropic

virus). Many viral strains are able to use both co-receptors for entry and might also utilize some additional atypical co-receptors such as CCR2, CCR3, CCR8, Ajp, and CX3CR1. [9-12].

4. Disease Progression

Primary HIV-1 infection is associated with clinical symptoms such as general malaise and lymphoadenopathy approximately 3-6 weeks following infection. The severity and persistence of these symptoms vary considerably from patient to patient. A burst of viral replication can be detected in the blood approximately 3-weeks after infection with levels reaching 10^6-10^7 copies of viral RNA per ml [13]. A decline in peripheral CD4 T cells is also noted [14]. Antiviral immune responses are detected approximately 3-6 weeks after infection followed by a decrease in plasma viral load [15,16]. Following the acute phase a phase of clinical latency begins which is mostly asymptomatic and can vary between 8-12 years in humans [17]. During this period there is continual viral replication at fairly constant levels even in the presence of the antiviral immune responses [18] likely due to the multiple immune evasion strategies adopted by the virus. Clinical disease begins when plasma CD4 T cell levels begins to drop. When CD4 cell counts drops below 200 cells/µl, the patient becomes susceptible to AIDS-defining opportunistic infections and neoplasms [3].

The most important correlate of disease progression is the viral load set point at the end of acute infection. When viral load is high at this time, progression to disease is faster [19,20]. Both viral and host genetics are thought to affect the rate of disease progression. For example, in both humans [21] and macaques [22] a deletion or mutation of the viral *nef* gene has been described to inhibit rapid disease progression. Individuals who do not progress to AIDS also show a more sustained immune response, including for example, maintenance of a vigorous CD8 response

throughout the course of infection [23]. A number of host genetic factors have also been associated with slower rates of disease progression. The most striking is a CCR5 deletion mutation. Individuals who are homozygous for a 32 base pair (bp) deletion of the CCR5 gene (co-receptor for HIV) are resistant to infection and heterozygous individuals have a slower rate of progress [24,25].

Importantly, despite 20 years of intensive research, the precise mechanisms by which HIV-1 infection causes AIDS have not been clearly identified.

B. Experimental animal models

Since analyses of HIV and its effects in humans are generally limited to autopsy specimens, an animal model is essential to study the changes at the cellular and molecular level that occur in tissues, particularly at the earlier stages of disease.

1. Nonhuman primate models

The SIV-infected macaque system is widely used to model HIV-1 infection and disease and the advantage to this system is that tissues can be examined from infected hosts throughout the course of infection including the early stages of infection. SIV and HIV-1 are related genetically, have similar genome structures and infect the same target cell types [26] [27]. SIV infection of macaques shows very similar disease progression and immunodeficiency when compared to HIV infection of individuals [26,28] [29]. The acute phase of infection is very similar to that of HIV-1 with peak plasma viremia observed at 2 weeks post infection [30]. Like HIV infection in the CNS, SIV primarily infects macrophage/microglia (MF/Mgl) cells, specifically perivascular MFs [31]. Widespread astrocytosis [32], CNS infiltration by CD8 T cells [33] and apoptosis of multiple cells

5

types [34] are associated with end stage disease. As in HIV, vacuolization of white matter is observed in areas of abundant inflammatory and SIV-expressing cells [28]. The histopathological findings are similar in HIV and SIV except that vacuolar myelopathy and peripheral neuropathy associated with HIV are not observed during SIV infection [28]. SIV also causes neurophysiologic abnormalities detectable by neurobehavioral testing [32]. As in HIV-associated dementia (HAD), the neurobehavioral dysfunction associated with SIV infection does not correlate with CNS viral burden [32]. Instead, the best correlates are the amount and the extent of MF/Mgl activation within the CNS [35-37].

One challenge in studying HIV/SIV neuropathogenesis is that, SIV-infected macaques like HIV-1 infected humans develop overt neurological symptoms in only a small percentage of infected cases [38-40]. Host genetic factors as well as the strain of the infecting virus can affect extent of CNS disease [28]. There are poor correlations between lesions, viral burden, and clinical neurological manifestations [38]. Strong correlations have been described between neurological symptoms and productive infection of MF/Mgl and higher viral RNA levels in the CNS [41]. Attempts have been made to develop models of encephalitis that provide higher rates of disease development within a reasonable period of time. These models include CD8 T cell depletion strategy [42] in rhesus macaques, coinoculation of pigtailed macaques with the neurovirulent strain SIV/17E-Fr plus the immunosuppressive strain SIV/DeltaB670 [43][44], and infection with SIV/17E-Fr plus SHIV(ku2) of rhesus macaques [45].

2. Murine models

Murine models have also provided information regarding the development of HIV associated neuropathology. A model described by Tyor *et al.* [46], involves the inoculation of severe combined immunodeficiency (SCID) mice with HIV-infected human monocyte-derived macrophages. This results in neuropathology extending beyond the region of the xenograft [46 47]. The pathology includes astrocytosis, activation of Mgl, formation of multinuclear giant cells (MNGCs), and neuronal apoptosis [48]. Behavioral abnormalities have also been described for these animals [49]. Transgenic mice over-expressing HIV/gp120 also demonstrate Mgl activation, astrocytosis, blood brain barrier (BBB) permeability, and altered neuronal morphology [50-52]. These mice also developed neurobehavioral abnormalities [50]. These studies suggest that certain viral proteins by themselves might have neurotoxic effects as described below.

C. HIV encephalitis and dementia

HIV can affect the nervous system directly by producing neurological pathologies and symptoms as well as indirectly by causing immunodeficiency, which results in increased susceptibility to opportunistic infections and neoplasms [53]. HIV-1-associated neuropathologies include HIV-1 - associated encephalopathy, cognitive-motor disorder, vacuolar myelopathy, and peripheral neuropathies. The opportunistic infections associated with HIV-1 neuropathology are toxoplasmosis, tuberculosis, cryptococcal meningitis, and cytomegalovirus-associated retinitis and encephalitis. Neoplasms include primary CNS lymphomas as well as metastatic Kaposi sarcoma [53]. HAD has been described as a subcortical dementia that affects approximately 25% of

infected individuals. The early symptoms of HAD includes psychomotor slowing and behavioral changes such as apathy and irritability. At a later stage, almost all aspects of cognition, motor functions and behavior are affected resulting in dementia and paraplegia [54] [53]. HIV encephalitis is assumed to precede dementia and consists of pathological changes such as perivascular infiltrates, MNGCs, microglial nodules, astrocytosis, loss of white matter, and loss of neurons. There does not appear to be a strong correlation between plasma viral load and encephalitis [55], although correlations have been noted between HAD and CNS viral load [56], neuronal dendritic pathology [57] and neuronal loss [58-61]. The best correlates of HIV-associated encephalitis (HIVE) described so far are the number of MFs present in the CNS. Levels of local viral RNA and antigens can also be correlated to encephalitis [55,62,63]. With the advent of highly active antiretroviral therapy (HAART), the incidence of HAD has decreased, however, the cumulative prevalence of HAD has increased possibly because of the increased lengths of survival in AIDS patients [53,64]. Several host genetic factors have been implicated as having an increased or decreased risk toward development of HAD. MHC Class I haplotypes B51 and A24 have been described as neuroprotective whereas MHC class II alleles DQA1-03000, DQB1-05000 and DRB1-09199 were associated with a higher risk for developing HAD [53]. An Apolipoprotein E4 allele and specific polymorphisms in the MCP-1 gene were also found to increase the risks for developing HAD [65,66].

1. Early stages of CNS infection by HIV/SIV

Studies examining the early stages of CNS infection have mostly been performed in the SIV-infected macaque model. SIV can be detected in the CNS as early as 7-day post infection (dpi). The primary infected cell population in the CNS is considered to be cells of the myeloid lineage,

monocytes (MO), MF, Mgl. These cell types have been shown to express the necessary receptor (CD4) and co-receptor (CCR5) required for viral entry [67,68]. At the early stage viral replication is mostly observed in perivascular macrophages suggesting that these cells are infected in the periphery and might traffic through the BBB and seed the brain parenchyma with virus [30,31]. Intracerebral inoculations studies [69] showing lack of infected cells around site of inoculation suggest that parenchymal Mgl are poorly infected by SIV. In a study by Williams *et al.*, the authors used cell surface markers to distinguish between perivascular MF (CD11b+, CD68+, CD14+, CD45+) and parenchymal Mgl (CD11b+, CD68+) and showed that perivascular MF are primarily infected by SIV [31]. However, this observation was not replicated in HIVE tissues where parenchymal Mgl accounted for the majority of HIV p24 antigen positive cells and were found to express both CD14 and CD45 [70]. It is possible that this reflects a difference between humans and primates and this issue currently remains unresolved. Early SIV infection of the CNS is accompanied by mild gliosis and the presence of perivascular infiltrates [30]. Early infection is also associated with an upregulation of cytokines IL-1β, TNFα, and IL-6 [35,71]. No clear correlations have been found between neuropathology, SIV replicating cells, and T-cell infiltration [71]. There is evidence of early neuronal injury in the absence of high CNS viral load. Gonzalez *et al*, have found decreases in the levels of n-acetylasparate, calbindin, and synaptophysin, (indicating neuronal damage), along with increases in the levels of GFAP (indicating gliosis) during early infection [72]. Increased expression of vascular cell adhesion endothelial molecule 1 (VCAM-1), and the tryptophan metabolite quinolinic acid [73,74] have also been noted. The clinical manifestations of the acute symptoms in macaques are similar to humans, noted by an increase in body temperature, lymphadenopathy, and a decrease in gross motor activities [75]. A decrease in the activity of choline acetyltransferase (chAT), a biochemical

marker of cognitive function, was noted during early infection [76]. This decrease in activity was restored by treatment with a dopaminergic drug selegiline [77], suggesting that dopaminergic regions of the CNS, such as the basal ganglia (BG), are affected early during SIV infection causing cognitive impairments [78].

2.   Late stages of CNS infection by HIV/SIV

After the resolution of acute infection viral mRNA is no longer readily detectable in the CNS [31,43,79]. Microglial activation and MF infiltration are inapparent [73]. However, body temperatures can remain elevated [75] and behavioral changes have been noted [80] suggesting that the early CNS invasion does cause some damage even though the viral levels are undetectable.

During late infection, the extent of gliosis and MF/Mgl activation increases within the CNS [72]. In fact, Mgl activation is believed to play a central role in the development of the pathology associated with HIV/SIV CNS infection. Mgl can be activated by systemic viral infection as well as by the presence of infected cells within the CNS. Infected and/or activated MF/Mgls secrete a number of neurotoxins that could be involved in the development of CNS pathology. These include proinflammatory cytokines (IL-1β, IL-6, TNFα), nitric oxide (NO), neopterin, eicosanoids (arachidonic acid), Ntox, β2-microglobulin (B2M), platelet activating factor (PAF), quinolinic acid, prostaglandins and excitatory amino acids (EAAs) (glutamate, aspartate, L-cystein), all of which have been found to be upregulated in CNS tissues of patients with end stage AIDS [81-86]. Astrocytes function in maintaining the homeostasis of EAAs by regulating their uptake. Mgl activation can alter astrocyte physiology resulting in glutamate release, impaired glutamate uptake, NO production, and further cytokine/chemokine secretion [85]. Impaired glutamate uptake by astrocytes can result in neuronal death due to glutamate

excitotoxicity [87]. Soluble factors released from activated Mgl can directly damage neurons by releasing substances that produce excessive activation of the NMDA subtype of glutamate receptors [88]. Furthermore the presence of high levels of EAAs due to damage of astrocytes and neurons can promote neuronal calcium influx [89], which, in addition to the over-stimulation of the glutamate receptors can activate apoptotic pathways. The presence of HIV or SIV in the CNS can also activate the resident Mgl directly. HIV gene products Tat and gp120 can stimulate Mgl to produce a host of toxic products (PAF, arachidonic acid, glutamate, NO), which can cause damage to both neurons and astrocytes leading to apoptosis [90-92]. In addition, Tat has been shown to upregulate expression of adhesion molecules, increase permeability of BBB and thus influence MO trafficking [93,94]. Activation of MF/Mgl can also lead to increased production of reactive oxygen and nitrogen species that could be responsible for oxidative stress. Evidence for increased oxidative stress has been found in the CNS of patients with HAD [95,96].

3.   Neurovirulent strains of HIV/SIV

The issue of whether specific neurovirulent strains of HIV and SIV exist is not resolved. Previous reports of viral genome sequence analysis support the idea that neurotropic forms of the virus exist [97,98]. Gene sequences in the V3 loop of HIV-1 *env* as well as sequences within the *nef* gene may be responsible for conferring neurotropism [99-101]. However, other studies have demonstrated that viral sequences within the CNS phylogenetically match those of the bone marrow [63,102]. This argues for a hematogenous route of viral entry into the CNS.

4.   CNS Cells involved in HIVE/SIVE

MO/MF/Mgl

Infection of MO/MF/Mgl by HIV/SIV is of paramount importance to the development of encephalitis and dementia and has also been described in other sections of this dissertation. Briefly, there is clear evidence that MO/MF/Mgl constitute the primary population of CNS cells infected by HIV/SIV. These cells express CD4 and CCR5 [67] and also an atypical co-receptor CCR3 [67]. The principal strains associated with neuropathological disease are macrophage-tropic with MF/Mgl cells being productively infected during disease [103]. Whereas the controversy of perivascular MF versus parenchymal Mgl as the major population of virus infected cells have not been resolved [31,70], the "Trojan horse" hypothesis (described below) of MO trafficking playing a major role in the development of encephalitis is generally accepted [54,85].

T Cells

T-cells, both CD4 and CD8, express the required receptors for HIV/SIV entry and although CD4 T cells are infrequently detected [104] in the brain, HIV/SIV antigen-specific CD8 T cells have been detected in the CSF and CNS parenchyma during HIVE/SIVE [33,39,105-109]. HIV-1-specific cytotoxic T lymphocyte (CTL) responses have been detected in the cerebrospinal fluid (CSF) of patients with HAD and suppression of viral replication has been observed [108,110]. CD8 T cells isolated from the CNS of infected macaques are functional and express granzymes A and B, perforin, and IFNγ [33] suggesting that even though T cells constitute a minor population within the CNS, they might still play an active functional role. In the CD8 depletion model for SIVE [42],

a high percentage of the CD8 depleted animals develop severe encephalitis, thereby demonstrating the importance of these cells in the development of HIVE/SIVE. This could be a consequence of systemic immunosupression, which might allow an increased number of infected MOs to traffic to the CNS.

Oligodendrocytes

Few studies [111,112] have reported *in vitro* or *in vivo* infection of oligodendrocytes by HIV. It is generally accepted that these cell populations are not productively infectable by HIV or SIV. Human and simian oligodendrocytes do not express CD4 or the chemokine co-receptors utilized by HIV/SIV for entry [113], so even if rare infections would occur *in vivo* it is unlikely that would contribute significantly toward disease. Nevertheless abortive infection of these cells could still have effects on the alteration of the immune environment of the CNS leading to encephalitis.

Endothelial cells

 Whether HIV/SIV can productively infect endothelial cells *in vivo* and contribute to the disease process is not clear. The current consensus is that these cells comprise a potential avenue for the virus to enter the CNS. Endothelial cells express the chemokine co-receptors CCR5 and CXCR4 that are utilized by HIV/SIV for entry [114,115]. In addition they express other chemokine receptors such as CCR1, AJP, CCR3 and DC-Sign [115-117] that can potentially be utilized by HIV/SIV for entry into CNS cells. Even if not used for productive infection these virus binding cell surface proteins could hold virus present in the plasma in a form that could subsequently infect other cells that pass through the BBB and enter the CNS. Whereas some studies report the presence of CD4 receptors on endothelial cells [118], others find no evidence of it [117,119]. It seems that infection

of endothelial cells *in vivo* might occur but viral replication is minimal [119]. In another study, endothelial cells were found to not support HIV-1 replication by themselves, but direct cell to cell contact between MF and endothelial cells in co-cultures increased HIV-1 replication considerably [120]. This kind of interaction might occur at the BBB during HIV infection. Therefore, it is possible that HIV/SIV uses endothelial cells as an entry point into the CNS through the BBB rather than as a cell population to be productively infected.

Neurons

Neurons in the human and macaque brain have been shown to express CXCR4, CCR5, and CCR3, CX3CR1 chemokine receptors [12,115,121] but only certain subtypes of neurons have been shown to express CD4 [122]. A CCR3-mediated, CD4-independent mechanism of infection has been suggested for neurons [123]. It has also been proposed that the virus can enter neurons by a trans-receptor mechanism where cell-to-cell contact between neurons and MO/MF or T cells allows the virus to first bind to the gp120 of the MO/MF/T cell and then to the co-receptors present on the neurons, thereby entering the neuronal cell [124,125]. Whether this actually happens in an *in vivo* situation is unclear. In summary, although *in vitro* infection of neuronal cell lines by HIV has been observed [126], there is little evidence that productive infection of these cells occurs *in vivo*.

Astrocytes

Astrocytes do not express CD4 but do express CCR5 and CXCR4 on their cell surfaces. Therefore it is possible that they can be infected by HIV/SIV via a CD4-independent mechanism [115,121]. There is a lack of convincing evidence that astrocytes can be productively infected by

HIV/SIV *in vivo*. Infection of astrocytes leads to an abortive replication where early viral proteins (Tat, Nef, Rev) are expressed but late structural proteins (Gag) are not [127,128]. Evidence for *in vitro* infection has been conflicting. There are studies that suggest such an infection is possible and other studies that suggest that is not the case. There is also a lack of consensus regarding the mechanism and the extent of such an infection [127,129-131].

D. Mechanisms involved in the development of encephalitis and dementia

The underlying mechanisms by which encephalitis and dementia develop are incompletely understood. Studies using the macaque model have shown that the virus enters the CNS as early as 7 dpi when low levels of productive infection are found [30,31,43]. However, after resolution of acute infection, productive viral replication is not seen in the brain until end stage AIDS [43,132]. The currently accepted "Trojan horse hypothesis" [54,85,86] suggests that during early infection, infected MO enter the CNS through the BBB where they might differentiate into perivascular MFs or infect the already existing perivascular MFs. This occurs during peak systemic viremia when viral DNA, RNA, and protein are detected in the CNS [30,31]. During the clinical latency period MO still continue to traffic to the CNS, but due to systemic immune responses the numbers of infected MO entering the CNS might be greatly reduced. Later in disease when the individual progresses to AIDS, immune control of virus becomes greatly reduced and the number of infected MO that can carry the virus to the brain increases again. This allows further spread of virus in the brain and also reactivates the latent virus population that entered the CNS during early infection [54]. Figure 1 shows a schematic describing this process.

EARLY INFECTION

VIRUS → Monocyte / MØ → CNS

VIRUS → Marrow - MØ Precursors → CNS

ASYMPTOMATIC PHASE

CD4$^+$ T Cells
CD8$^+$ T Cells
B Cells

Are jointly effective in keeping retrovirus in check while immune system function is adequate

AIDS EMERGENCE
PROGRESSIVE NERVOUS SYSTEM DAMAGE

IMMUNE FAILURE
- Loss of CD4$^+$ T lymphocytes
- Failure of CD8$^+$ T lymphocytes to control virus
- Increase numbers of viral$^+$ MØ in CNS

MACROPHAGE DYSREGULATION
- Productive MØ infection
- MØ activated via multiple mechanisms in the CNS
- Macrophage production of high levels of cytokines, etc.
- Enhanced production of viral$^+$ cells from the marrow
- Increased dependence on "innate" immune mechanisms to deal with environmental flora and pathogens

Figure 1   Schematic of early, asymptomatic, and AIDS stages of HIV/SIV CNS infection

Figure taken from Williams *et al*., Annual Review of Neurology, Vol. 25, 537-562, March 2002. Reprinted with permission from the Annual Review of Neuroscience, volume 25 ©, 2002 by Annual Reviews www.annualreviews.org

Mgl activation is thought to play a major role in the pathology observed in HIVE/SIVE. Mgl activation can occur as a result of systemic infection as well as due to direct viral infection of the CNS. MO in blood activated in response to systemic infection produce inflammatory factors such as TNFα, IL-1β, and IL-6. This results in an increase in MO migration into the CNS compromising the integrity the BBB. Evidence of serum proteins in the CNS [133,134] and disruption of tight junctions of endothelial cells [135] in HIVE points to increased permeability of the BBB as a factor in the disease process. In response to the presence of proinflammatory

cytokines, endothelial cells of the BBB over-express adhesion molecules such as E-selectin, ICAM-1 and VCAM-1 [136,137] that bind the approaching MO and further expedite their migration into the CNS. An over-expression of specific matrix metalloproteinases (MMPs) has also been observed in HIV infected MF/Mgl and HIVE tissue [138]. The MMPs are proteolytic enzymes responsible for the maintenance of the extracellular matrix and aberrant expression of these products can further compromise the BBB and influence MO trafficking. As MO migration increases, further production of proinflammatory cytokines and release of viral products prompt the endothelial cells to maintain high expressions of adhesion molecules and allow a continuous flow of MO infiltration. HIV proteins can also stimulate gelatinase B (MMP 9) to compromise the integrity of the BBB [139]. The proinflammatory cytokines produced as a result of the interaction between infected MO and the BBB can also induce the expression of CC chemokines MCP-1, MIP1α, MIP1β, and RANTES which then increases migration of more infected and/or activated MO into the CNS [140]. Therefore, once initiated, chronic activation associated with inflammation may be self-perpetuating, maintained in an autocrine and paracrine fashion. Although, the motor and cognitive impairments associated with HIVE are presumed to be linked to neuronal injury and damage [141,142], the virus does not infect neurons productively [143-145]. Neuronal damage is thought to occur indirectly through networks of dysregulated cytokines and chemokines along with the production of viral or cellular neurotoxins [85,115,146]. Specifically, neurons are damaged by toxins released by activated Mgl, particularly the EAAs, via over-stimulation of glutamate receptors [85,147]. Immunomodulatory factors such as SDF1 or PAF may promote further calcium influx or like TNFα, may directly initiate caspase-dependent apoptotic pathways [147]. A currently accepted model showing mechanisms of neuronal damage in HIVE/SIVE is shown in Figure 2.
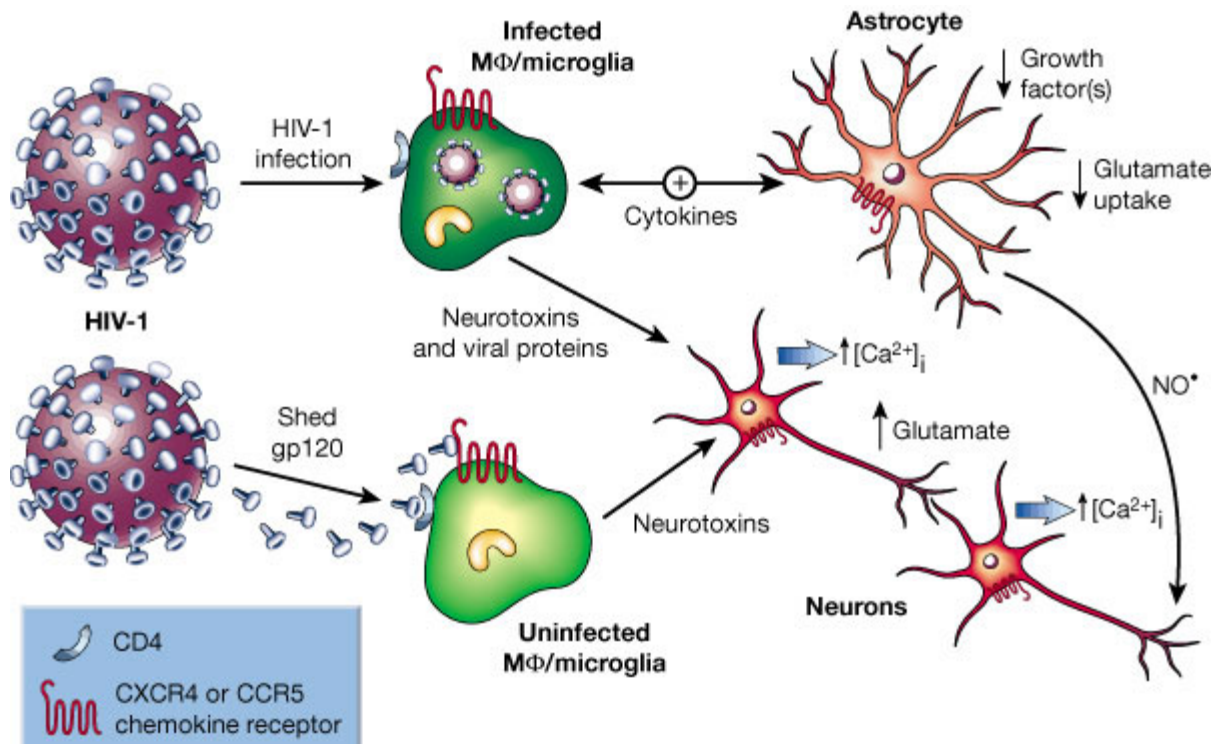
Figure 2   Mechanisms of neuronal damage in HIVE/SIVE.

Figure from Kaul *et al.*, Nature, Vol. 410, 988-994, April 2001. Reprinted with permission from Nature (www.nature.com).

Evidence for MO/MF trafficking playing a major role in the development of HIVE, comes from patients on HAART. Since the introduction of HAART, the incidence of HAD has decreased [53] in spite of the poor penetrance of protease inhibitors [148]. A reason for this observation might be that as HAART treatment reduces the number of infected MO in the periphery, fewer infected cells traffic to the CNS thereby causing a reduction in the incidence of

HAD [148]. Furthermore, CD14+ CD16+ and CD14+ CD69+ subsets of MO in the blood increases during HIV/SIV infection and the increased percentages have been found to correlate with HAD [149]. In the CD8 depletion model of SIVE, $CD14^{lo}$ $CD16^{hi}$ blood MO levels peak at 7 dpi, drop, and rise again with the development of AIDS and SIVE following the pattern of virus infection of the CNS [149].

The scenario described above is called the "indirect mechanism model" hypothesis because injured neurons that contribute toward the development of HAD, are damaged mostly by indirect mechanisms involving activation of Mgl, a wide-spread dysregulation of cytokines, chemokines, immunomodulatory factors, and production of neurotoxins.

## E.	Differential Gene Expression: Overview

Traditionally gene expression studies have been approached at the single gene level using classical techniques such as northern blot analysis and *in situ* hybridization (ISH). Such techniques allow the analysis of a limited number of genes in a single study. Other techniques such as subtractive hybridization and differential display do not allow global quantitative analysis of transcript levels. During the last decade a number of new methods have been developed that can assess and quantify the expression levels of up to thousands of genes simultaneously. Two such high-throughput gene expression techniques, SAGE and microarray analysis have revolutionized the field by permitting the generation of large-scale gene expression profiles.

1.   SAGE

SAGE is a comprehensive approach to analyze global gene expression patterns where prior knowledge of the genes and their sequences is not a requirement. SAGE relies upon the generation of unique 10 bp sequence tags from a defined position within the transcript near the 3' end. Multiple transcript tags are concatenated and sequenced thus allowing simultaneous analysis of thousands of genes. An evaluation of the gene expression profile is made by determining the relative abundance of individual tags as well as identifying the gene corresponding to each tag [150,151].

In order to generate SAGE libraries, double stranded cDNA is synthesized from total RNA or mRNA using a biotinylated oligo (dT) primer. The cDNA is then digested with the restriction enzyme *Nla*III, which recognizes the sequence CATG and therefore is expected to cut the cDNA once every 256 nucleotides (4^4). Using streptavidin-coated magnetic beads the 3' end of each cDNA closest to the last CATG sequence is isolated. A linker containing a restriction enzyme site for *Bsm*F1 is then ligated to the cDNA. This enzyme cleaves the cDNA in a sequence independent manner at a distance of 10 nucleotides (nt) 3' from its recognition site thereby releasing short cDNA fragments that are known as the SAGE tags. The ends of the tags are blunted, combined and ligated as ditags, the linkers are released by *Nla*III digestion, and the ditags are concatenated, cloned, and sequenced. By computer analysis tags from each library are counted and matched against Genbank or Unigene databases (www.ncbi.nlm.nih.gov/SAGE) [150-152]. A schematic of the SAGE procedure is shown in Figure 3.

The strength of this approach is that simultaneous, quantitative analysis of tens to hundreds of thousands of transcripts is possible. Prior information about the genes is not required for this
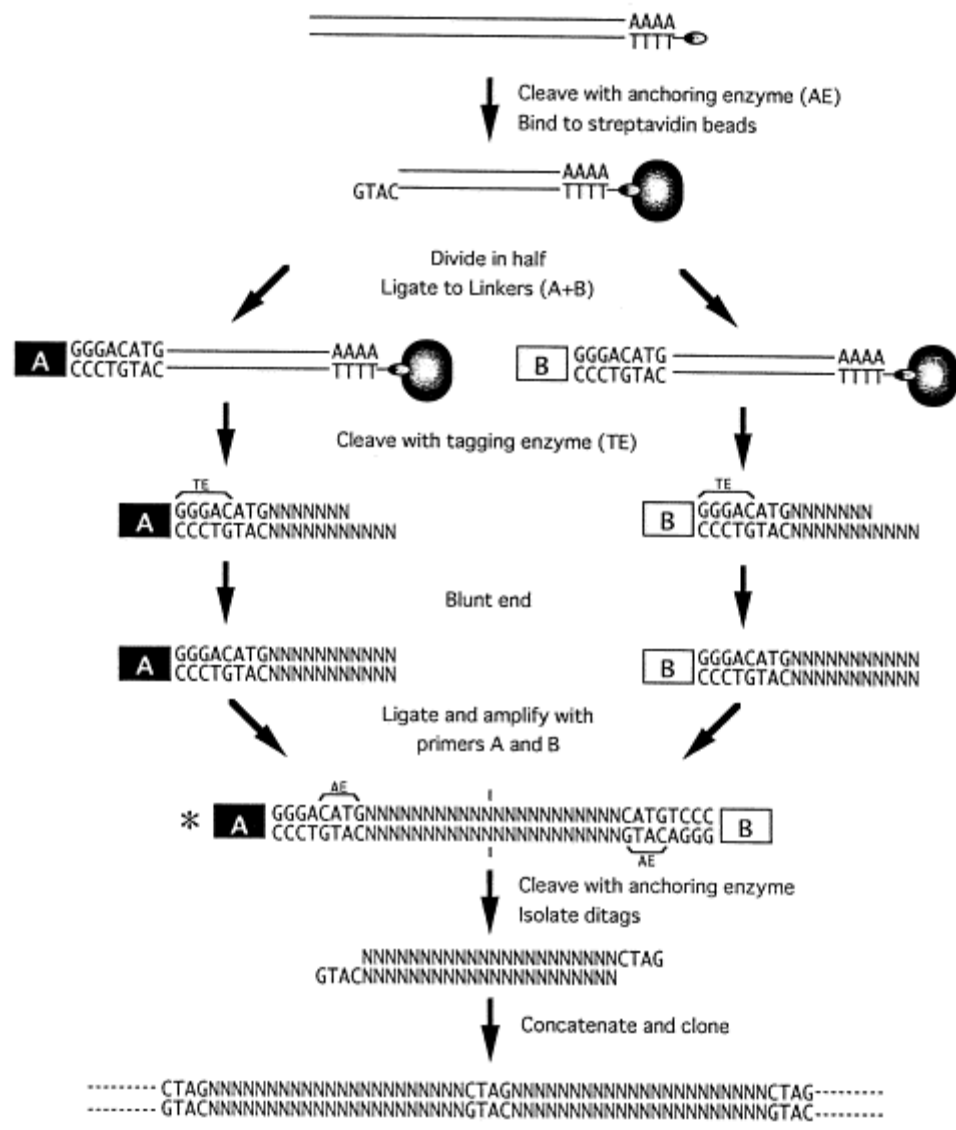
Figure 3 Schematic of SAGE procedure

The anchoring enzyme (AE) is *NlaIII* and tagging enzyme (TE) is *Bsm*FI. Boxed A and B are independent linkers, whose 3′ portions are designed to contain TE sequence. Transcript-derived tag sequences are denoted by Ns.

Figure from Yamamoto *et al*., Journal of Immunological Methods, Vol 50, Pages 45-66, April, 2001. Reprinted with permission from Elsevier.

method. As such, this approach should allow the discovery of novel genes. Results obtained by

SAGE have been validated by other methods including parallel analysis of clone frequencies in

cDNA libraries, northern blot, RT-PCR, ISH, and microarray analyses [153-156]. In addition, since expression levels of transcripts are represented by absolute numbers of SAGE tag counts, data sharing and comparison between different experiments and different research groups is facilitated.

Although SAGE is a powerful technique it does have several limitations. The process of constructing the SAGE libraries, sequencing and analyzing the tags is time consuming, labor-intensive and expensive [151]. It has been shown that detection of low abundance transcripts can be challenging particularly in complex heterogeneous tissues [152]. Also a large amount of input RNA is required for SAGE, which might not always be feasible.

Recently modifications of the SAGE technique have been developed allowing smaller amounts of input RNA [157], microSAGE [158], SAGE-Lite [159], PCR-SAGE [160] and MiniSAGE [161]. Often, computer analyses of SAGE tags result in tags that do not match to any known gene in the databases, perhaps corresponding to novel transcripts. Additionally, a SAGE tag might match to more than one gene in the database making unigene identification difficult. In order to identify these tags more accurately, several PCR-based strategies have been developed. These include the techniques rapid analysis of unknown SAGE tags (RAST)-PCR [162], and generation of longer cDNA fragments from SAGE tags for gene identification (GLGI) [163]. The GLGI approach is designed to isolate a population of cDNAs representing only the 3' ends of the mRNAs, thus creating a smaller, more specific pool for the amplification of a gene sequence associated with a particular 14 nt SAGE tag. Methods such as LongSAGE utilize a different type IIS restriction enzyme, *Mme*I to generate 21 bp tags. This method has been shown to better facilitate gene identification over the standard SAGE [164]. Another approach has found that using the restriction

enzyme *Sau*3A instead of *Nla*III as the anchoring enzyme increases the tag length by 2-3 bp and improves the potential for transcript detection and identification [165].

The SAGE technique was originally developed by Velculescu *et al*. to study the patterns of gene expression in the adult pancreas [150]. Since its inception, SAGE has been successfully applied to studies of gene expression in multiple types of cancer [166,167], cell typing studies such as comparison of mature versus immature dendritic cells [168], as well as gene expression studies of CNS abnormalities[155] [169]. In HIV-1 infected T cell lines, SAGE has identified upregulation of genes associated with transcription and T-cell activation and downregulation of genes involved in defenses against oxidative stress [170]. Notably, all of these studies involved analysis of human genes in human cells or tissues. SAGE analysis of gene expression profiles in other species might be limited by the ability to identify the genes from which the SAGE tags were derived.

2.   **Microarrays**

DNA microarray technology permits the analysis of the expression levels of thousands of genes simultaneously [171,172]. The array consists of a highly ordered matrix of hundreds to thousands of different DNA sequences immobilized on a solid surface such as a nylon membrane, glass, or silicon chip. Arrays can be spotted with presynthesized cDNA fragments or oligonucleotides varying in length from 40-70-nt. In this method, a labeled cDNA target is hybridized to a DNA microarray and the gene expression levels assed by quantifying hybridization intensities. Specifically, two samples are labeled with different fluorescent nucleotides (Cy3 and Cy5) and are subsequently co-hybridized to the same array. Genes that are expressed at equal levels in both samples will have a mixture of both fluorescent nucleotides hybridized whereas genes
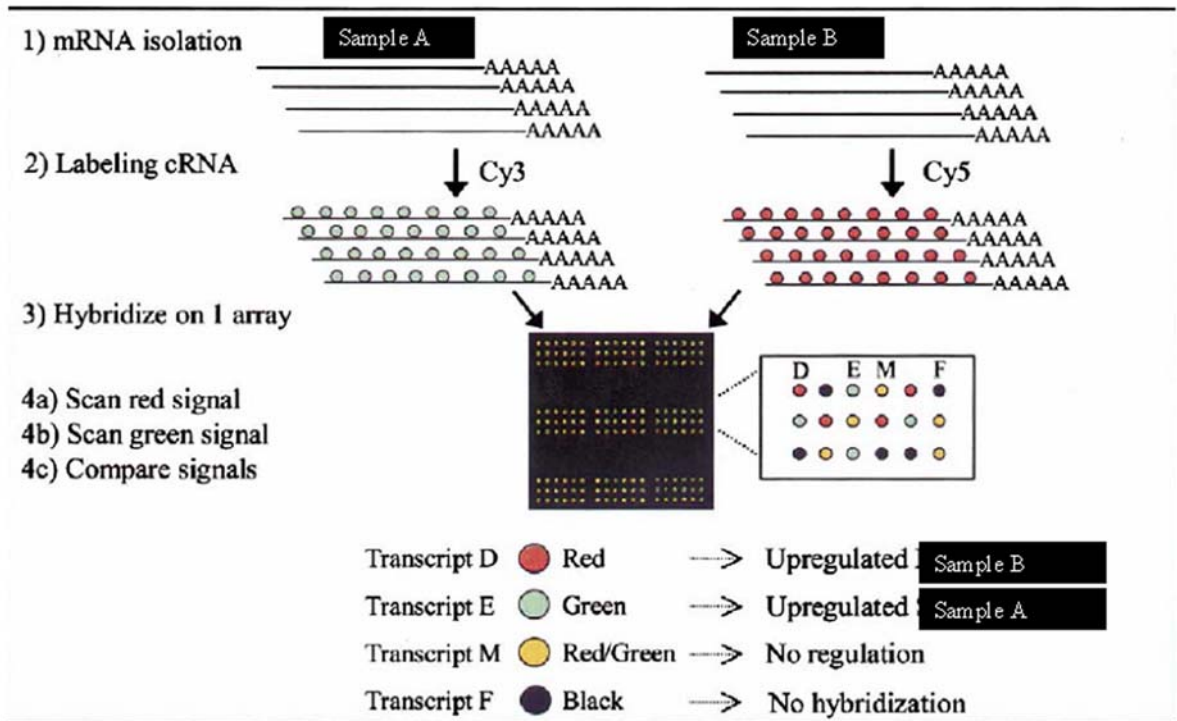
Figure 4 Schematic of Microarray technique

Figure modified from Feldker *et al.*, Behavior Genetics, 33 (5): 537-548, Sept 2003. Reprinted with permission from Springer Science and Business Media.

expressed at different levels between both samples will display predominant hybridization of one of the fluorescent nucleotides over the other [152]. A schematic of the procedure described above is shown in Figure 4.

Results from microarray experiments have been confirmed by ISH and real-time RT-PCR [173] indicating the reliability of the procedure. Although the experiments are fast and efficient, commercially available arrays can be expensive and the bioinformatical analysis can be time

consuming and complicated. A major limitation is that gene expression levels can be assessed only for the genes that are spotted on the array. That is, discovery of novel genes is not possible by this method. Also DNA arrays have been shown to lack the sensitivity to detect low abundance mRNAs particularly in complex tissues [174]. Furthermore, different protocols, reagents, and analyses used in different studies make it difficult to compare microarray data between laboratories.

3.   Comparison of SAGE and microarray approaches

Although large-scale gene expression profiling by SAGE and microarray hybridization are being used extensively by researchers, both methods have their limitations. The biggest advantage of SAGE over microarray is the fact that it does not require prior knowledge of the transcriptosome and thus is not limited to known genes spotted on a chip. On the other hand, the microarray technique is faster and less challenging than SAGE. Since both SAGE and microarray are popular techniques for studies attempting large-scale gene expression profiling, some researchers have compared the two methods to observe if the same genes are found to be up- or down-regulated when these different methods are utilized. A study by Feldker *et al.,* attempting to detect CNS genes responsible for certain behavioral abnormalities in different strains of mice, found that for medium to high abundance genes, the two techniques are fairly comparable. However, results were undependable by either method when looking at low abundance genes, including genes that are known to play a role in these behavioral problems [152]. Another study by Ishii *et al.* [156] compared the top 20 genes upregulated in MO/MF expression profiles and compared microarray chip intensity to SAGE tag frequencies. They found that whereas both techniques identified similar subset of genes, each also identified genes that the other did not and

the rankings did not always match. They did note, however, that whereas the two techniques did not always identify the same gene, often genes that belonged to the same pathway were identified [156]. Therefore, ideally, SAGE can be used to generate an initial picture of the trascriptosome and then microarray technology can be used to expand the study further. In fact, a study by Sawiris *et al.*, [175] identified 516 SAGE tags that were upregulated in ovarian cancer and used these tag sequences to build a diagnostic microarray chip known as Ovachip.

F.   Summary

One of the biggest challenges with SAGE is that the databases used for tag-to-gene mapping, or identification of the genes encoding the tags, are crucial for all downstream applications and understanding. Currently comprehensive sequence databases exist for only certain species. In the study described in this dissertation, we performed SAGE on macaque RNA and since macaque sequence specific databases for analyzing SAGE tags are currently not available, we had to perform all analyses against existing human sequence databases. This attempt at cross-species analysis of SAGE tags was novel. This problem in the field has been recognized by others [176] as a recent paper describes development of a bioinformatics tool that facilitates cross-species tag to gene mapping. How well this tool functions remains to be seen.

Although HIVE/SIVE has been studied for many years, until recently, the focus has not been on large-scale differential gene expression profiling to globally identify genes that are up- or down-regulated. This approach is useful for identifying pathways that might be involved in the disease process. Also, early studies of HIV/SIV infection of the CNS showed no local viral replication at the early stages of infection. Therefore, what happens in the CNS during acute systemic infection has not been well addressed. Only recently studies are finding evidence of

early damage and immune activation to the CNS during HIV/SIV infection [74]. In this dissertation, I focused on utilizing differential gene expression techniques to identify genes that might be involved during early CNS infection by SIV and therefore contribute to early previously unrecognized changes in the CNS, or to the later development of encephalitis and dementia.

II.   Specific Aims

HAD is a severely debilitating neurological disorder that affects approximately 25% of infected individuals in terminal stages of AIDS [54]. The overall aim of this dissertation was to investigate potential changes in the CNS that might elucidate the mechanisms underlying the development of HAD, using SIV-infected rhesus macaques as a model system. The mechanisms underlying the early viral entry in the brain, the changes during the acute phase of infection and the events preceding encephalitis have not been fully elucidated. The current consensus is that an "indirect mechanism" of neuronal damage occurs where multiple cellular factors may play an important role. It is generally believed that systemic viral infection causes infected MO to traffic to the CNS and enter through the BBB. This results in an activation of tissue MF and Mgl, which then produce a host of toxic factors and release chemokines to attract more peripheral MO into the CNS. A vicious cycle ensues which might be self-perpetuating, maintaining itself in an autocrine and paracrine manner. The toxins produced by the activated MF/Mgl act directly on astrocytes and neurons causing their death [54] [85,86]. The details of this model are however poorly understood. **My hypothesis was that during disease progression after infection with SIV, subsets of cellular genes would be differentially expressed in the brain. These genes will be expressed by specific cell types within specific micro-anatomic compartments within the CNS, and might have a role in the development of encephalitis and potentially in downstream neurologic dysfunction.** I have approached this hypothesis by studying differential gene expression profiles using an unbiased method, SAGE and a biased method, microarray hybridization.

The specific aims that were used to address the central hypothesis are described below.

28

Specific Aim 1: To identify differentially expressed CNS genes during different disease states in SIV-infected rhesus macaques by using an unbiased approach, SAGE and a biased approach, microarray technology. The subcortical regions of the CNS are major anatomic targets for HIV/SIV infection and the BG, thalamus and hippocampus regions are areas of high viral load and virus-mediated damage [56,177]. Multiple studies have previously addressed the condition of the CNS during severe encephalitis. Since the virus has been described to enter the CNS very early during infection, I hypothesized that there might be changes at the molecular level in the CNS long before severe encephalitis sets in and that these changes might explain some of the mechanisms that are involved in development of encephalitis and dementia. Therefore I focused on defining the immune environment of the CNS during acute infection (AcSIV) (2 weeks post infection) and during mild encephalitis (mSIVE). The expectation was that at least a proportion of the SIV-infected rhesus macaques that developed AIDS would also develop fulminant SIVE so that these could be compared with the AcSIV and mSIVE animals. However, in our cohorts none of the animals developed fulminant encephalitis. The mSIVE status of the animals was defined by the number of viral RNA positive cells and CD68 positive macrophages. SAGE was performed on RNA samples obtained from the caudate (CA) and the globus pallidus (GP) regions of uninfected, AcSIV and mSIVE rhesus macaques through collaborative efforts with Dr. David Peters (Currently at the Department of Pharmacology and Therapeutics, University of Liverpool).

The SAGE data generated were in the form of lists of tag frequencies. Each tag is a 10 bp sequence that is generated from a unique mRNA within the population. To identify the genes represented by the tags, I attempted to obtain more complete sequence information for the gene from which a particular tag was generated by using a PCR-based technique known as rapid

amplification of cDNA ends (RACE). The products that were successfully identified by RACE were then analyzed further by multiple methods.

Microarrays have been used extensively for studying differential gene expression. Our laboratory has developed an immunologically focused custom microarray that contains 256 macaque cDNAs. These genes included cytokines, chemokines and chemokine receptors, all of which might have a role in the SIV-associated disease process. The array also includes a large number of macrophage, dendritic cell, and lymphocyte related genes as well as genes involved in innate immunity and adhesion. This custom-built array was used as a second approach to identify differentially expressed genes using RNA from uninfected, AcSIV, and mSIVE tissues.

Specific Aim 2: To perform additional analyses of the genes identified in Specific Aim 1 in order to confirm and quantify their differential expression. Techniques for global differential gene expression studies such as SAGE or microarray hybridizations are designed for large scale screening experiments that are semi-quantitative. Therefore any gene are identified as differentially expressed by those techniques must be confirmed using other techniques that are more quantitative in nature. I focused on two tags that were predicted by SAGE to be differentially expressed and successfully identified by RACE. These genes were MHCI and Nrg. MHCI was found to be differentially expressed in between of disease states whereas Nrg was found to be differentially expressed in the CA relative to the GP of the CNS. I developed real-time RT-PCR assays specific for MHCI and Nrg to accurately quantify their levels of expression. I also generated riboprobes from these genes by *in vitro* transcription of cDNA template and used those to probe CNS tissues by ISH in order to determine patterns of expression within the complex tissues from which the original RNAs were obtained.

Specific Aim 3: To elucidate the roles of differentially expressed genes identified in Specific Aim 1 in the disease process. Since I found MHCI to be upregulated in the CNS, I next focused on characterizing immune-associated genes that might act as upstream activators of MHCI. Using a combination of molecular and tissue based techniques I investigated selected molecules that might be responsible for MHCI upregulation. The molecules I investigated included cytokines, ISGs, and toll-like receptors (TLRs). I also investigated what the types of cells express MHCI mRNA in the CNS and whether this population changes during the different disease states. To address this I used simultaneous ISH and IHC to label for MHCI mRNA and cellular markers specific for macrophages (CD68), T-cells (CD3), neurons (NeuN), astrocytes (GFAP), and oligodendrocytes (MBP). I also characterized these cells on the basis of their states of activation (HLA-DR) and proliferation (Ki67). Finally, as potential downstream effects of MHCI upregulation, I investigated whether there was evidence of mitochondrial damage and oxidative stress in the diseased tissues, by IHC staining for Cyt C and Hsp70.

Collectively the studies described in this dissertation were designed to define the state of immune activation of the CNS during SIV infection. Whereas the immune state of the CNS during HIVE or SIVE has been well studied previously, here I have focused on the immune environment of the CNS during early acute infection and mild encephalitis when local viral replication is absent or at very low levels.

Chapter III consists of data from Specific Aims 1, 2, and 3, focused mainly on the SAGE studies, its confirmation and the potential functions of differentially expressed genes identified by SAGE. Chapter IV contains the microarray analyses from Specific Aim 1 and follow-up

studies with stress related genes as described in Specific Aim 3. A schematic describing the samples and methods used in this dissertation is presented as a flowchart in Figure 5.
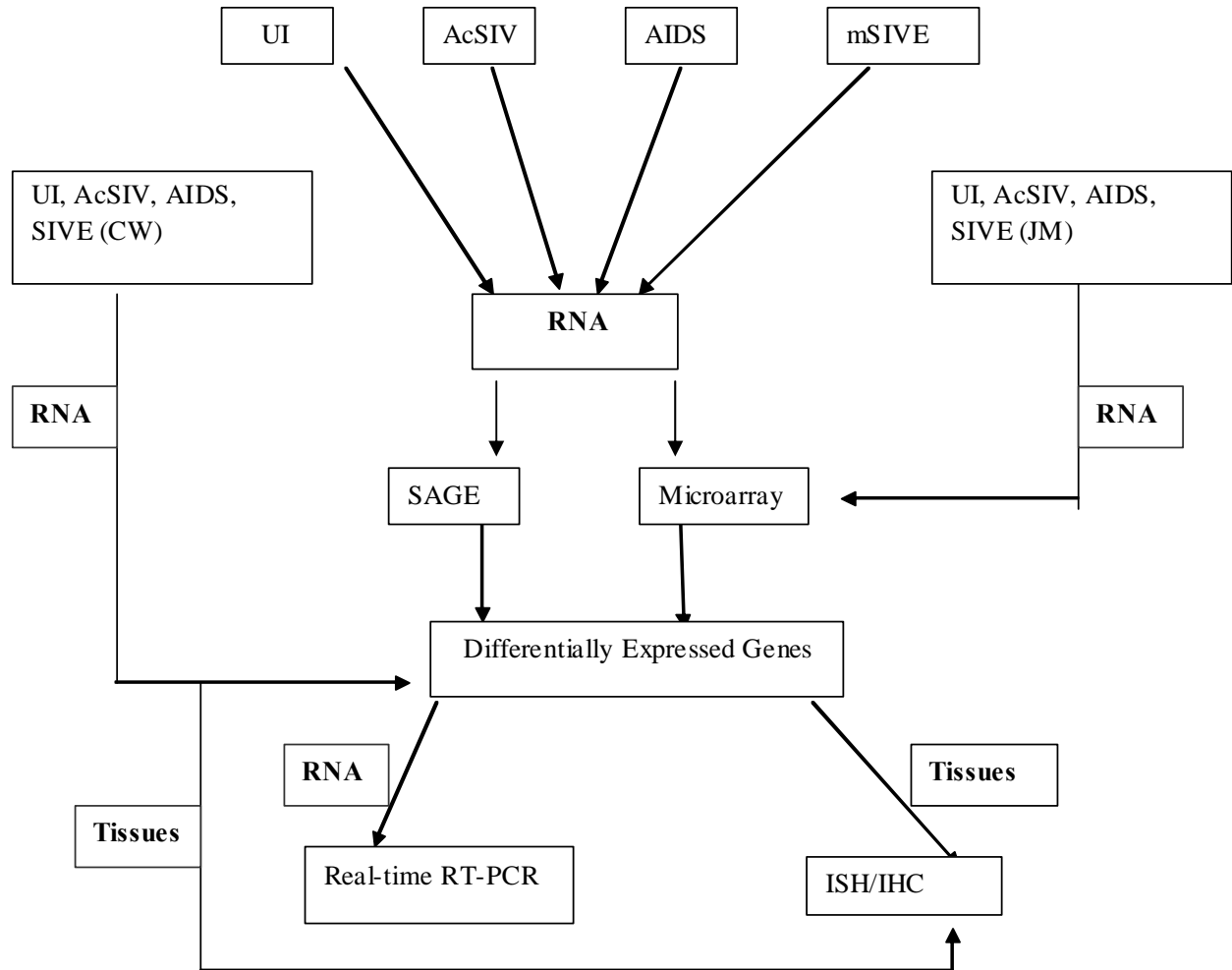
Figure 5   Flowchart of samples and methods.

RNA and/or tissues from UI, AcSIV, AIDS and mSIVE macaques were used to identify differentially expressed genes by SAGE and microarray hybridizations. In depth analyses for differentially expressed genes were performed by real-time RT-PCR and ISH/IHC. RNA/tissue samples obtained from collaborators Dr. Clayton Wiley and Dr. Joseph Mankowski are denoted by CW and JM, respectively.

III. Upregulation of MHCI in the central nervous system of Simian immunodeficiency virus-infected Rhesus macaques in the absence of encephalitis

(Manuscript in preparation)

This chapter consists of data that are currently being prepared as a manuscript for submission in a peer-reviewed journal.

The data described here consisted in part of collaborative efforts within Dr. Reinhart's laboratory and between Dr. Peter's and Dr. Reinhart's laboratories. To ensure appropriate credit is given for such collaborations, I note here those individuals who contributed to these studies. The SAGE data were generated by Elisa O'Hare in Dr. David Peters' laboratory. Macaque-specific ISGs were cloned by Dr. D.H. Kim (at the time at Dr. Reinhart's laboratory). Primers for Sybrgreen Real-time RT-PCR assays were developed by Dr. D.H. Kim (all ISG assays) and Dr. Sonali Sanghavi (cytokine and TLR assays) (Reinhart Laboratory). Data for IFNα mRNA levels in axillary lymph nodes (Ax LN) were obtained from Dr. Sonali Sanghavi. Viral load data (SIV ISH) for Ax LN was obtained from Beth Fallert (Reinhart Laboratory). Taqman Realtime RT-PCR assays were purchased directly from Applied Biosystems.

A.   Preface

The following section contains data that are part of a manuscript in preparation. Here I have described the SAGE data and analyses, the RACE procedure attempted to accurately identify the SAGE tags, and how the RACE procedure was found to be inefficient for identifying macaque SAGE tags using human nucleotide sequence databases. I have also described follow up studies on the tags MHCI and Nrg. The differential expression of these two tags was confirmed by ISH as well as real-time RT-PCR. I further investigated the cell types expressing MHCI in the CNS during the different disease states and whether these cells were activated, and/or proliferating. In addition, I also investigated the differential expression of other immune markers in the CNS, such as the ISGs that might be related to the MHCI upregulation.

Upregulation of MHCI in the central nervous system of Simian immunodeficiency virus-infected Rhesus macaques in the absence of encephalitis

Mimi Ghosh[1], Elisa O'Hare[2], Craig Fuller[1], Joseph Mankowski[3], Clayton Wiley[4], David Peters[2] and Todd A. Reinhart[1]

Running title: *Differential gene expression/SIV/CNS/MHCI*

[1]Department of Infectious Diseases and Microbiology, Graduate School of Public Health, University of Pittsburgh, Pittsburgh, PA; [2]Department of Human Genetics University of Pittsburgh, Pittsburgh, PA; Department of Neuropathology, [4]University of Pittsburgh, Pittsburgh, PA; [3]Department of Comparative Medicine, Johns Hopkins University, Baltimore, MD

[‡]Corresponding author and reprint requests: Mailing address: Department of Infectious Diseases and Microbiology, Graduate School of Public Health, University of Pittsburgh, 130 DeSoto St., Pittsburgh, PA 15261. Phone: (412) 648-2341. Fax: (412) 624-4873. (reinhar@pitt.edu)

B.   Abstract

Although a majority of HIV infected individuals show evidence of some neurological symptoms, only about 25% develop HIV-associated dementia. The underlying mechanisms responsible for the development of encephalitis and dementia are poorly understood. To gain insights into the events that take place at the molecular level following viral infection, we attempted to study global differential gene expression using SAGE in a SIV-infected rhesus macaque model. We studied two different brain compartments, CA and GP in uninfected, AcSIV, and mSIVE animals. The putative genes from which the differentially expressed SAGE tags were derived could be broadly categorized into genes associated with immune function, signal transduction, metabolism/stress, cytoskeleton, replication/transcription/RNA processing, and protein synthesis/trafficking/degradation. The SAGE tags were identified by using an online tool that matches them to existing nucleotide sequence databases. Since our SAGE data were generated from macaque RNA, and currently no comprehensive macaque sequence database exists, we matched our tags against current human sequence databases. Since such a cross-species match might not be fully accurate, we performed the RACE technique in an attempt to accurately identify the SAGE tags. Using strict criteria, we successfully RACE-amplified two cDNAs, MHCI and Nrg. The MHCI tag was upregulated during disease whereas the Nrg tag was more highly expressed in CA relative to GP. We were able to confirm the differential expression of these two genes using real-time RT-PCR and ISH techniques. We further characterized the expression of MHCI in the CNS and found that in the absence of disease MHCI RNA was expressed at low levels by endothelial cells. During AcSIV and mSIVE, other cell types of the CNS including MF/Mgl, neurons, astrocytes, and oligodendrocytes were found to express MHCI. We also observed an upregulation of interferon-stimulated genes (ISGs) early in

infection (MxA, OAS2 and G1P3), both locally and systematically, that remained elevated in AIDS and mSIVE. Our data indicate that cross-species analyses of SAGE tags are challenging and must be rigorously confirmed by other experimental strategies. The data also indicate that MHCI is upregulated in the CNS of SIV-infected rhesus macaques in the absence of local virus replication and encephalitis. This suggests that during SIV infection of the CNS, immune activation might occur early and even when local viral replication is absent or at low levels and persist in a chronic manner until end stage disease when encephalitis develops. The upregulation of ISGs also points toward a general state of immune activation that is persistent in nature. The development of encephalitis might therefore depend on the extent of early CNS immune activation.

C.   Introduction

HIV-1 neuropathogenesis is defined by encephalitis and dementia, the latter characterized by progressive cognitive, motor, and behavioral impairments [54]. Approximately 60% of HIV-1-infected individuals ultimately demonstrate some type of neurological abnormalities throughout the course of infection and approximately 90% of autopsy cases show signs of neuropathology. However, only 25-30% of infected individuals develop HAD [86]. In HIV-1 infected individuals as well as in SIV-infected nonhuman primates, CNS dysfunction has not been shown to correlate well with viral load in the CNS or at the periphery, or with the route of infection. The best correlates of dysfunction seem to be the levels of activated MF/Mgl in the brain [55]. The pathological hallmarks of HIVE consists of perivascular infiltrates, microglial nodules, presence of MNGCs, astrocytosis, and later in disease, vacuolization of white matter, myelin pallor and neuronal loss [28,178]. The virus enters the CNS as early as 7 dpi when only low levels of productive infection are found [30,31,43]. However, after resolution of acute infection, productive viral replication is not seen in the brain until end stage AIDS [43,132]. The changes in cellular gene expression that occur due to the early viral assault are not clearly understood and might explain some of the mechanisms of development of encephalitis and/or neurologic dysfunction. The motor and cognitive impairments associated with HIVE can be linked to neuronal injury and damage [141,142]. Since the virus does not infect neurons efficiently [85], neuronal damage is thought to occur through networks of dysregulated cytokines and chemokines along with the production of viral or cellular neurotoxins [115,146,179].

The SIV-infected macaque system is widely used to model HIV-1 infection and disease and one advantage of this system is that tissues can be examined from infected hosts throughout the course of infection including the early stages of infection. SIV infection of macaques show

very similar disease outcomes, including immunodeficiency, as compared to HIV-infected individuals [26,28] [29], albeit within a shorter period of time. One challenge in studying HIV/SIV neuropathogenesis is that SIV-infected macaques, like HIV-1 infected humans, develop overt disease in a small percentage of infected cases [38]. Attempts have been made to develop models of encephalitis that provide higher rates of disease development within a reasonable period of time. These models include CD8 T cell depletion strategy [42] in rhesus macaques, coinoculation of pigtailed macaques with the neurovirulent strain SIV/17E-Fr plus the immunosuppressive strain SIV/DeltaB670 [43] [44], and infection with SIV/17E-Fr plus SHIV(ku2) of rhesus macaques [45].

Multiple studies have previously addressed the condition of the CNS during severe encephalitis. Since the virus has been described to enter the CNS very early during infection, we hypothesized that there might be changes at the molecular level in the CNS long before severe encephalitis sets in and that these changes might contribute to the mechanisms that are involved in development of encephalitis and/or neurologic dysfunction. Our cohort of 12 rhesus macaques was infected with the immunosuppressive SIV/DeltaB670 strain, and none developed severe encephalitis. In this study we focused on defining changes to the CNS gene expression profile during AcSIV (2 week post infection) and during mSIVE. The mSIVE status of the animals was determined by measuring the numbers of viral RNA positive cells and CD68 positive macrophages in the CNS tissue [180]. All animals described in this paper were SIV/DeltaB670 inoculated except one mSIVE animal, which was from a different cohort that was inoculated with a macrophage-tropic genetically homogenous isolate referred to as SIV/DeltaB670 Clone 12.

To understand the changes that occur at the molecular level in the CNS during SIV infection, we used SAGE. SAGE is a powerful technique used to study differential gene

expression in a global manner, where prior knowledge of the genes is not a requirement. This technique was originally developed by Velculescu *et al*. to study the pattern of gene expression in the adult pancreas [150]. Since it's inception, SAGE has been successfully applied to studies of gene expression in multiple types of cancer [166,167], cell typing studies such as the comparison of mature versus immature dendritic cells, [168], and gene expression studies of CNS abnormalities [152,169]. The subcortical regions of the CNS are major anatomic targets for HIV/SIV infection and the BG, thalamus and hippocampus regions are areas of high viral load and virus-mediated damage [56,177 181]. We therefore used RNA samples obtained from the CA and the GP regions of the BG from uninfected, AcSIV and mSIVE rhesus macaques to construct the SAGE libraries.

Putatively identified genes associated with differentially expressed tags during AcSIV and mSIVE could be broadly categorized into genes involved in functions associated with the immune system, signal transduction, metabolism/stress responses, cytoskeleton, replication/transcription/RNA processing and protein synthesis/trafficking/degradation. Some of the tags identified by SAGE were further analyzed by RACE in attempts to confirm their identities. Once the genes associated with the tags were identified, they were analyzed by ISH, IHC and real-time RT-PCR techniques to further characterize their expression levels and patterns.

Since we encountered difficulties with the analysis of macaque SAGE tags using human databases our experiences suggest that cross-species analyses of SAGE tags must be confirmed rigorously by other experimental strategies and might require modifications that provide greater than 14-nt of gene-specific sequence information.

From the SAGE analysis, we found MHCI to be differentially expressed in the CNS of AcSIV and mSIVE rhesus macaques. We found MHCI to be expressed by endothelial cells in

uninfected as well as infected macaque CNS. However, during infection MHCI was found to be expressed by other cell populations of the CNS including MF/Mgl, neurons, astrocytes, and oligodendrocytes. We observed this MHCI upregulation during AcSIV and mSIVE when local viral replication was absent or low, as well as during SIVE when productively infected cells were present in the brain. In addition to the MHCI upregulation, we also observed an upregulation of ISGs interferon-α inducible gene (G1P3), myxovirus influenzae resistance 1 (MxA), and oligoadenylate synthetase 2 (OAS2), both locally and systematically. These molecules were expressed at elevated levels during AcSIV and the levels remained high in AIDS non-SIVE, mSIVE, and SIVE animals.

The data described here indicate that MHCI is upregulated in the CNS of SIV-infected rhesus macaques during both the acute phase and mild encephalitis, possibly as an indicator of local CNS immune activation. In addition, the observed upregulation of ISGs MxA, G1P3, and OAS2 might be potential surrogate markers for SIV infection and immune activation. Therefore immune activation of the CNS might occur early in infection and persist in a chronic manner thereby causing continuous damage, which might affect the development of end stage encephalitis and dementia.

D. Materials and methods

Animals and Tissue Processing

All animal studies were performed under the approval and guidance of the University of Pittsburgh Institutional Animal Care and Use Committee. The 12 adult rhesus macaques (*Macaca mulatta*) used in this study tested negative for SIV, simian retrovirus (type D), and simian T-lymphotropic viruses -1, -2, and -3 and have been described previously [182-184]. Briefly, all animals were inoculated intravenously and sacrificed either at 2 weeks post-infection during the acute phase of infection or upon progression to AIDS. At necropsy, transcardial perfusion was performed with 0.9% saline to remove contaminating blood cells from tissues. Dissection of brains was performed within 1 hour of death using a protocol developed in consultation with Dr. Ronald Hamilton (University of Pittsburgh). Tissue specimens were fixed in 4% paraformaldehyde (Sigma Co., St. Louis, MO)/phosphate-buffered saline (Biowhittaker, Walkersville, MD) (PF/PBS) and processed as described previously [185], or snap frozen in liquid nitrogen and stored at -140^0C. Details of the animals used in this study are tabulated in Table 1.

SAGE

Snap-frozen tissues from specific CNS regions were homogenized and total RNA was extracted by using the Trizol reagent (Life Technologies, Rockville, MD). For generation of the SAGE tags, we generated pools of total RNA from the CA and/or GP of 2 uninfected animals and 3 AcSIV animals. SAGE was performed essentially as described [159].

Table 1 Infection status and clinicopathological findings of animals used in this study

Animals	Infection duration (wk)[a]	Infection stage	Plasma viral copies/mL	Virus in Brain[d]	Clinicopathological findings
M5299	2	Acute	10 000 000	+/-	Mild hypercellularity in LN, gastritis
M5499	2	Acute	6 500 000[b]	-	Reduced % CD4$^+$ T lymphocytes
M5699	2	Acute	63 000 000	-	None
M0999	2	Acute	29 000 000	+/-	None
M5899	2	Acute	14 000 000[b]	+/-	Reduced % CD4$^+$ T lymphocytes, mild LH, gastritis
M5999	2	Acute	7 000 000	-	Reduced % CD4$^+$ T lymphocytes
M6299	2	Acute	34 000 000	-	Reduced % CD4$^+$ T lymphocytes
M1799	21	AIDS	780 000	+/-	Weight loss, CD4$^+$ T-lymphocyte loss, Pc, LH
M5199	24	AIDS	540 000	+/-	Weight loss, CD4$^+$ T-lymphocyte loss, Pc, LH
M6199	32	AIDS	940 000	+ (++++)	Weight loss, CD4$^+$ T-lymphocyte loss, mild encephalitis, LH
M6200	8 [c]	Clinical latency	41 600 000	+(+++)	Mild encephalitis
M5600	NA	Uninfected	ND	-	None
M6600	NA	Uninfected	ND	-	None

LH indicates lymphoid hyperplasia; Pc, *Pneumocystis carinii* infection; NA, not applicable; and ND, not done.

[a] **All macaques were inoculated intravenously with a characterized stock of the pathogenic isolate SIV/DeltaB670.**

[b] **Values for samples obtained 2 weeks after infection were not available; values are for the week 1 time point.**

[c] **M6200 was inoculated intravenously with a characterized stock of pathogenic isolate SIV/DeltaB670 Clone 12.**

[d] **SIV RNA positive cells detected by ISH were graded on a +/- scale where +/- indicates 1-2 viral RNA positive cells, + indicates 5-10, ++ indicates 10-20, +++ indicates >20 viral RNA positive cells per tissue section. + signs within parentheses indicate a cluster of positive cells within a tissue where overall number of positive cells could be lower.**

RACE

3' RACE was performed using the RLM-RACE kit that included 3'RACE specific primers (Ambion, Austin, TX). The 14 bp SAGE tags were used as gene-specific primers. Briefly, first strand cDNA was synthesized from total RNA samples that were originally used for SAGE, using a 3' RACE adapter primer (5'-GCGAGCACAGAATTAATACGACTCACTATAGGT$_{12}$VN-3'). The cDNA was then PCR amplified using 3' RACE outer primer complimentary to the anchored adaptor primer (5'-GCGAGCACAGAATTAATACGACT-3') and a primer based on the SAGE tag sequence. The

resultant PCR products were purified on a 2% agarose gel, excised, and cloned into the pGEMT

vector (Promega, Madison, WI). The cloned products were sequenced and analyzed by basic

local alignment search tool (BLAST) sequence homology analysis. For some RACE products, a

second round of amplification was performed by hemi-nested PCR using the same 14 bp SAGE

tag sequence as the sense primer and a nested 3' RACE inner primer (5'-

CGCGGATCCGAATTAATACGACTCACTATAGG-3') prior to gel purification, cloning and

sequencing analyses.

Cloning of macaque-specific MHCI and Nrg partial cDNAs

Rhesus macaque specific MHCI and Nrg cDNAs were generated from total RNA extracted from

snap-frozen brain tissue using RT-PCR (Access RT-PCR System Promega Corporation,

Madison, WI). The following cycling parameters were used, 48°C for 45 min; 94°C for 2 min;

30 cycles of 94°C for 30 sec, 54°C for 30 sec, and 68°C for 2 min; and 68°C for 3 min. The

primer sequences used were MG.MHCIA.F1 (5'-ATGGCGATCATGGCGCCCCG-3'),

MG.MHCIA.R1 (5'-TCACACTTTACAAGCCGTGAGAG-3'), MG.Nrg.F2 (5'-

CTTTTGCTTCTCGCCCACCTCT-3') and MG.Nrg.R2 (5'-

AACACTTGGACATTCCTCTTTATTATTG-3'). These primer sequences were based on a

macaque MHCIA sequence (GenBank accession number NM_002116) and a human Nrg

sequence (GenBank accession number AJ317956). A 1097 bp fragment that encompassed the

MHCI open reading frame and a 554 bp fragment of Nrg were amplified by RT-PCR. The

amplified products were ligated to the pGEM-T vector (Promega, Madison, WI) and sequenced.

Riboprobe synthesis and ISH

ISHs were performed as described [185]. The macaque MHCI and Nrg cDNAs cloned as described above were used to generate riboprobes. [^{35}S-UTP]-labeled riboprobes were synthesized by *in vitro* transcription using the Maxiscript SP6/T7 kit (Ambion, Austin, TX) and the amount of incorporated radioactivity was determined by liquid scintillation. Optimized exposure times were determined to be 3 days for both MHCI and Nrg ISHs.

Simultaneous ISH and IHC

Simultaneous ISH and IHCs were performed as described [184]. ISH was performed using the MHCI riboprobe. Following stringent washing, tissue sections were equilibrated in 1X PBS for 5 min, and incubated in primary antibody for 1 hr. The primary antibodies that were used are as follows: anti-CD68 mAb, 1:25 dilution (clone KP1, Dako Corp., Carpinteria, CA); anti- MHC class II antibody, 1:50 dilution (HLA-DR; TAL.1B5, Dako); anti-NeuN, 1:100 dilution (clone A60, Chemicon, Temecula, CA); anti-GFAP, 1:500, (rabbit Ig, Dako Corp., Carpinteria, CA), anti-MBP, undiluted, (clone MBP88, Biogenex, San Ramon, CA); Antigen-positive cells were detected using the Super PicTure kit (Zymed, Valencia, CA) using 3,3'-diaminobenzidine (DAB) as the substrate. MHCI and Nrg RNA+ cells were then detected by emulsion autoradiography with exposure times of 2 days.

For some antigens ISH caused a reduction or abrogation of the subsequent IHC signals. For the localization of these antigens, ISH and IHC were performed separately on immediately subjacent sections. The antibodies used for these experiments were anti-CD34, 1:50 dilution (clone BI-3C5, Zymed, San Francisco, CA); anti-CD3, 1:100 dilution (NCL-CD3-12, Novocastra, Newcastle, UK); and anti-Ki67, 1:100 dilution (NCL-Ki67-MM1, Novocastra, Newcastle, UK). For anti-CD3, anti-CD34, and anti-Ki67 antibodies, Retrievogen B (BD

Pharmingen, San Jose, CA) was used for microwave antigen retrieval and tissues were blocked for 1 hr at room temperature in 1X PBS supplemented with 1.6% normal horse serum (Dako Corps, Carpinteria, CA).

Image Capture and Quantitative Image Analysis (QIA)

To quantify the levels of ISH signal as well as the numbers of antigen and RNA positive cells in tissue sections, 10 random microscopic fields from brain tissue sections were captured through a 40X or 60X Plan apochromat objective on a Nikon E600 microscope using the Metaview software package (Universal Imaging Corp., West Chester, PA) and a RT Slider Spot camera (Diagnostic Instruments, Inc., Sterling Heights, MI). For combined ISH/IHC experiments, the manual counting feature of Metaview was used to count total cells, and cells that were mRNA+, antigen+ and mRNA+/antigen+ from each captured image and the percentages of mRNA+/antigen+ (double positive) cells were calculated. For quantifying ISH signals, silver grains were differentiated from other structures using the color separation feature of Metaview software, and surface areas (pixels) were measured with the threshold and measure tools of Metaview. ISH signals were calculated for each of the microscopic fields and presented as the percentage of total image surface area covered by silver grains.

Real-time RT-PCR

Real-time RT-PCR was performed using a 2-step protocol as described [186,187]. For each specimen, 200 ng of total RNA was reverse transcribed using random hexamers and Superscript II RT (Life Technologies, Rockville, MD) in a 100-µL reaction. RT-negative controls were also performed in parallel for each RNA sample. Five (5) µl of each cDNA was amplified using

MHCI and Nrg specific, commercially available Taqman Assays (PE Applied Biosystems, Foster City, CA) and a Taqman assay for 18S rRNA (PE Applied Biosystems, Foster City, CA) was used as the endogenous control. PCR reactions were cycled at 95°C for 10 min followed by 40 cycles at 95°C for 15 sec and at 60°C for 1 min on an ABI Prism 7700 Sequence Detection System (PE Applied Biosystems, Foster City, CA). Relative quantification of MHCI and Nrg mRNA expression levels was calculated using the comparative C_T method [187], with the ΔCT value from an uninfected macaque (M5600) serving as the calibrator.

Statistical analyses

All statistical analyses were done with Minitab software (State College, PA). Data from ISH QIA and real-time RT-PCR experiments were analyzed by pair-wise T-Test comparisons, repeated measures analysis of variance (ANOVA) and Kruskal-Wallis tests. A *p*-value of <0.05 was considered to be significant.

SAGE analysis of mRNA expression profiles in uninfected, AcSIV and mSIVE rhesus macaque CA and GP.

To identify CNS genes that were differentially expressed during different SIV infection states, we created six different SAGE libraries using RNA extracted from uninfected, AcSIV and mSIVE CA and GP. The mSIVE status of these tissues was determined in a semi-quantitative manner by the presence of viral mRNA+ cells (ISH) and the extent of MF/Mgl immunoreactivity (CD68 IHC) (Figure 6). This approach has been used previously by others [180]. The CA and GP regions were chosen as they have been shown to be important targets of viral replication and subsequent development of pathology [56,177]. The numbers of tags in the SAGE libraries were 28,164 and 26,728 in uninfected CA and AcSIV CA, respectively and 35,361, and 31,283 in uninfected GP and AcSIV GP, respectively. The mSIVE CA and GP libraries contained 35,215 and 32,756 tags, respectively. The frequencies for each of these tags were calculated, normalized per 10^6, and the normalized expression levels of the tags between all SAGE libraries were compared.

Abundantly expressed SAGE tags.

The 20 most abundantly expressed SAGE tags in the CNS of uninfected, AcSIV and mSIVE animals are shown in Table 2. The tag sequences were queried using the NCBI SAGE tag-to-gene mapping tool (www.ncbi.nlm.nih.gov/SAGE) against a comprehensive database of human sequences. Eleven out of the top twenty most abundant tags were identical in both CA and GP. One of the exceptions was Nrg, which was highly expressed in CA but not in GP. Nrg is a

postsynaptic protein kinase substrate that binds to calmodulin and is thought to play an important role in learning, memory, and neuroplasticity [188]. CNS microanatomic specific differential expression of this gene has been previously described in other studies [189,190]. In addition, several tags did not match with any known human genes. They were unidentifiable using the tag-to-gene mapping technique. This could mean these genes are novel and not yet identified or characterized or that the analysis of macaque tags using a human database might not be optimal.

Differentially expressed SAGE tags in AcSIV and mSIVE CA and GP.

Differentially expressed SAGE tags were identified by calculating the ratio between the normalized frequency of a given tag from uninfected, AcSIV and mSIVE SAGE libraries. The top 20 differentially expressed tags from the CA and GP libraries are shown in Tables 3 and 4, respectively. Comparing AcSIV with uninfected CA libraries, 65 unique tags with 10-fold or greater increased expression and 23 unique tags with 10-fold or greater decreased expression were identified (Table 3). In the GP libraries 26 unique tags with 10-fold or greater increased expression and 21 unique tags with 10-fold or greater decreased expression were identified (Table 4). Comparing the mSIVE with the uninfected SAGE libraries, 59 tags with 10-fold or higher upregulation and 41 tags with 10-fold or higher downregulation in CA and 142 similarly upregulated tags and 92 similarly downregulated tags in GP were identified (Tables 3 and 4). Some of the tags that were upregulated in the AcSIV were also upregulated in mSIVE whereas other tags were specifically upregulated in AcSIV and/or mSIVE. In CA the tag representing MHCI (AGAGGTTGAT) was upregulated 27.4-fold in AcSIV and 5.7-fold in mSIVE. In GP this same tag was upregulated by 11.9-fold in AcSIV and 8.1-fold in mSIVE. Other than the tag representing MHCI, only one more unidentifiable tag was present amongst the top 20 most

upregulated tags in both CA and GP (Tables 3 and 4). The most significantly downregulated tag putatively identified as PITPNM family member 3 (CTGCTAACAG) was downregulated by 80.5-fold in AcSIV CA and by 66-fold in AcSIV GP, but was not differentially expressed in either mSIVE SAGE libraries. This was the only tag that was present among the top 20 downregulated tags in both CA and GP (Tables 3 and 4). Therefore, the tags most up or down regulated in CA and GP were mostly mutually exclusive. Twelve out of the top twenty upregulated tags in AcSIV CA were also 5-fold upregulated in mSIVE CA. In GP, 3 out of the top 20 upregulated tags in AcSIV were also found to be >5-fold upregulated in mSIVE. Out of the 20 most downregulated tags in AcSIV CA, 5 were also downregulated by >5-fold in mSIVE CA whereas in the GP, 7 out of the 20 most downregulated tags were found to be downregulated by >5-fold in mSIVE.

Based on the putative gene identification, the SAGE tags from our libraries could be grouped into genes associated with the immune system, signal transduction, metabolism/stress, cytoskeleton, replication/transcription/RNA processing, and protein synthesis/trafficking/degradation.
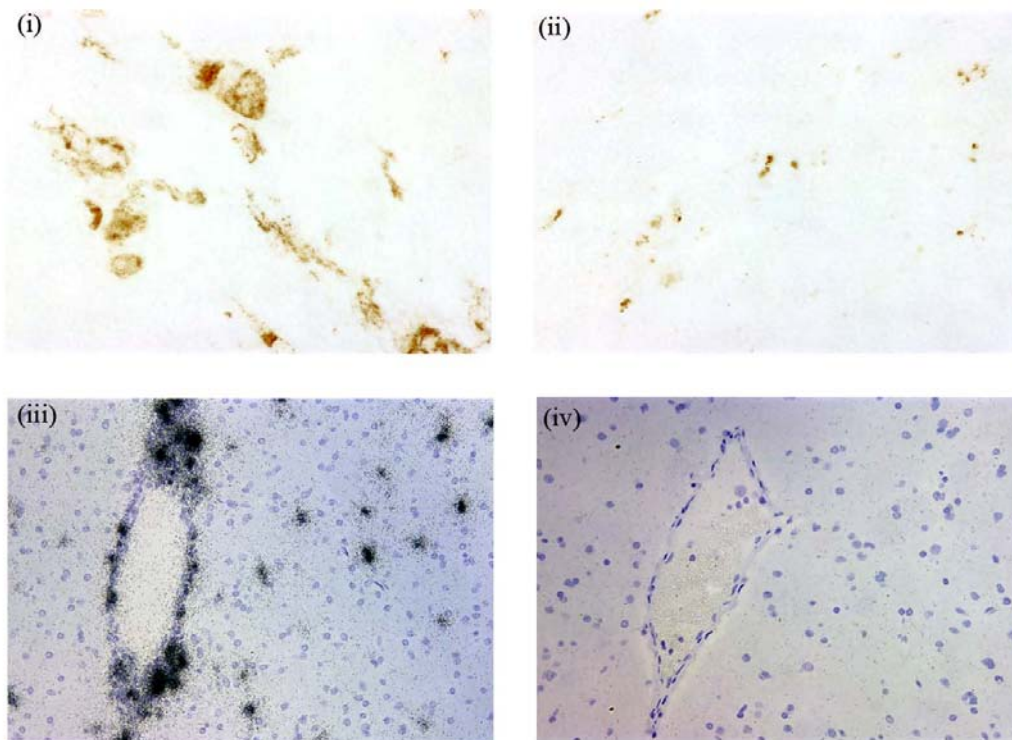
Figure 6   Comparison of SIVE and non-SIVE tissues

MFs were detected by CD68 immunostaining in BG tissues from macaques with SIVE (i) and non-SIVE (ii). SIV viral RNA positive cells detected in SIVE (iii) and non-SIVE (iv) tissues by ISH. Isotype controls for IHC and sense controls for ISH (not shown) showed little background. Size bar 50 μm. Original magnification 400x.

Use of RACE to identify genes containing SAGE tags.

Although the human and macaque genomes are highly homologous, it is conceivable that any given 14-nt SAGE tag sequence (*NlaIII* site, CATG plus 10 nt unique sequence) might not be exactly the same between humans and macaques. Since we used the available human nucleotide sequence databases to putatively identify our macaque-derived SAGE tags with limited success, given the large frequencies of unmatched tags, it was important to attempt to unequivocally determine the identity of the genes from which the differentially expressed SAGE tags were derived.

RACE is an application of RT-PCR that can be used to obtain additional sequence information for a given gene using only one gene-specific primer. We employed this method in an attempt to obtain more sequence information from the gene containing the 14-nt SAGE tags. Using total RNA extracted from macaque brain tissue we performed RT-PCR using a 3' RACE adapter primer and then hemi-nested PCR using the 14-nt SAGE tag as forward primer and 3' RACE outer and inner primers as reverse primers. The products of these PCR reactions were gel purified, cloned into pGEMT vector and sequenced. To obtain gene identity information, online BLAST search analyses were performed. This approach was attempted for 8 different SAGE tags. Using this method, we obtained 2 cDNAs that when aligned with the most homologous

human sequences were 100% homologous across the 14-nt SAGE tag for MHCI and Nrg. Although cDNAs were amplified from all attempted RACE reactions, overall, this method of follow-up proved to be inefficient. Use of 14-nt tag-specific primers for RACE yielded RACE products with a perfect match at the 14-nt area of the sequence for only 2 out of 8 attempted SAGE tag specific RACE reactions. These mismatched RACE products, when sequenced, did not match the identity of the original tag-to-gene output. Table 5 lists 8 SAGE tags for which RACE was attempted and compares them with the RACE products that were obtained. Figure 7 shows sequence alignments of cDNA products from the 3'RACE using the Nrg SAGE tag sequence as the 14-nt primer. For one sequenced clone, the tag region showed a perfect 14 bp match and the identity of the gene matched with the putative identity predicted by the tag-to-gene analysis. However, for a different clone from the same RACE reaction and subsequent ligation, the tag region showed only a 10/14 bp match and the amplified gene was identified as stannin instead of the expected Nrg. This could have been due to sequence differences between macaque and humans, technical limitations resulting from performing PCRs with unusually short length primers, or due to homology of a short stretch of sequence in the gene with the 3' end of the 14-nt primer causing it to amplify.

Table 2 Abundantly expressed SAGE tags in the rhesus macaque CNS

Caudate

Tag Sequence	UI Freq[a]	AcSIV Freq[a]	mSIVE Freq[a]	Tag-to-gene Output[b] (*Unigene ID*)	Putative Function[c]
GACTCCACGT	15836	17622	5168	Copper chaperone (*Hs.5002*)	Delivers Cu to and activates copper/zinc superoxide dismutase
ACCAAGAGGA	15303	10700	5793	No Match	
ACAACTCGAA	15268	17023	14880	No Match	
GTAAGCGTAC	13563	11187	10904	No Match	
CTAAGACCAC	13563	9990	10989	Max protein (*Hs.42712*)	Basic helix-loop-helix leucine zipper transcription factor
TACCCGTACC	11433	6397	2782	Disheveled associated- activator of morphogenesis 1 (*Hs.19156*)	Controls cell polarity and movement during development
CTTCGCCACC	9693	8867	12267	No Match	
CAGTTGTTGA	9232	17136	4685	Viperin (*Hs.17518*)	Interferon inducible viral inhibitory protein
CAGCTAAAGC	9054	6697	7383	No Match	
AACTATCCCC	7669	9316	4373	Ngg1 interacting factor 3 like binding protein 1 (*Hs.288151*)	Unknown
ATCTGAGAAG	7349	6098	6872	Forkhead box P1 (*Hs.431498*)	Transcription factor
TGACTGTGCT	6462	6996	6730	Neurogranin (*Hs.232004*)	Calmodulin-binding protein kinase substrate
CAAACATCCT	6355	5050	4089	Partitioning defective 6 homolog gamma (*Hs.436554*)	Signal Transduction
AGGCCAAATA	5041	3741	3578	Hypothetical protein MGC34713 (*Hs.425123*)	
CAGCCAAATG	4686	4265	2726	Hippocalcin (*Hs.288654*)	Neuron specific calcium binding protein
TGGACACTCA	4438	3217	4799	Neurochondrin (*Hs.121870*)	Development of CNS
GTGAAACCCC	4367	4340	8746	Hypothetical protein MGC11332 (*Hs.98798*)	
CCACTGCACT	2982	3067	5253	Carbonic anhydrase XII (*Hs.210995*)	Zinc metalloenzyme
CTGCGCCCTT	2201	4527	6105	No Match	
GGGGTCAGAA	2166	1122	539	Glu rich tetratricopeptide repeat containing, alpha (*Hs.203910*)	Unknown

Globus Palidus

Tag Sequence	UI Freq[a]	AcSIV Freq[a]	mSIVE Freq[a]	Tag-to-gene Output[b] (*Unigene ID*)	Putative Function[c]
GACTCCACGT	16148	15791	2747	Copper chaperone (*Hs.5002*)	Delivers Cu to and activates copper/zinc superoxide dismutase
ACAACTCGAA	15526	10325	10325	No Match	
CTAAGACCAC	9163	5434	8517	Max protein	Basic helix-loop-helix leucine zipper transcription factors
CAGCTAAAGC	8795	5466	4640	No Match	
ACCAAGAGGA	8738	5466	4396	No Match	
CTGCGCCCTT	8427	15568	15539	No Match	
AACTATCCCC	7466	6841	1831	Ngg1 interacting factor 3 like binding protein 1 (*Hs.288151*)	Unknown
GTAAGCGTAC	7409	6329	7021	No Match	
CAGTTGTTGA	7324	9846	1557	Viperin (*Hs.17518*)	Interferon inducible viral inhibitory protein
ATCTGAGAAG	6759	4763	6502	H2A histone family, member Z (*Hs.119192*)	Embryonic development
AGGCCAAATA	5938	2653	2564	Hypothetical protein MGC34713 (*Hs.425123*)	
CTTCGCCACC	5713	7512	10654	No Match	
CAAACATCCT	5118	2589	3846	Partitioning defective 6 homolog gamma (*Hs.436554*)	Signal Transduction
TACTTCTGCC	4015	3676	1801	Myeloid differentiation primary response gene (88) (*Hs.82116*)	Adaptor protein for TLR signaling pathway
GTGAAACCCC	3930	3772	8914	Retinol dehydrogenase 11 (*Hs.226007*)	Oxidoreductase activity toward retinoids
TTGGGGTTTC	3704	3420	3083	Ferritin heavy polypeptide 1 (*Hs.448738*)	Iron storage and metabolism
TTGGAGATCT	3054	2717	1251	NADH dehydrogenase 1alpha subcomplex (*Hs.50098*)	Electron transfer from NADH to respiratory chain
AATATTTTCT	2941	1118	2045	RASp21 protein activator 1 (*Hs.292524*)	Control of cell proliferation and differentiation
CTATATTTAG	2884	1603	1251	Adrenergic alpha 1A receptor (*Hs.52931*)	Regulation of cell proliferation
CATACATACA	2856	1886	3632	Proteolipid protein 1 (*Hs.1787*)	Development of myelin sheath, oligodendrocytes

[a]frequencies were calculated for all SAGE libraries and normalized per 10^6. To avoid division by 0, a tag value of 0.5 was used, whenever a tag was not detected in a library.

[b]Putative identification for a given tag was obtained by using the tag-to-gene mapping tool at www.ncbi.nlm.nih.gov/sage

[c] Putative functions were obtained by using online tools and databases locuslink and OMIM at www.ncbi.nlm.nih.gov

Although most of the RACE products we obtained did not show a perfect 14-nt match at the SAGE tag region, a number of genes were amplified that had anywhere between 8 to 13 nt of identity with the tag primer sequence. Based on our criterion for a successful RACE reaction being obtaining a product that had a 14/14 homology at the tag region, all but 2 (MHCI and Nrg) RACE products were considered unsuccessful. The identity of many of these RACE products could not be established as their sequences aligned with poorly characterized regions of human chromosomes, clones from the I.M.A.G.E (Integrated Molecular Analysis of Genomes and Expression) consortium collection (IMAGE Clones) or bacterial artificial chromosome (BAC clones) with undefined functions. However, the RACE products that we were able to identify could be functionally grouped into categories similar to the SAGE tag-to-gene outputs and included genes associated with immunity, signal transduction, metabolism/stress, replication/transcription/RNA processing and protein synthesis/trafficking/degradation. These "misprimed" genes were likely to have been amplified because of their abundant expression in the tissue samples and/or because of homology of a stretch of sequence of the gene with the 3' end of the primers containing SAGE tag sequences. Table 5 lists putative functions of the RACE products that were obtained.

For the mismatched RACE products, when the corresponding human sequences were analyzed, they often did not show a perfect 14 bp match at the tag region. A number of strategies were attempted in order to obtain RACE products perfectly matched at the 14-nt tag region. We attempted to optimize the primers by increasing their lengths (by adding a 6 bp restriction site or 3 bp GCG sequence to the 5'end of the tag sequence), and by designing redundancies (Ns) at the 3', 5', or both ends of the primer sequences, in order to generate a primer pool with a fraction of the primers having the correct end sequence.

Table 3 Differentially expressed SAGE tags in Rhesus macaque CA during SIV infection

Upregulated Tags

Tag	AcSIV:UI [a]	mSIVE:UI [a]	Tag to Gene Mapping Output [b] *(Unigene ID)*	Functional Category
AGAGGTTGAT	27.4	**5.7**	HLA-A major histocompatibility complex, class I, A *(Hs.181244)*	Immune associated
GGTGACCACC	24.9	**15.2**	Ferritin, light polypeptide *(Hs.433670)*	Metabolism/Stress
CCTTTCACAC	24.9	**5.7**	DKFZp434A0131 protein *(Hs.416436)*	
TGAGGTGGGA	24.9	**7.6**	No match	
GTCGTGGAAA	17.5	1	No match	
CTTCCTGTAC	17.5	3.8	Peptidylprolyl isomerase F (cyclophilin F) *(Hs.381072)*	Protein folding
CAAATCCAAA	15.8	0.4	No match	
CTCGCGTGCT	15.0	**9.5**	No match	
GACGTGTGGG	15.0	**5.7**	H2A histone family, member Z *(Hs.119192)*	Replication
TGGGGAAATC	15.0	**5.7**	Thymosin, beta 10 *(Hs.446574)*	Cytoskeleton associated
TATATATCTT	12.5	**7.8**	No match	
AGAACCTGCA	12.5	3.8	E4F transcription factor 1 *(Hs.154196)*	Transcription
CAAAGCACCG	12.5	**15.2**	No match	
TTTAACTGAC	12.5	3.8	LOC51123 HSPC038 protein *(Hs.374485)*	
AATTCATAGG	12.5	1	Ribosomal protein L21 *(Hs.381123)*	
TAAAGACACA	12.5	**5.7**	Tyrosyl DNA phosphodiesterase 1 *(Hs.209945)*; Poliovirus receptor related 3 (Hs.293917)	Replication; Cytoskeleton associated
TTTTTCTCCC	12.5	3.8	DORA reverse strand protein 1 *(Hs.279583)*	Unknown
TGAGGTTTTC	12.5	**7.8**	Dystonin *(Hs.485616)*	Cytoskeleton associated
TGGAAGGCGC	12.5	**7.8**	N acetylglucosaminyltransferase protein *(Hs.352622)*; GTPase activating protein 1 *(Hs.25584)*	Metabolism/Stress; Signal transduction
CAAATTAGGT	12.5	3.8	No match	

Downregulated Tags

Tag	UI:AcSIV [a]	UI:mSIVE [b]	Tag to Gene Mapping Output [b] *(Unigene ID)*	Functional Category
CTGCTAACAG	80.5	1.0	PITPNM family member 3 *(Hs.183983)*	Signal transduction
GGAGGTGCTC	14.2	3.8	Hypothetical protein MGC4093 *(Hs.31895)*	
GAGGCCAATG	14.2	**14.2**	Hypothetical protein FLJ33996 *(Hs.436550)*	
GCTACCCTCA	14.2	**14.2**	No match	
TGAAAGCAAA	14.2	0.8	LOC440135 *(Hs.375776)*	
GAAATGCAGC	14.2	**7.5**	Leucine proline enriched proteoglycan 1 *(Hs.437656)*	Cell proliferation suppressor
TCTGTCAAGA	14.2	1.9	ATP synthase, H+ transporting, mitochondrial F1 complex, O subunit *(Hs.409140)*	Metabolism/Stress
GGTCACCAGC	14.2	2.5	Phospholipase C, delta 1 (Hs.80776); Mastermind like 3 (Drosophila) *(Hs.444627)*	Signal transduction; Transcription
GCACAGATTA	11.8	1.3	Importin 13 *(Hs.158497)*	Protein trafficking
TGTGGCCTCC	11.8	**12.5**	C11orf2 chromosome 11 open reading frame2 *(Hs.277517)*	
GTTGTCTTTG	11.8	1.6	C10orf86 Chromosome 10 open reading frame 86 *(Hs.258798)*	
GTACATTGTA	11.8	3.1	Transcription elongation factor A (SII) like 3 *(Hs.311776)*	Transcription
AGATGGCACA	11.8	0.6	Ribosomal protein L39 *(Hs.300141)*	Protein synthesis
GGTGACAGCC	11.8	2.1	GlcNAc:betaGal beta 1,3 N acetylglucosaminyltransferase 6 *(Hs.8526)*	Metabolism/Stress
TCAGGAAACA	11.8	1.6	Dual specificity phosphatase 3 (vaccinia virus phosphatase VH1 related) *(Hs.181046)*	Signal transduction
TGCAATATGG	11.8	2.1	Fibrillin 1 (Marfan syndrome) *(Hs.750)*	Cytoskeleton associated
TGCCCACACA	11.8	**6.3**	ATP synthase, H+ transporting, mitochondrial F1 complex (Hs.177530); Transcribed locus *(Hs.448741)*	Metabolism/Stress
GAATTGGTGC	11.8	3.1	Collagen, type IX, alpha 1 *(Hs.149809)*	Structural
TAGACATTGC	11.8	1.3	No match	
GGATAATGTG	11.8	3.1	No match	

[a]**For all SAGE libraries, frequency of a given tag was calculated within each library and normalized per 10^6. For obtaining fold differences, the frequency of a tag in one library was divided by the frequency of the same tag in a different library. To avoid division by 0, a tag value of 0.5 was used, whenever a tag was not detected in a library.**

[b]**Information on the putative identity of a given tag was obtained by using the tag-to-gene mapping tool at www.ncbi.nlm.nih.gov/sage.**

Numbers in bold indicate tags that were up or down regulated by >5-fold in mSIVE SAGE libraries

Table 4 Differentially expressed tags in Rhesus macaque GP

Upregulated Tags

Tag	AcSIV: UI[a]	mSIVE:UI[a]	Tag to Gene Mapping Output [b] (Unigene ID)	Functional Category
GTCGTGGAAA	23.4	1.0	No match	
TATATATCTT	14.9	2.0	No match	
GTGGAGCGGA	14.9	4.1	DEAD/H (Asp-Glu-Ala-Asp/His) box polypeptide 30 (Hs. 323462)	RNA processing
TTTCTGGAGG	14.9	2.0	Mannose phosphate isomerase (Hs. 75694)	Metabolism/Stress
TTTTACAGTA	12.8	4.1	Hypothetical protein PTD004 (Hs. 475012)	
GAGGGAGGGC	12.8	1.0	CDNA FLJ26120 fis, clone SYN00419 (Hs. 433995)	
CCGCCCGCCT	12.8	4.1	No match	
GTGTGGGGTG	12.8	2.0	C17orf28 chromosome 17 open reading frame 28 (Hs.11067)	
AGAGGTTGAT	11.9	**8.1**	HLA-A major histocompatibility complex, class I, A (Hs. 181244)	Immune associated
GCGGAGGTTG	11.3	2.2	No match	
GGGCAGCTGG	10.7	4.1	FLJ20512 hypothetical protein FLJ20512 (Hs. 105606)	
TGTATATAGA	10.7	**8.1**	RNA polymerase II, polypeptide A small phosphatase 1 (Hs. 444468)	Signal transduction
ACTTCTCCTG	10.7	1.0	No match	
CGGGTGGTAA	10.7	1.0	No match	
GAAATCCAAA	10.7	1.0	Myotrophin (Hs.21321)	Signal transduction
GCAAAACTCC	10.7	2.0	REV1 like (yeast) (Hs. 443077)	
GCTATAGGGA	10.7	2.0	No match	
CACTATCCCC	10.7	1.0	Autism susceptibility candidate 2 (Hs. 296720)	Unknown
GAGGGTGCCA	10.7	**20.4**	Complement component 1, q subcomponent, beta polypeptide (Hs.8986)	Immune associated
TATATGCCTA	10.7	4.1	HERC2 hect domain and RLD 2 (Hs. 434890)	Protein trafficking/Degradation

Downregulated Tags

Tag	UI:AcSIV[a]	UI:mSIVE[a]	Tag to Gene Mapping Output [b] (Unigene ID)	Functional Category
CTGCTAACAG	66.0	2.0	PITPNM family member 3 (Hs.183983)	Signal transduction
ACCTCAGGAA	18.9	2.3	High density lipoprotein binding protein (vigilin) (Hs. 427152)	Metabolism/Stress
AGGGAAAAAA	18.9	1.2	Guanine nucleotide binding protein (G protein), beta polypeptide 1 (Hs.304694)	Signal transduction
AATAAAGGTG	17.0	4.2	Heat shock factor binding protein 1 (Hs. 250899)	Metabolism/Stress
TGTAAAATAA	17.0	1.7	LOC400076, mRNA (Hs. 131598)	
CTGTGTAAAG	15.1	1.1	AF 1 specific protein phosphatase (Hs. 7314)	Signal transduction
AGGCCCAAAT	15.1	3.7	KIAA1416 protein (Hs. 397426)	
AATAAAAAAA	15.1	1.1	Mediterranean fever (Hs.173730); Protein tyrosine phosphatase, receptor type, G (Hs.89627)	Immune associated/Signal transduction
CAGCCTGAT	13.2	**6.5**	N-myristoyltransferase 1 (Hs.346743)	Metabolism/Stress
ACAAGCAAAC	11.3	2.8	No match	
GATGAAGACT	11.3	**5.6**	Loss of heterozygosity, 11, chromosomal region 2, gene A (Hs. 152944)	Unknown
TAACCAGAG	11.3	**11.3**	Transthyretin (prealbumin, amyloidosis type I) (Hs.427202)	Retinol/Steroid Binding
CAGATTAAAG	11.3	1.9	No match	
AAGTGAAAAA	11.3	**11.3**	Ring finger protein 12 (Hs. 122121)	Protein degradation
AATGAAAAAA	11.3	**11.3**	RAD51 homolog C (Hs.412587)	DNA repair
ACTAGTTGAT	11.3	**11.3**	No match	
CAGCCAAATG	11.3	2.8	Hippocalcin (Hs.288654)	Signal transduction
TACCAATCCA	11.3	2.8	No match	
CATACCTGAA	10.6	**22.6**	CDNA FLJ25076 fis, clone CBL06117 (Hs.351357)	
ACTAGAGAAA	9.7	1.0	No match	

[a] **For all SAGE libraries, frequency of a given tag was calculated within each library and normalized per 10^6. For obtaining fold differences, the frequency of a tag in one library was divided by the frequency of the same tag in a different library. To avoid division by 0, a tag value of 0.5 was used, whenever a tag was not detected in a library.**

[b] Information on the putative identity of a given tag was obtained by using the tag-to-gene mapping tool at www.ncbi.nlm.nih.gov/sage.

Numbers in bold indicate tags that were up or down regulated by >5-fold in mSIVE SAGE libraries

For optimizing the PCR reactions, we tested a range of $MgCl_2$ concentrations (1, 1.5, 2 mM) and a range of annealing temperatures (45^0C, 55^0C, 58^0C, 60^0C). We also attempted two techniques known as "hot start" PCR and "touch-down" PCR, which are designed to minimize spurious binding of the primer to the template and thereby reduce nonspecific amplification products. In hot start PCR the polymerase remains inactive until heated to 94^0C minimizing low temperature non-specific amplification. In touch-down PCR the annealing temperature is increased or decreased by 2^0 every 2 cycles for the first 10 cycles. For the remaining cycles the annealing temperature is set at 58-60^0C. All these strategies were attempted on a single tag, however, none yielded a product with a 14 bp sequence match at the tag region. We also attempted to repeat a published method known as GLGI [163]. In this method double stranded cDNA is synthesized by use of a biotinylated oligo (dT) primer followed by digestion with the restriction enzyme *Nla*III. The products are ligated to linker sequences and PCR amplified in a first round reaction using primers specific for the linker and the oligo (dT) sequences (universal anti-sense primer) and PCR amplified in a second round reaction using the SAGE tag specific primer and the universal anti-sense primer. This approach should result in the isolation of a population of cDNAs representing only the 3' ends of mRNAs, thus creating a smaller, more specific pool for amplification of a gene sequence associated with a particular SAGE tag. Although in theory this technique should enable more accurate identification of the SAGE tags, in our case the efficiency of obtaining a 14/14-nt match at the tag region remained low. Specifically, we attempted to optimize four SAGE tags by the GLGI method and compared 19 different RACE products. Out of them, only 2 (10%) showed a perfect match across the tag region.

Table 5 Sequence comparisons between SAGE tags and RACE products at the tag region

SAGE Putative ID[a]	Tag Sequence	Length of homology across tag region[b]	RACE Gene ID[c]	% homology with highest ranking BLAST result[d]	Putative Function
MAP3K4	CAAATCCAAA	10 out of 14	Macaque cytochrome B	94%	Stress
Neurogranin	TGACTGTGCT	14 out of 14	Human neurogranin	100%	Signal transduction
		10 out of 14	Human stannin	95%	Mediates neurotoxicity
Collagen, type XVIII, alpha 1	CTGCTAACAG	10 out of 14	Macaque mitochondrial dehydrogenase subunit 4, 5	99%	Stress
		9 out of 14	Macaque mitochondrial cytochrome oxidase subunit, 1	98%	Stress
		13 out of 17	Human brain cDNA KIAA0626	93%	Unknown
Unknown (2)	GTCGTGGAAA	13 out of 18	Human EMS1	91%	Cancer associated
MHCI	AGAGGTTGAT	13 out of 18	Human bleomycin hydrolase	98%	Cysteine proteinase
		11 out of 14	Human GDP dissociation inhibitor1	94%	Signal transduction
		13 out of 16	Human heat shock protein	98%	Stress
		14 out of 14	Human MHCI	99%	Immune-associated
		8 out of 13	Hypothetical protein FLJ20156	67%	Hypothetical
		12 out of 18	Human large cell hypothalamic nuclei protein	93%	Hypothetical
		14 out of 14	Macaque MHCI A*11	96%	Immune associated
Unknown (3)	CATACCTGAA	10 out of 15	Human H+-ATPaseB	97%	Metabolism
Unknown (1)	TGGTATACCT	9 out of 14	Human thioredoxin	97%	Oxidoreductase enzyme
General transcription factor II	CCTTTCACAC	9 out of 14	Macaque mitochondrial genomic DNA	71%	Stress

[a] **Result of tag-to-gene mapping using online tool at www.ncbi.nlm.nih.gov/SAGE**

[b] **Sequence homology across the 14 bp tag region**

[c] **Result of BLAST search for the RACE product obtained**

[d] **RACE amplified sequences along with tag sequence were analyzed by BLAST**

Quantification of differential gene expression by Real-time RT-PCR.

MHCI and Nrg were two SAGE tags that were differentially expressed and for which the RACE products identified genes containing the exact tag sequence. To accurately quantify the levels of gene expression for MHCI and Nrg, real-time RT-PCR was performed using RNA extracted from CA and GP tissues of uninfected, AcSIV, and mSIVE rhesus macaques. Based on the SAGE data, the tag associated with the MHCI mRNA was predicted to be 27-fold higher in AcSIV versus uninfected CA and 12-fold higher in AcSIV versus uninfected GP (Table 3 and 4). The same MHCI tag was also predicted to be upregulated 6-fold in mSIVE CA and 8-fold in mSIVE GP compared to uninfected CA and GP respectively. By real-time RT-PCR, we compared the levels of expression of MHCI mRNA in uninfected, AcSIV, AIDS non-SIVE, and mSIVE animals. When group means were compared, levels of MHCI mRNA expression were found to be 3.5-fold higher in AcSIV CA and 6-fold higher in AcSIV GP compared to uninfected CA and GP, respectively (Figure 8 A). In similar comparisons, AIDS non-SIVE animals showed a 4.3-fold upregulation and mSIVE animals showed 5.2-fold upregulation when compared to uninfected CA. In GP, we found MHCI to be similarly upregulated, by 4.6-fold in AIDS non-SIVE and 5.3-fold in mSIVE compared to uninfected animals (Figure 8 A). In CA, the group mean differences were statistically significant between uninfected and AcSIV ($p = 0.02$) and uninfected and AIDS ($p = 0.04$) but not between uninfected and mSIVE disease groups. In GP, the differences were statistically significant between uninfected and AcSIV disease groups only ($p = 0.01$).

A Hu Nrg **CATGTGACTGTGCTG**GGTTGGAATGTGAACAATAAAGAGGAATGTCCAAGTGAAAAAAAAAAAAA

  Rh.Nrg.5a **CATGTGACTGTGCTG** ....

  Hu Nrg.5a AAAAAAA

  Rh.Nrg.5a ....

B Hu Stannin **CATGTGACTGTGCT**ACTGTTTTTGTTTCAAAGCTACCAAGTTTGTGCAATAAGTGGAAGGGATG

  Rh.Nrg.6a A.**A..GACTGTGCT**.....A...

  Hu Stannin TCATCTCTCTTCAATAAATGCTGAATGACATTCAAGTTGATTTTCTAGACCACTGAGAAAATCT

  Rh.Nrg.6a   .....C.. .C...

  Hu Stannin TTATTTACAATAAATTTCAATAAAATTTGCATAAATATAAAAAAAAAAAAAAAAAAAAAAAAAAAA

  Rh.Nrg.6a ....

  Hu Stannin AAAAA

  Rh.Nrg.6a ....

Figure 7 Nucleotide sequence alignments of Nrg

Alignment of sequence of Nrg RACE products obtained with the Nrg SAGE tag and corresponding human sequences. Alignments show a perfect 14 bp match at the primer region for Nrg clone 5a (A) and an imperfect match using the same primers and conditions for Nrg clone 6a, Stannin (B). Dots represent identical nucleotides. Sequences in blue indicates the tag regions

By SAGE analysis, comparing across microanatomic compartments, the Nrg tag was predicted to be expressed 73-fold higher in AcSIV CA versus AcSIV GP and 46-fold higher in uninfected CA versus uninfected GP. This tag was also predicted to be 37-fold upregulated in mSIVE CA compared to mSIVE GP. By real-time RT-PCR levels of Nrg mRNA were found to be 5.2-fold higher in acute and uninfected CA compared to acute and uninfected GP when group means were compared (Figure 8 B). The differences between CA and GP were statistically significant ($p = 0.02$). Therefore these real-time RT-PCR results confirmed the higher levels of expression of MHCI during SIV infection and of Nrg in CA relative to GP, although the levels of increase were not as large as what were predicted by the SAGE data.

In order to determine whether MHCI expression in the CNS corresponds to expression levels in a peripheral tissue compartment, we performed real time RT-PCR on RNA extracted from Ax LN. In this tissue compartment, the levels of MHCI RNA expression did not rise significantly in any of the disease states, with the exception of a single outlier AcSIV animal (Figure 8 C). Whereas in the CNS MHCI expression remained elevated in both AIDS and mSIVE, in the Ax LN the expression levels were low in both AIDS non-SIVE and mSIVE animals (Figure 8 C). No correlations were observed between the levels of MHCI expression in CNS CA and Ax LN and the differences between disease groups were not statistically significant. These findings indicate that the upregulation of MHCI in the CNS was most likely independent of the upregulation in peripheral Ax LN.
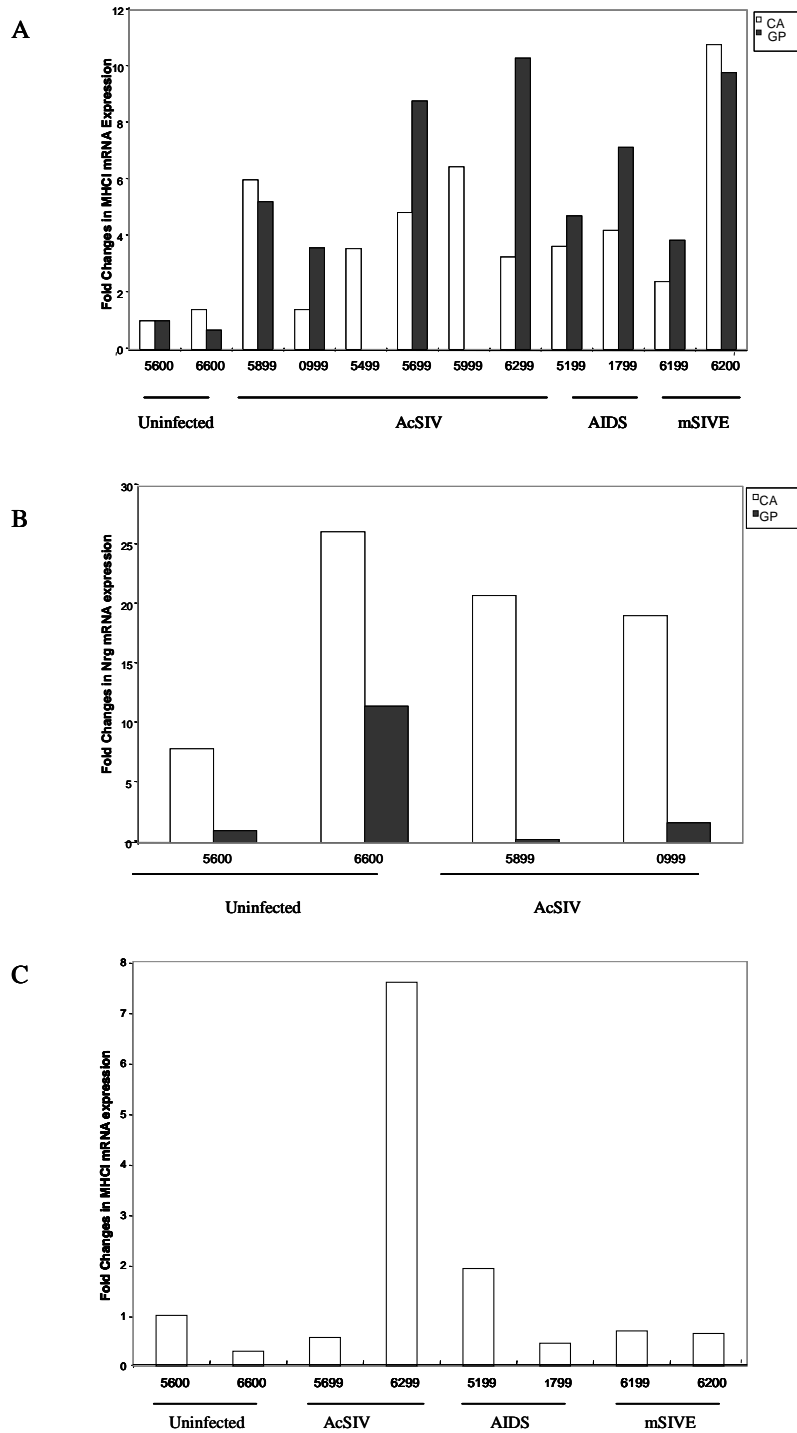
Figure 8   Differential expression of MHCI and Nrg RNA by Real time RT-PCR.

Upregulation of MHCI was observed among disease states in the CNS (A) and Ax LN (C). Differential expression of Nrg was observed in the CNS CA compared to GP (B). Taqman realtime RT-PCR was performed using 40 cycles of amplification with 18S as endogenous control and fold changes were calculated by the comparative C_T method.   For MHCI assays M5600 was used as calibrator. For Nrg assays M5600 GP was used as calibrator. For (A), GP RNA was not tested for 5499 and 5999.

Single cell analysis of differentially expressed genes.

ISH was performed to better understand the patterns of expression of MHCI in macaque CNS tissues. For comparison purposes Nrg mRNA expression pattern was also examined. MHCI mRNA expression was higher in tissues from AcSIV and mSIVE animals when compared to uninfected animals (Figure 9). In uninfected tissues the MHCI signal was mostly localized in perivascular regions of the CNS. In the AcSIV and mSIVE tissues, perivascular pattern of MHCI expression was retained although signal was more intense. Also, in AcSIV and mSIVE, MHCI mRNA was observed throughout the CNS parenchyma. Nrg mRNA expression was found to be higher in CA of both AcSIV and uninfected samples when compared to GP, irrespective of disease state (Figure 11).

ISH signals for MHCI mRNA were quantified using quantitative image capture and analysis (QIA) such that the surface areas of images covered by silver grains were thresholded and measured. Ten randomly captured microscopic fields were examined from each tissue section hybridized with the antisense riboprobe and analyzed by QIA (Figure 10). Measuring the amount of silver grains over each cell, the mean surface area covered by the silver grains was 4.3 μm^2 per cell in uninfected CA whereas the ISH signals in tissues from AcSIV and mSIVE animals were 9.4 and 16.7 μm^2 per cell, respectively. In GP tissues, the uninfected mean surface area covered by silver grains was 6.0 μm^2 per cell compared to the AcSIV and mSIVE, which were 11.7 and 12.2 μm^2 per cell respectively. This difference was found to be statistically significant (*p-value* of <0.01) when comparing the uninfected samples to AcSIV and mSIVE in both CA and GP.
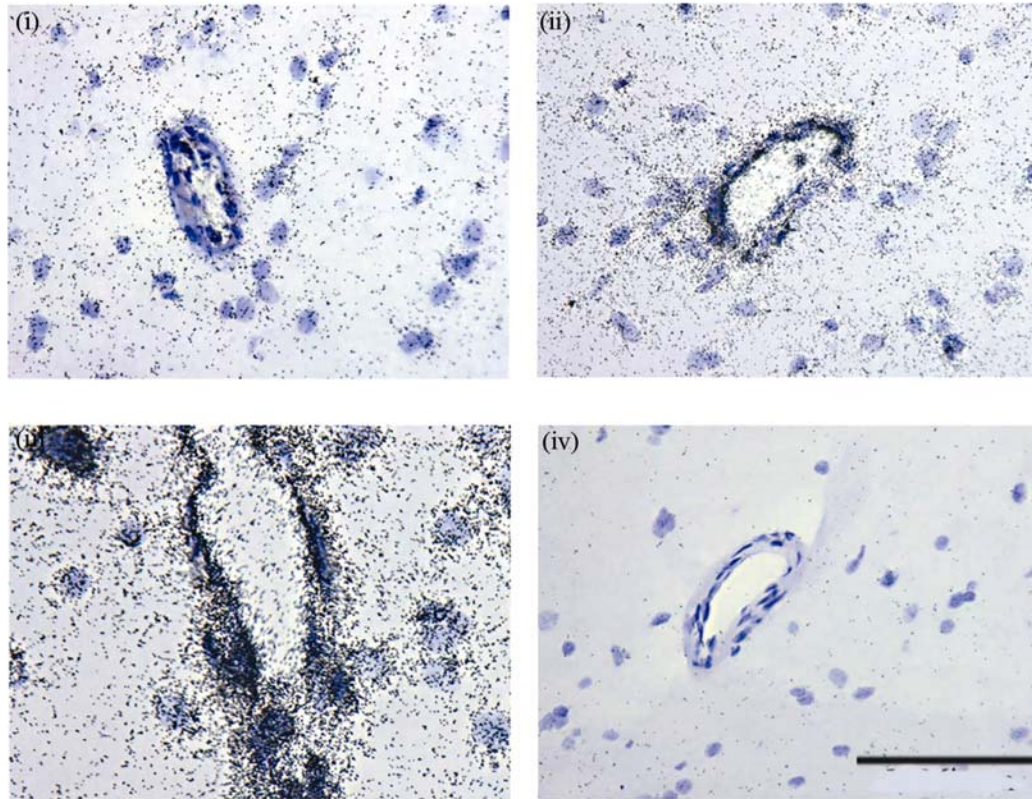
Figure 9   Tissue expression of MHCI mRNA by ISH

ISH were performed using MHCI specific riboprobes on CNS tissues and exposed for 3 days. Upregulation of MHCI mRNA was observed in uninfected (i), AcSIV (ii), and mSIVE (iii). Sense control is shown in (iv). Size bar 50 μM. Original magnification of images 400x.

(i)
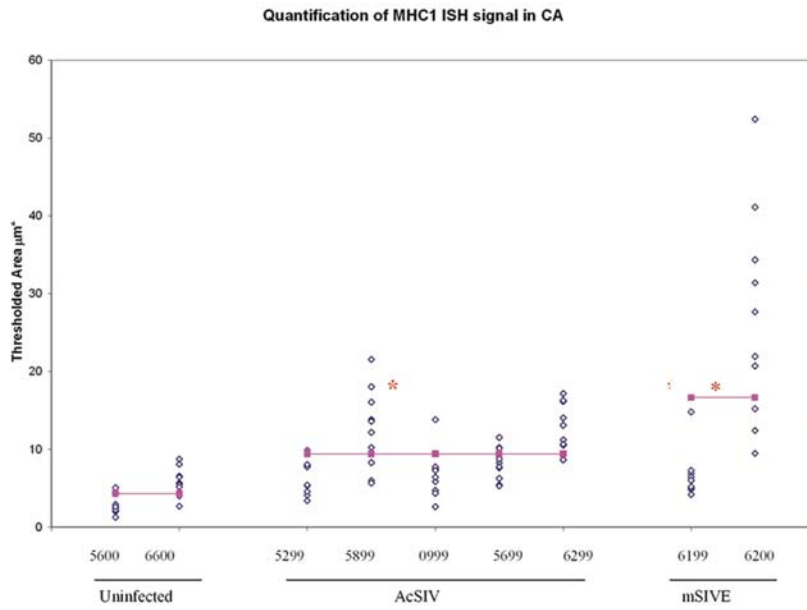
(ii)
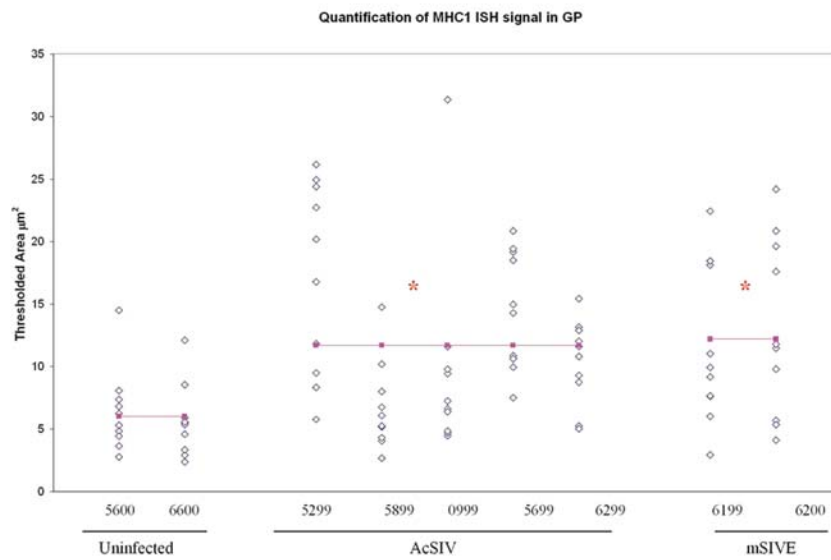
Figure 10 QIA of MHC1 ISH

QIA was performed in uninfected, AcSIV and mSIVE ISH tissues by capturing 10 random images and the amount of silver grains over each cell was quantified using the Metaview software. Comparing the mean values of each disease group, upregulation of MHCI was observed in (i) CA and (ii) GP. Bars in graphs indicate mean values for each disease group. * indicates $p<0.05$.

66
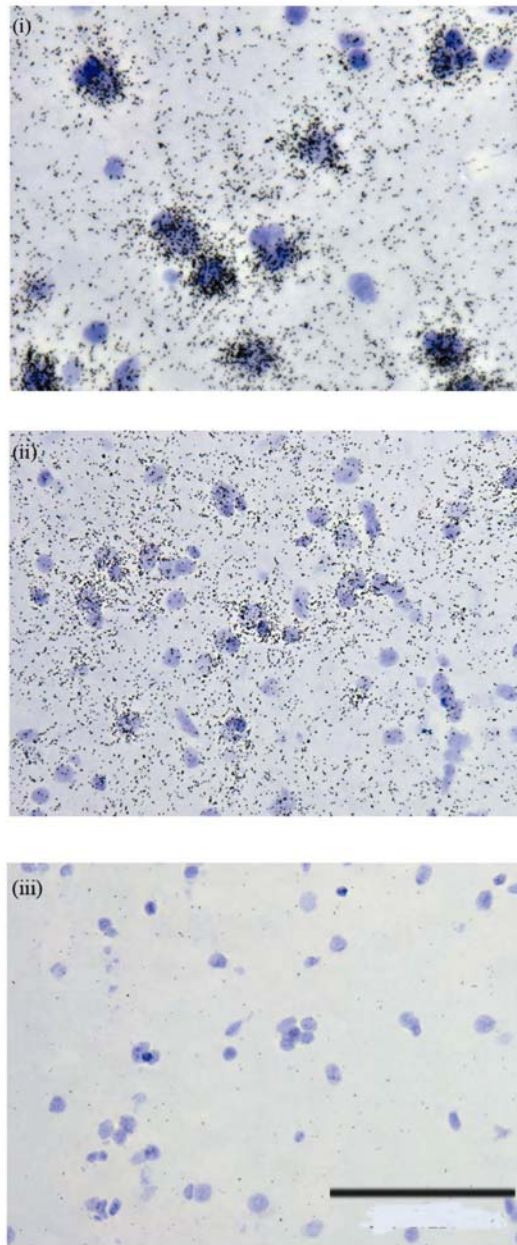
Figure 11 Tissue expression of Nrg by ISH

Nrg specific riboprobes were used to perform ISH on CNS tissues and exposed for 3 days. Higher expression of Nrg in the CA area of the CNS was observed (i) compared to the GP (ii). Tissue probed with a sense control riboprobe is shown in (iii). Size bar at 50 µM. Original magnification 400x.

Characterization of MHCI expressing cells in the CNS

To better understand the cells involved in the upregulation of MHCI mRNA in CNS tissue during acutely infected and mildly encephalitic stages of SIV infection, we sought to determine the cell types expressing MHCI mRNA. To this end, we performed combined ISH/IHC experiments for MHCI mRNA and cell type specific antigens (CD34, CD68, CD3, NeuN, MBP, and GFAP). we also characterized these MHCI mRNA$^+$ cells further in terms of their states of activation (HLA-DR) and cell proliferation (Ki67). For a subset of antibodies, it was difficult to optimize the combined ISH/IHC experiments and for these, we performed ISH and IHC in immediately subjacent sections of tissue. Due to limiting amounts of CA and GP tissues from the macaques used for the RNA studies, we used frontal cortex (FC) tissue sections for these analyses. By ISH we found comparable levels of virus-infected cells in this region as in the CA and GP of the mSIVE animals (Table 6). Two animals per disease state were used for the combined ISH/IHC analyses.

MHCI/CD68 and MHCI/HLADR ISH/IHC experiments showed predominantly perivascular colocalization for MHCI and both CD68 and HLA-DR (Figure 12). Staining for the monocyte/macrophage marker CD68, we found that MHCI$^+$/CD68$^+$ cells increased from 2.9% of total cells in uninfected animals to 4.4% in AcSIV and 7.7% in mSIVE animals (Figure 13). Using HLA-DR (MHCII) as an activation marker, we found that the percentage of MHCI$^+$/HLA-DR$^+$ cells increased from 1.1% of total cells in uninfected tissues to 3.9% in AcSIV and 7.1% in mSIVE tissues. Although there was a distinct increase in the proportion of activated cells with disease progression (Figure 13), overall, a low percentage of cells were activated even in tissues with active viral replication (in both mSIVE animals).

Table 6 Presence of SIV RNA positive cells in the CNS tissues of animals used in this study

Animals	Disease States	Area of brain	SIV RNA positive[a]
5600	UI	CA	-
		GP	-
		FC	-
6600	UI	CA	-
		GP	-
		FC	-
5299	AcSIV	CA	NT
		GP	+/-
		FC	-
5899	AcSIV	CA	NT
		GP	+/-
		FC	-
0999	AcSIV	CA	NT
		GP	NT
		FC	+/-
5499	AcSIV	CA	NT
		GP	NT
		FC	-
5699	AcSIV	CA	-
		GP	NT
		FC	-
5999	AcSIV	CA	-
		GP	NT
		FC	-
6299	AcSIV	CA	-
		GP	-
		FC	-
5199	AIDS	CA	NT
		GP	+/-
		FC	NT
1799	AIDS	CA	NT
		GP	+/-
		FC	NT
6199	mSIVE	CA	+
		GP	+
		FC	+/- (+++)
6200	mSIVE	CA	+ (+++)
		GP	+(+++)
		FC	+ (+++)

[a]SIV RNA positive cells within each region of the CNS were graded on a +/- scale where +/- indicates 1-2 viral RNA positive cells, + indicates 5-10, ++ indicates 10-20, +++ indicates >20 viral RNA positive cells per tissue section. + signs within parentheses indicate a cluster of viral RNA positive cells within a tissue where overall SIV positive cells could be lower. NT, not tested.
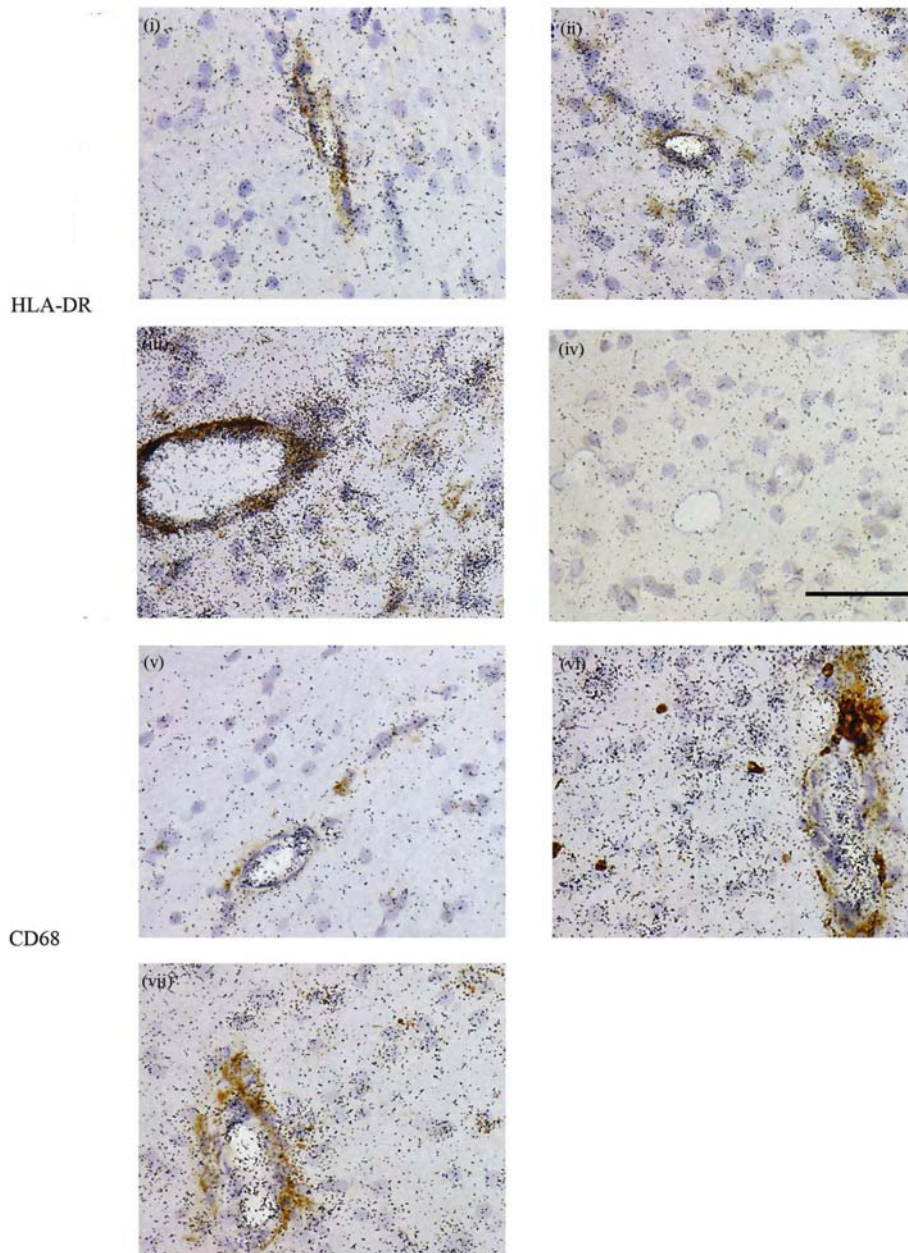
Figure 12 Detection of MHCI mRNA expressing cells that were CD68 and HLA-DR positive

Simultaneous ISH and IHC detection of MHCI mRNA and HLA-DR (i-iv) and CD68 (v-vii) antigens in the FC of SIV infected animals. In uninfected animals both CD68 and HLA-DR were expressed mostly at the perivascular regions where they colocalized with MHCI (i, v). In AcSIV and mSIVE, perivascular staining for MHCI and the antigens were more intense. Although punctuate staining for CD68 and HLA-DR were observed throughout the parenchyma in AcSIV and mSIVE, the colocalization of both antigens with MHCI remained primarily perivascular (ii, iii, vi, vii). Negative controls included tissue probed with a sense control riboprobe and stained with an isotype antibody, as shown in (iv). Size bar at 50 μm. Original magnification at 400x.
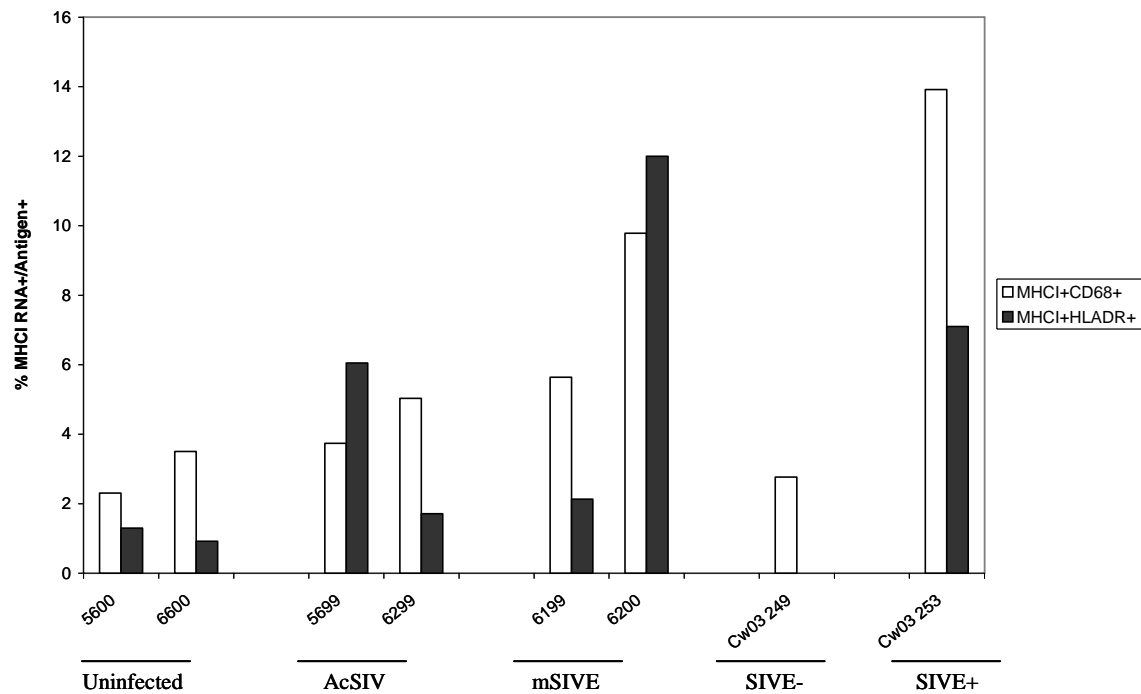
Figure 13 QIA for MHCI RNA and CD68 or HLA-DR antigen positive cells.

Semi-quantitative analysis of data obtained from simultaneous ISH and IHC experiments detecting MHC1 mRNA and CD68 and HLA-DR antigens in the FC of SIV infected animals. Ten random images were captured per tissue section and the percentage of double positive cells out of total cells was calculated. The percentage of double positive cells was found to increase with the progression of disease. Animal Cw03-249 showed 0% of MHCI+/HLA-DR+ cells out of total cells. Animals Cw03-249 and Cw03-253 were kindly provided by Dr. Clayton Wiley.

Since MF/Mgl have been well described to be the key cell population that is likely to be activated during HIV/SIV infection, the MHCI-CD68 and the MHCI-HLADR cell populations could be overlapping. In order to compare our tissues from AcSIV and mSIVE macaques with those from animals with severe encephalitis, we obtained one SIVE negative (SIVE-) and one SIVE positive (SIVE+) macaque brain tissue sample (kindly provided by Dr. Clayton Wiley, Department. of Neuropathology, University of Pittsburgh). With these additional tissues we found the percentage of MHCI-CD68 double positive cells to increase from 2.8% of total cells in SIVE- to 14% of total cells in SIVE+ whereas the MHCI-HLA-DR increased from 0% of total

71

cells in SIVE- to 7% of total cells in SIVE+ (Figure 13). This again suggests that most of the MHCI-CD68 double positive cells are activated i.e. expressing HLA-DR in disease.

In the macaque CNS, I found MHCI expressed at low levels even in uninfected animals. In uninfected tissues MHCI mRNA was localized almost exclusively in association with the vasculature. ISH and IHC on subjacent sections showed that the cells expressing MHCI were endothelial (Figure 14). In AcSIV and mSIVE, the endothelium continued to express MHCI mRNA however, in these infected tissues, additional cell types in the CNS were also found to express MHCI mRNA (Figure 15). During AcSIV the mean percentages of neurons (NeuN+) expressing MHCI mRNA increased from 6.9% in uninfected to 21% in AcSIV. This number decreased slightly to 16.2% in the mSIVE animals (Figure 16). The mean percentages of oligodendrocytes (MBP+) expressing MHCI mRNA increased from 4.8% in uninfected to 13% in AcSIV and further increased to 22 % in mSIVE (Figure 16). Finally, the numbers of astrocytes (GFAP+) that were also positive for MHCI mRNA did not show many changes in the different disease states. The mean percentages of MHCI+/GFAP+ cells were found to be 11.4%, 10.2%, and 14.2% in uninfected, AcSIV, and mSIVE respectively (Figure 16). These findings indicate that the expression patterns of MHCI mRNA alter during SIV infection. Whereas in uninfected tissues MHCI mRNA is mostly expressed at the perivascular regions by endothelial cells, in AcSIV and mSIVE neurons, oligodendrocytes, and astrocytes, can all express MHCI.

In addition, we observed a limited number of proliferating cells based on Ki67 positivity that slightly increased during AcSIV and mSIVE (Figure 17). In uninfected tissues Ki67 positive cells were rare located both at the vasculature and scattered through the parenchyma. In AcSIV and mSIVE increased numbers of Ki67 positive cells were observed in both of these locations particularly in the parenchyma. We also observed a limited number of CD3 positive T cells

present during AcSIV and mSIVE mostly around the vasculature (Figure 18). The numbers of CD3+ cells increased slightly in AcSIV and mSIVE animals but expression patterns remained perivascular. Some of these limited numbers of Ki67 and CD3 positive cells particularly around the perivascular regions were likely to be expressing MHCI mRNA. However since these cells were so few in number they were not likely to be the major producers of MHCI mRNA in these animals.

MHCI mRNA expression in other models of SIV encephalitis.

As described earlier, for the majority of these studies, we used an infection model in which rhesus macaques were infected with SIV/DeltaB670. Using this system, none of the animals became severely encephalitic and only two could be categorized as mildly encephalitic by SIV ISH and CD68 IHC methods. To determine if the MHCI upregulation that was observed in this model was reflected in other established models of SIV encephalitis, we examined MHCI expression in two other established models of SIVE.

We were able to obtain RNA extracted from the BG of two each of AcSIV, AIDS non-SIVE and SIVE samples from rhesus macaques that had been depleted of CD8 T cells, (kindly provided by Dr. Clayton Wiley, Department of Neuropathology, University of Pittsburgh). In addition we obtained RNA extracted from the CA from two each of uninfected, AcSIV, AIDS non-SIVE and SIVE pigtailed macaques that were coinoculated with SIV/17E-Fr SIV/DeltaB670 (kindly provided by Dr. Joseph Mankowski, Department of Comparative Medicine, Johns Hopkins University).
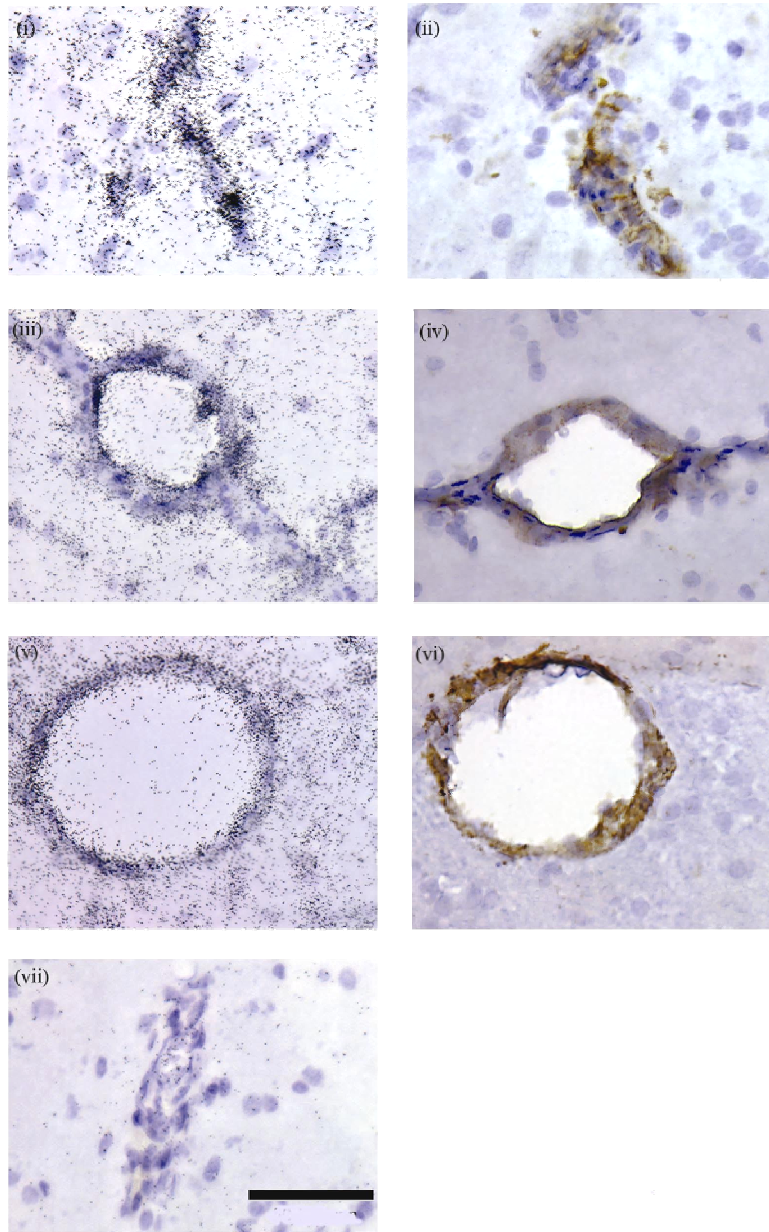
Figure 14 Detection of MHCI mRNA expressing cells that are CD34 positive.

Subjacent tissue sections were probed with MHCI specific riboprobe and stained with anti-CD34 antibody. MHCI mRNA was found to colocalize with CD34 positive endothelial cells in uninfected (i-ii), AcSIV (iii-iv) and mSIVE (v-vi). Negative control tissue probed with a sense orientation MHCI riboprobe is shown in (G). Size bar at 50 μm. Original magnification 400x.
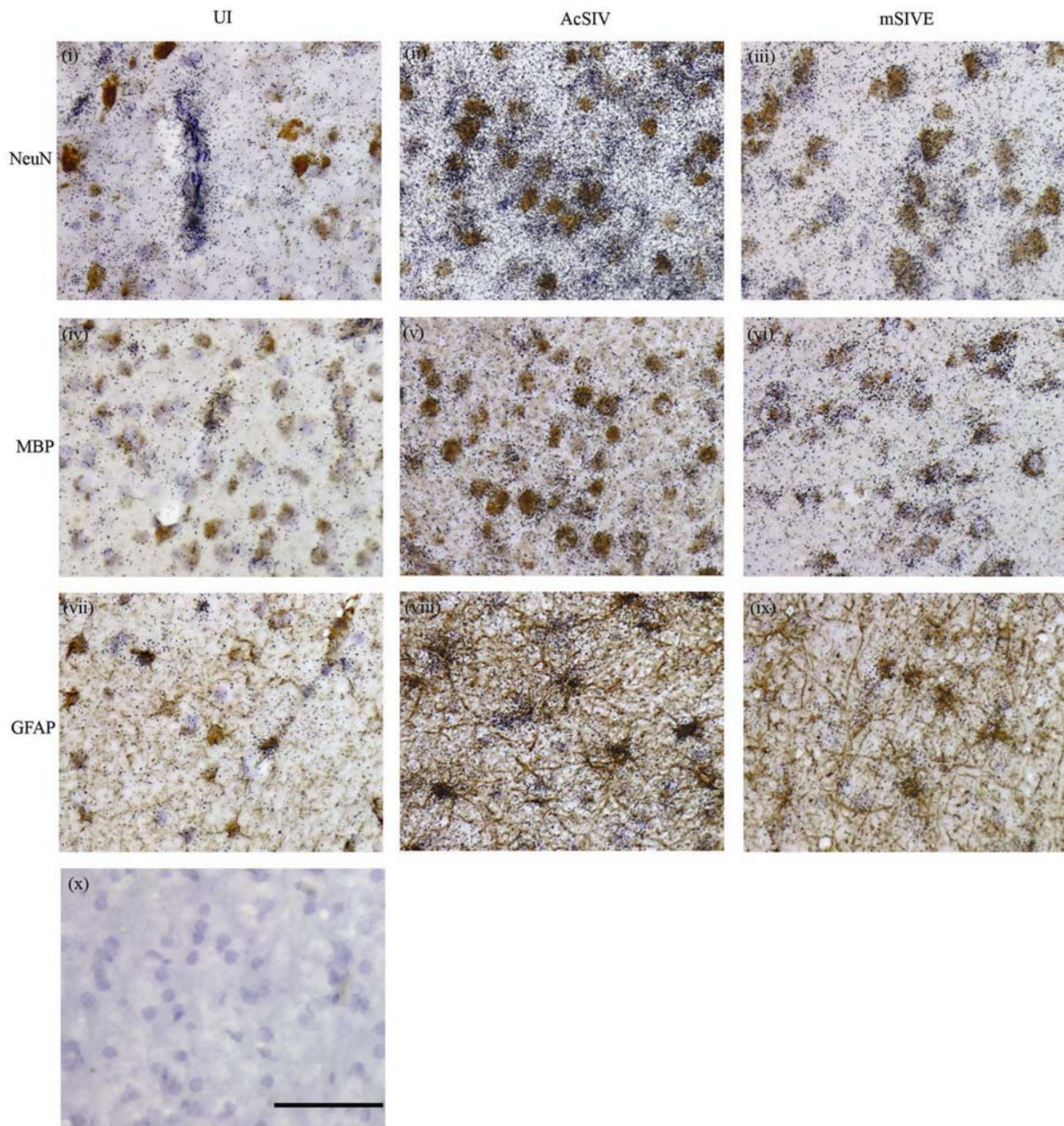
Figure 15 Detection of MHCI mRNA and NeuN, MBP, GFAP double positive cells in SIV infection.

Simultaneous ISH and IHC for the detection of MHCI mRNA and NeuN+ neurons (i-iii), MBP+ oligodendrocytes (iv-vii), and GFAP+ astrocytes (vii-ix) in the FC of SIV infected macaques with (x) showing a negative control probed with a sense orientation riboprobe and stained with isotype control antibody. A small number of neurons, oligodendrocytes, and astrocytes were found to express MHCI mRNA in uninfected animals (i, iv, vii). The percentages of double positive cells out of total number of cells for NeuN and MBP increased in infection (ii-iii, v-vi) whereas the proportion of MHCI mRNA+ cells that were GFAP positive remained relatively unchanged. Size bar at 50 μm. Original magnification 400x.
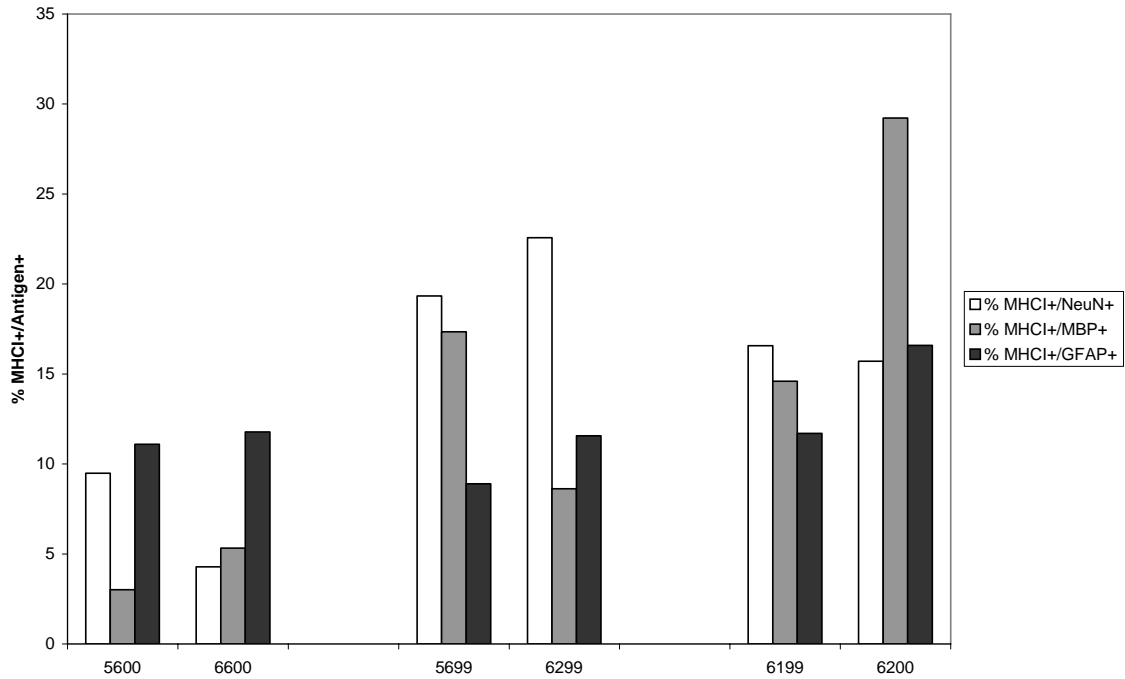
Figure 16 QIA for MHCI mRNA and NeuN, MBP, and GFAP double positive cells.

Semi-quantitative analysis of data obtained from simultaneous ISH and IHC experiments detecting MHCI mRNA and NeuN, MBP and GFAP antigens in the FC of SIV infected macaques. Ten random images were captured per tissue section and the percentage of double positive cells out of total cells was calculated. QIA showed an increase in percentages of double positive NeuN and MBP in AcSIV decreasing slightly in mSIVE. For GFAP, the mean percentages of double positive cells remained more or less unchanged with disease progression.
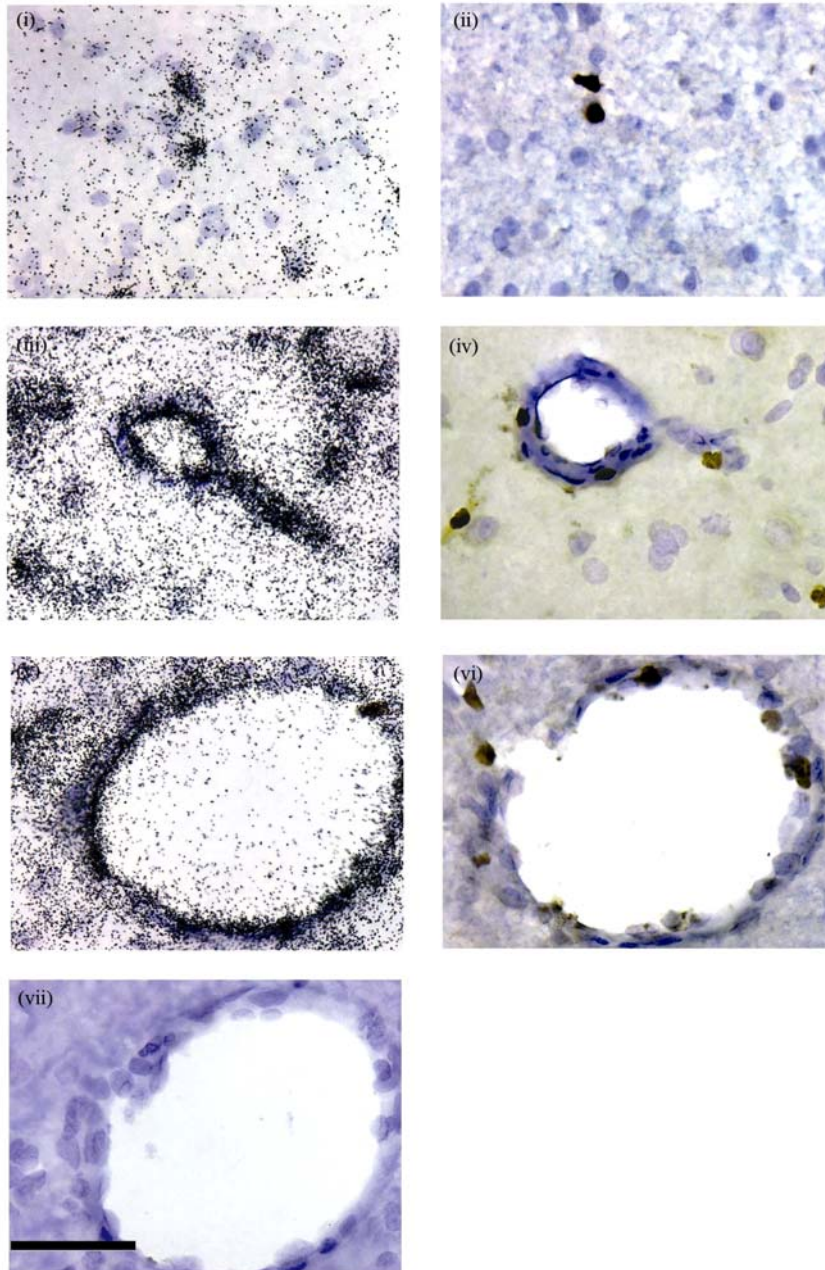
Figure 17 Detection of cells positive for MHCI mRNA and Ki67 antigen in SIV infected CNS

ISH and IHC on subjacent tissue sections detected limited number of Ki67 positive cells in the CNS parenchyma of uninfected animals (i-ii). These numbers were found to increase slightly in AcSIV (iii-iv) and mSIVE (v-vi). Limited colocalization of MHCI and Ki67 was observed. Negative control tissue probed with a sense orientation riboprobe is shown in (vii). Size bar 50 μm. Original magnification 400x.
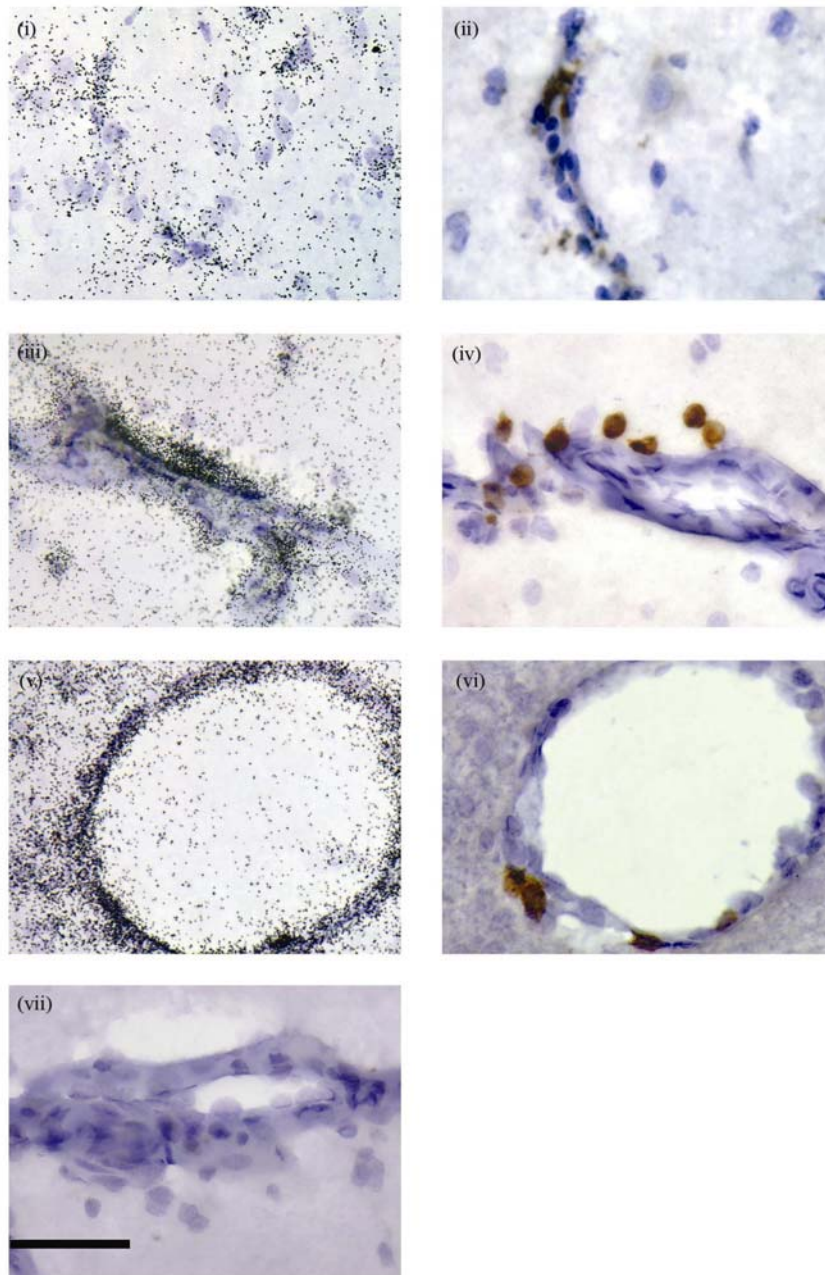
Figure 18 Detection of cells positive for MHCI mRNA and CD3 antigen in SIV infected CNS

ISH and IHC on subjacent tissue sections detected rare CD3 positive T cells in the CNS of uninfected animals (i-ii). These numbers were found to increase slightly in AcSIV (iii-iv) and mSIVE (v-vi) particularly around the perivascular regions. Limited colocalization of MHCI and CD3 was observed. Negative control tissue probed with a sense orientation riboprobe is shown in (vii). Size bar 50 µm. Original magnification 400x.

Comparing group mean levels in the macaques coinoculated with SIV/17E-Fr SIV/DeltaB670, MHCI mRNA expression increased by 11.3-fold in AcSIV but only a 2.8-fold increase was observed in AIDS non-SIVE animals when compared to uninfected (Figure 19 A). In SIVE animals a group mean increase of 49-fold was observed when compared to uninfected macaques. However, this high value was mostly due to a single animal producing high levels of MHCI mRNA (Figure 19 B). The differences between the uninfected and AIDS groups were found to be statistically significant ($p = 0.02$). In the BG of CD8-depleted macaques MHCI was found to be upregulated 7-fold in AcSIV, 2.5-fold in AIDS non-SIVE and 10-fold in SIVE relative to uninfected tissues when group means were compared and no statistical significance was observed. Therefore although only 2 animals per group were used for both of these models, overall, a trend toward MHCI mRNA upregulation was observed in the AcSIV and SIVE animals.
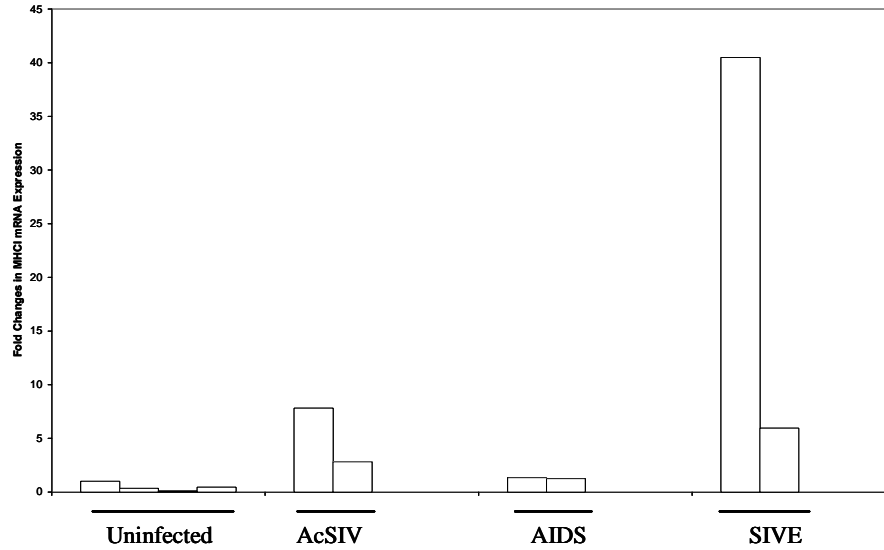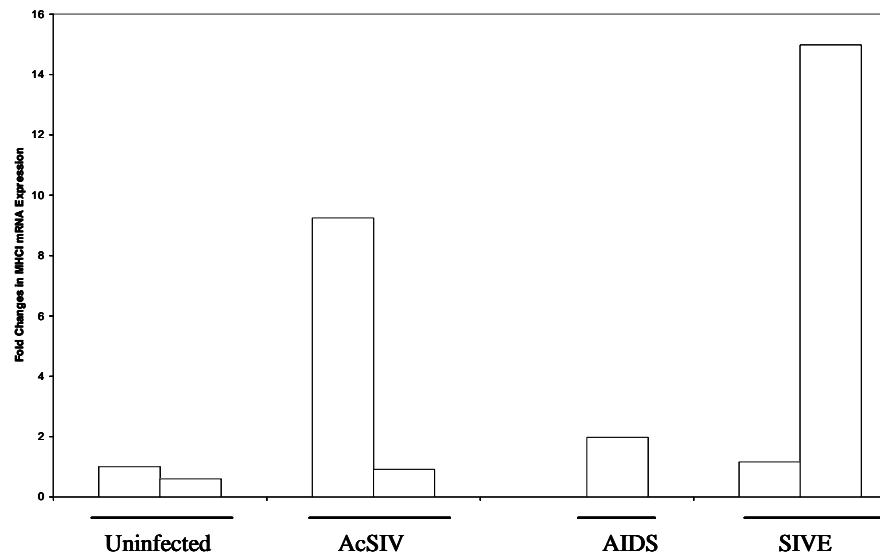
Figure 19 Differential expression of MHCI mRNA in established models for SIV encephalitis.

MHCI upregulation was observed in the CA of coinoculated pigtailed macaques (A) and BG of CD8-depleted rhesus macaques (B). For (A), two animals were used for each group with the exception of uninfected where four animals (2 from our cohorts) were used. For (B), two animals for each group were used but RNA from one AIDS animal did not amplify. Taqman realtime RT-PCR was performed using 40 cycles of amplification with 18S as endogenous control and fold changes were calculated by the comparative C_T method. M5600 was used as a calibrator for both data sets.

Local and systemic expression of cytokines, TLRs and ISGs

The MHCI upregulation that I observed might indicate a state of immune activation in the CNS. To better understand the mechanisms responsible for the CNS immune activation possibly leading to the development of encephalitis and dementia, we focused our attention to the study of the expression patterns of molecules that might be responsible for the MHCI upregulation. Some of the molecules that respond to pathogen invasion and cause early immune activation of the CNS are proinflammatory cytokines IL-1β, TNF-α, and IL-6 [191-193]. Other molecules that have been described to cause upregulation of MHCI are IL-2, IL-12, and IFNγ [194]. IFNα and IFNβ are antiviral molecules that are expressed early during infection and they activate innate and acute phase response immune molecules and can cause upregulation of MHCI [194]. We also studied the expression patterns of a number of ISGs, which are induced by IFNα and IFNβ and participate in innate antiviral immune responses [195]. The ISGs we studied were G1P3, MxA, OAS2, interferon induced protein tetratricopeptide repeats 1 (IFIT1), interferon induced protein tetratricopeptide repeats 2 (IFIT2), interferon alpha inducible protein 27 (IFI27), myxovirus influenzae resistance 2 (MxB), and oligoadenylate synthetase like (OASL). These particular ISGs were selected because they were found to be upregulated in SIV infected lung tissue in a different study in our laboratory (Dr. D.H.Kim, Reinhart laboratory, unpublished observations).

TLRs form a major group of pattern recognition receptors of the innate immune system that sense molecular patterns on microbes. Although TLRs have been described in the past as being involved in bacterial infections, TLR2 and TLR4 have both been recently described to be involved in herpes simplex virus (HSV) encephalitis and respiratory syncytial virus (RSV)[196,197].

We investigated the differential expression of these two TLRs in our SIV-infected macaque CNS to see if these genes might be playing a role in the CNS immune activation that we observe.

To examine potential upstream mediators of MHCI upregulation, we studied the expression patterns of IL-6, IL-1β, IL-2, IL-12, TNFα, IFN α, IFN β, and IFN γ, by real-time RT-PCR. For all real-time RT-PCR experiments, RNA from uninfected animal M5600 was used as a calibrator, 18S rRNA was used as endogenous control and all reactions were amplified for 40 cycles.

No detectable expression was observed for IL-6, IL-12, IL-2, IFNα, IFNβ, IFNγ, and TLR2 in the CNS (Table 7). Consistent with these findings, ISH also showed no positive signal for IL-6, IL-12, IL-2, IFNγ, and TNFα (data not shown). In the case of IFNα and IFNβ, controls that lacked reverse transcriptase amplified to similar C_T values as samples subjected to reverse transcription. This was most likely due to genomic DNA contamination of the RNA samples used. Unfortunately, due to limiting amount of tissue to extract RNA, the genomic DNA could not be removed enzymatically without the risk of losing a majority of the RNA during clean up. For these reasons the results were therefore uninterpretable for these genes.

Table 7 Differential expression of cellular genes by Real time RT-PCR

		$2^{-\Delta\Delta C_T}{}^a$																	
Animals	Disease State	IL-1β	TNFα	IL-6	IL-2	IL-12	IFNα	IFNβ	IFNγ	TLR2	TLR4	G1P3	IFIT1	IFIT2	IFI27	MxA	MxB	OAS2	OASL
5600	UI	1.0	-	-	-	-	g	g	-	-	1.0	1.0	g	g	-	1.0	g	1.0	g
6600	UI	3.4	-	-	-	-	g	g	-	-	1.7	0.4	g	g	-	0.8	g	0.3	g
5899	AcSIV	2.0	-	-	-	-	g	g	-	-	2.3	0.6	g	g	-	4.0	g	0.0	g
0999	AcSIV	2.0	-	-	-	-	g	g	-	-	4.6	3.6	g	g	-	1.8	g	0.0	g
5499	AcSIV	2.6	-	-	-	-	g	g	-	-	5.5	2.3	g	g	-	0.9	g	0.0	g
5699	AcSIV	3.8	-	-	-	-	g	g	-	-	2.5	16.2	g	g	-	77.8	g	2.6	g
5999	AcSIV	6.2	-	-	-	-	g	g	-	-	1.3	3.3	g	g	-	1.0	g	0.0	g
6299	AcSIV	2.6	-	-	-	-	g	g	-	-	2.7	12.0	g	g	-	1.7	g	0.6	g
5199	AIDS	x	x	x	x	x	x	x	x	x	x	49.2	x	x	x	3.9	x	5.1	x
1799	AIDS	x	x	x	x	x	x	x	x	x	x	72.5	x	x	x	12.7	x	6.7	x
6199	mSIVE	13.1	-	-	-	-	g	g	-	-	1.1	5.6	g	g	-	37.4	g	6.6	g
6200	mSIVE	3.8	-	-	-	-	g	g	-	-	0.8	3.3	g	g	-	59.6	g	4.3	g

[a] **Fold change in expression given by $2^{-\Delta\Delta C_T}$**

[x] **Not tested**

[-] **Not detected after 40 cycles of amplification**

[g] **Not calculated due to genomic DNA contamination of RNA samples**

Expression of IL-1β mRNA was detectable but other than one mSIVE animal, no upregulation was observed (Table 7). For TLR4 mRNA large fold differences were not observed when comparing group means. However, the differences were significant between uninfected and AcSIV animals ($p = 0.05$) (Table 7).

Out of the eight ISGs that I investigated, I observed elevated expression levels of MxA, OAS2, and G1P3 in both CNS and Ax LN (Figure 20). All three molecules have previously been shown to have antiviral activity associated with early interferon-mediated immune response [198-

[201]. In CA, G1P3 mRNA was found to be upregulated in AIDS compared to other disease states. Comparison of the group means revealed an increase in G1P3 mRNA expression of 9.0-fold during AcSIV, 87.0-fold during AIDS non-SIVE and 6.4-fold during mSIVE (Figure 20 A). Group mean expressions of OAS2 mRNA levels were elevated by 2.5-fold during AcSIV, 9.4-fold during AIDS and 8.6-fold during mSIVE (Figure 20 B). Mean expression levels of MxA mRNA were found to be the most upregulated in mSIVE (55.0-fold) compared to 16.5-fold in AcSIV and 9.4-fold in AIDS (Figure 20 C).

Since elevated expression of G1P3, OAS2, and MxA was found in the CNS, we also investigated whether these three mRNAs were upregulated systematically. Mean expression levels of G1P3 mRNA was the highest in the two AcSIV animals (70.0-fold upregulated) then lower again in AIDS non-SIVE (20.0-fold upregulated) and mSIVE (10.0-fold upregulated) relative to uninfected samples (Figure 20 A). Mean expression levels of OAS2 were found to increase by 24.0-fold in AcSIV and remain at similar levels in AIDS and mSIVE. (Figure 20 B). MxA was upregulated by approximately 8.0-fold in AcSIV and mSIVE and by 15.2-fold in AIDS (Figure 20 C). These data indicate that during SIV infection, expression of ISGs G1P3, OAS2, and MxA are elevated both in the CNS and in the Ax LN. Although the data for all three genes indicated a trend toward upregulation, statistical significance was not achieved.

.
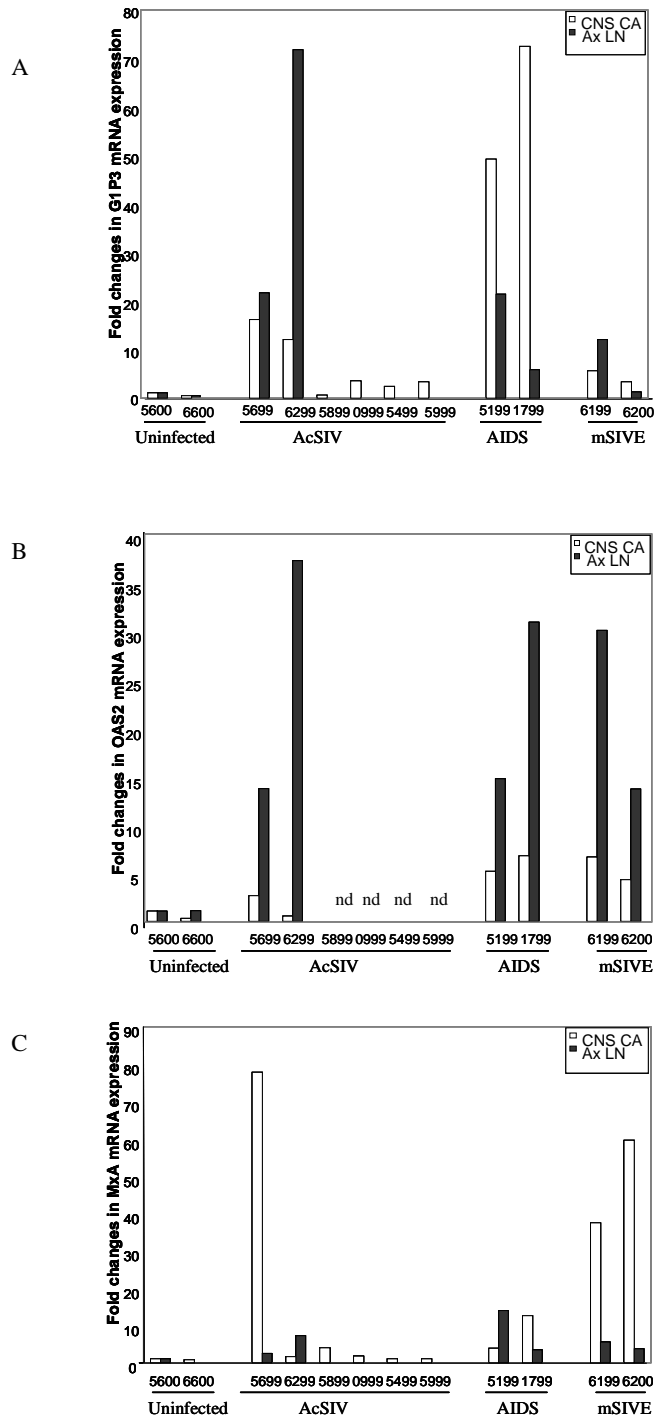
Figure 20 Differential expression of ISGs in CA and Ax LN

Upregulation of (A) G1P3 (B) OAS2, and (C) MxA mRNAs was observed by real-time RT-PCR. Each bar represents a single animal. Analyses of Ax LN total RNAs were not performed for AcSIV animals 5899, 0999, 5499, and 5999. Expression of OAS2 mRNA was undetectable in the CA tissue RNAs of the same four animals, which has been denoted by "nd". Taqman real-time RT-PCR was performed for OAS2 and MxA RNAs using 40 cycles of amplification with 18S as endogenous control and fold changes were calculated by the comparative C_T method. RNA from uninfected animal M5600 was used as a calibrator. For G1P3 sybrgreen real-time RT-PCR was performed with all other conditions kept the same as the assays for OAS2 and MxA mRNA

In the CNS, MxA mRNA levels were found to correlate with viral loads in plasma and in Ax LN as well as IFNα levels in Ax LN (r = 0.8, 0.7, 0.7 respectively with *p-values*<0.01). No correlations were observed between G1P3 and OAS2 mRNA levels and viral loads. Levels of all three ISGs in Ax LN were also not found to correlate with viral loads or with their respective expression levels in the CNS. Taken together, we found upregulation of ISGs G1P3, MxA, and OAS2 both in the CNS and in the Ax LN. Although these molecules have been shown to have antiviral activities, no correlations between elevation of these molecules and reduction of viral levels were observed. This suggests that high systemic levels of IFNα/β might stimulate the expression of ISGs in multiple tissue compartments. These ISG molecules, like MHCI, might be acting as markers for immune activation, both systematically and within the CNS.

**F.		Discussion**

In an attempt to identify differentially expressed genes in an unbiased manner in the CNS of SIV-infected rhesus macaques, we performed SAGE in the CA and GP regions of uninfected, acutely infected and mildly encephalitic animals. We focused mainly on changes in gene expression that occurred when local viral replication was absent or at low levels because none of the animals in our cohort developed encephalitis. Based on the SAGE data we found differential expression among tags that were putatively identified through *in silico* matching with human nucleotide sequence databases, as molecules related to immune-associated functions, signal transduction, metabolism/stress related pathways, cytoskeleton-associated, replication/transcription/RNA processing, protein synthesis/trafficking/degradation. However, attempts to confirm the identities of the genes from which these tags came were not highly successful despite intense efforts by three investigators within Dr. Reinhart's laboratory.

Follow-up studies on two tags, MHCI (differentially expressed between disease states) and Nrg (differentially expressed between microanatomic compartments) by RACE and sequence analysis confirmed their identities. However, overall the RACE procedure was found to be inefficient when looking for a perfect 14-nt sequence match in the tag region of the cloned and sequenced RACE product with the most homologous human sequence identified by BLAST analysis. This 100% homology across the 14-nt tag sequence was considered to be a logical criterion to confirm the identity of a gene represented by a specific tag. Among the PCR optimizations we attempted in order to increase the success of the RACE procedure, was the use of anchored primers with redundancy at either end, optimization of the annealing temperatures for PCR and attempt at a "hot start" PCR and a "touchdown PCR", all with similar inefficient results. Recent papers by Chen *et al*. [163,202], described a process called GLGI developed as a

high-throughput modified RACE method to identify SAGE tags accurately and efficiently. In our hands, however, the GLGI procedure was no more successful than RACE.

The difficulties we have encountered with analysis of SAGE might be due to several factors. In this paper, we were, for the first time, attempting to perform cross-species analyses comparing macaque-derived tags to human nucleotide sequence databases. Although, the macaque and human sequences are highly homologous, when looking for a specific 14-nt match, even a 1-nt difference might create difficulties in obtaining a correct tag-to-gene output. Technical issues such as errors due to either mutations during PCR or during sequencing although likely to be infrequent, cannot be ruled out and such errors can produce the wrong tag-to-gene output. Based on our results, we do not believe that the widely used SAGE tag-to-gene tool is an effective tool when performing cross-species analyses for the identification of the genes containing the SAGE tags. Therefore, until a macaque database is available for comparison, it will be necessary to conduct extensive confirmation studies using other experimental procedures. A recently published paper by Keime *et al.* describes a bioinformatics tool that facilitates cross-species analysis of SAGE tags [176]. The method is based on identifying transcript sequence pairs that are putatively orthologous between two species. How well this tool functions remains to be seen.

The limitations we encountered in obtaining a perfect 14-nt match at the 3' end of the RACE products relative to the most highly homologous human sequence obtained by BLAST analysis, might simply be due to the difficulties associated with performing PCR using such a short primer sequence which likely reduces the specificity of the amplification. It is possible that these genes were amplified by RACE because they were abundantly expressed in the tissues. Also this might be due to the homology of a short stretch of sequence in the gene with the 3' end

of the 14-nt primers causing these genes to be amplified. Even though most of our RACE products did not show a perfect 14-nt match at the tag region, these genes, like the SAGE tag-to-gene output, could also be roughly categorized into immune-associated, signal transduction, metabolism/stress, replication/transcription/RNA processing and protein synthesis/trafficking/degradation associated genes.

A seperate study in our laboratory points toward the possibility of mismatches within the 14-nt tag region when comparing macaque and human sequences. In this study cDNA libraries were created using the same mRNA pools that were used to generate the SAGE data. These libraries were then probed using the 14 bp tag sequence generated by SAGE. When the macaque sequence from the cDNA libraries were compared with the published human sequences, it was found that the tag region at the 3'UTR often did not have a perfect sequence homology between the two species (Dr. D. H. Kim, manuscript in preparation). Therefore, without a macaque sequence database that can be used to analyze SAGE tags, the method of tag-to-gene mapping will be an incomplete and suboptimal tool for gene identification.

The SAGE tags specific for MHCI and Nrg were confirmed as MHCI and Nrg by RACE and sequence analyses. Nrg is a postsynaptic protein kinase substrate that binds to calmodulin and is thought to play an important role in learning, memory, and neuroplasticity [188]. Nrg has previously been described to be microanatomic compartment specific. Represa *et al.* found Nrg to be expressed in the cerebral cortex but not in the thalamus or cerebellum of normal adult rats [189]. Nrg has been found to show region-specific upregulation in multiple SAGE CNS libraries (http://www.ncbi.nlm.nih.gov/SAGE). For example, Sui *et al.* found the same Nrg tag as ours (TGACTGTGCT) to be upregulated in cerebral cortex compared to thalamus and cerebellum [190]. In these studies Nrg was not differentially expressed in disease but within microanatomic

compartments and I followed up on this gene as a technical control. However, we have also shown for the first time the differential expression of Nrg in CA relative to GP in the rhesus macaque CNS.

The MHC I molecule is an important component of the immune system, particularly for antigen-specific T cell lysis of target cells via interactions between the T cell receptor and a MHC I /peptide complex on the target cell. In the normal CNS MHCI expression is low but is upregulated during an inflammatory response [203-205]. In the CNS, the potential candidates for MHCI expression are MF/Mgl, endothelial cells, astrocytes, oligodendrocytes, and neurons [203-206]. There are multiple reports of MHCI expression by brain MF/Mgl, particularly perivascular cells, in a variety of inflammatory conditions including HIV infection [207]. Both endothelial and perivascular cells are likely to be important for antigen presentation since they lie at the BBB through which both the virus and the immune cells must enter. In our studies we observed high levels of MHCI mRNA expression in the vascular/perivascular regions of the brain. However, simultaneous ISH/IHC detection analyses for CD68 revealed approximately 2-fold upregulation of MHCI$^+$/CD68$^+$ cells comparing uninfected and AcSIV animals, and a 4-fold upregulation comparing uninfected and mSIVE animals. Although there was upregulation, only approximately 8% of total cells were MHCI$^+$/CD68$^+$ even in the inflammatory mSIVE state. Nevertheless, with 8% of CNS cells in a given microanatomic compartment being potentially activated MO/MF/Mgl, there may be dramatic changes to the local immunological environment. ISH and IHC of subjacent sections showed that in uninfected tissues MHCI mRNA were expressed by endothelial cells with the expression levels becoming elevated during disease. Astrocytes, oligodendrocytes, and neurons have all been reported to be capable of MHCI expression particularly in *in vitro* studies, but also in some *in vivo* studies [203,205,206,208]. Neurons have been

reported to express MHCI mRNA but not necessarily a functional MHCI protein [206,209]. MHCI expression in certain subsets of neurons in developing and mature brain has been described as a requirement for CNS remodeling and synaptic plasticity [210,211] suggesting that this molecule has neurodevelopmental functions other than antigen presentation. Electrically silent neurons, such as those damaged by inflammation, have been shown to express MHCI, possibly to facilitate recognition by the immune system and subsequent elimination [206,212]. Therefore MHCI expressed by neurons could have other functions than the classic antigen presentation. In the studies described here, we have observed an increase in the percentages of neurons, and oligodendrocytes expressing MHCI, particularly during the acute phase of infection when replicating virus is not detectable locally. However systemic viral replication leading to increased plasma virus levels and immune factors could act on the CNS particularly at the vasculature due to higher numbers of infected MO trafficking through the BBB and entering the CNS.

The upregulation of MHCI and Nrg mRNA that we observed in our studies was much less than that predicted by the SAGE data. One reason for this could be that the macaque SAGE tag that were determined to be MHCI or Nrg by using a human sequence database, could represent multiple genes in the macaque genome, therefore showing a higher value of upregulation. The human MHCI gene has been found to be upregulated in other SAGE libraries including several of CNS origin (http://www.ncbi.nlm.nih.gov/SAGE). However, the particular tag representing the MHCI gene that we found to be upregulated in our SAGE libraries (AGAGGTTGAT) was not as abundant in the CNS as were some of the other tags that were predicted for the same gene (http://cgap.nci.nih.gov/SAGE/BrainViewer). This particular tag was present in brain medulloblastoma (SAGE brain medulloblastoma B 98 04 P494) and astrocytoma

libraries (SAGE brain astrocytoma grade II B H563) as well as non-CNS libraries created from AIDS-KS lesions (KS 48) and malignant carcinomas (SAGE breast carcinoma CL MDA435H48). Nrg has also been found to be upregulated in multiple CNS SAGE libraries. As already mentioned, Siu *et al.* [190] found Nrg to be 74-fold differentially expressed in the cerebral cortex compared to both the thalamus and the cerebellum. However, when they performed quantitative RT-PCR to confirm their results, the fold differences did not match the SAGE predictions showing 300-fold upregulation compared to the cerebellum and only 6-fold upregulation compared to the thalamus. Therefore, this lack of correlation between SAGE prediction of upregulation of a gene and the actual upregulation of the gene determined experimentally by other means is not limited to cross-species studies and has been observed by others as well. This could simply be the result of the difference in experimental approaches between SAGE and other quantitative assays. The 14-nt based "short" SAGE procedure has also been reported to result in some redundancies i.e. multiple matches for a single tag sequence, that are eliminated by the long SAGE approach [213] which, due to the longer tag sequence presumably allows for more accurate tag-to-gene identifications.

The CNS is a complex heterogeneous tissue where genes expressed at low abundance, can often be functionally important [214]. Also, due to the homeostatic balance that exists in the CNS, relatively small changes (i.e. 2-fold or less) are common and can be of great significance to altered brain functions [214]. Therefore, although we observed a small upregulation of MHCI mRNA expression by real-time RT-PCR and ISH, it is possible that this nevertheless is biologically significant. There is evidence that SIV enters the CNS as early as 7 dpi but no productive infection is seen by 14 dpi. Re-emergence of virus, either by reactivation of latently infected cells or by less controlled trafficking of infected MO through the BBB, occurs during

AIDS. In our cohort, at 14 dpi, we see evidence of MHCI upregulation. It is possible that the MHCI upregulation that we see is a marker for a general immune activation. In the CNS, MHCI mRNA levels were found to be elevated during acute infection and remained high in AIDS and mSIVE, suggestive of a persistent state of immune activation. In the CNS a number of the cells expressing high levels of MHCI mRNA are endothelial, located at the junctions of the BBB. I found MHCI levels in the CNS correlated with viral load in blood and Ax LN suggesting that virus in the periphery could potentially affect the CNS endothelium and cause immune activation even though no replicating virus is observed in the CNS. Both virus and/or cellular factors in the blood could potentially affect the CNS endothelium due to its location at the interface of the periphery and the CNS. Cellular factors that can affect the expression of MHCI locally and systematically are cytokines and cytokine-induced genes such as ISGs. The SAGE predicted genes as well as several of the RACE products were found to be metabolism/stress related suggesting that there is some immune activation and stress present in the CNS as early as 14 dpi. Therefore, after initial viral entry, some level of immune activation might persist in the CNS, which then increases during AIDS when peripheral immune control is lost. This is also validated by the fact that MHCI is upregulated in the majority of the cell populations within the CNS even when local viral replication is absent. During this phase, systemic viral loads are very high and it is conceivable that at least some of the CNS immune activation is a result of a widespread systemic immune activation.

Further proof of a state of immune activation of the CNS comes from our studies with interferons and ISGs. In characterizing the immune environment of the CNS, we found that the levels of proinflammatory cytokines were undetectable in AcSIV, AIDS non-SIVE and mSIVE animals. In addition, we did not observe detectable levels of IFNα mRNA in the CNS. It is

possible that the expression levels of IFNα mRNA in the CNS were simply very low in the animals studied here and below the limits of detection in our assays. In a recent study, Roberts *et al.* [178] examined macaques infected with SIVmac182 that were CD8-depleted to induce rapid development of encephalitis. They detected IFNα mRNA in the CNS during acute infection, but observed no changes in the expression levels between acute, asymptomatic and encephalitic disease states. In this same study elevated levels of ISGs were found in the CNS even in the absence of changes in the local IFNα expression levels. However plasma levels of IFNα mRNA did show an increase. Therefore, systemic immune activation can potentially cause an activation and upregulation of immune molecules in the CNS. Although the data from our IFNα and β real-time RT-PCR assays were uninterpretable, ISG mRNAs MxA, OAS2, and G1P3 were upregulated suggestive of an ongoing interferon-mediated immune response.

Mx proteins are interferon induced GTPases that appear to detect viral infection by sensing the presence of nucleocapsid-like structures and sequestering them so that assembly of new viruses is inhibited [199]. In humans there are two distinct Mx proteins, MxA and MxB and only MxA has been ascribed with antiviral activity [199]. The expressions of Mx proteins are induced by IFN-α/β via the Jak-Stat signaling pathway and not directly by double stranded viral RNA [200]. The MxA protein has been found to have antiviral activity against multiple members of the *Orthomyxo*, *Paramyxo*, *Rhabdo*, and *Bunyaviridae* families [200]. A study by Abel *et al.* [215] have found high viral loads associated with increased MxA levels in both acute and chronic infection suggesting that elevated levels of MxA were unable to control viral replication. Bosinger *et al.* also found robust induction of ISGs including MxA, OAS2, and G1P3, without any reduction in viral loads in the PBMC of SHIV89.6P infected cynomolgus macaques [216]. I observed a similar pattern in our studies where elevated levels of MxA were present in spite of

94

high viral levels (Figure 20 C). Also, with the exception of one AcSIV animal, the levels of MxA in the CNS were higher during mSIVE when replicating virus was present (Figure 20 C). The MxA mRNA levels in the CNS were strongly correlated to viral loads in plasma and Ax LN as well as to IFNα levels in Ax LN. Therefore, in our SIV infected macaques, MxA upregulation in the CNS could be due to high levels of virus and IFNα in the blood. As in other studies, MxA was present in spite of high viral loads possibly acting as a marker for IFN-mediated immune response.

The 2'5'OAS is constitutively expressed in normal cells in an inactive form and can be upregulated by IFN-α/β, IFN-γ, and viral dsRNA [201]. In humans, three forms of OAS (OAS1, 2, 3) as well as several OAS-like (OASL) or OAS-related proteins (OAS-RP) have been described [201]. The 2'5'OAS catalyzes the synthesis of short 2'-5' oligoadenylates and activates latent endoribonuclease RNAseL which then degrades the viral RNA. The antiviral activities of OAS proteins have been well described for multiple viruses including Herpes simplex virus and the Encephalomyocarditis virus [200]. In our studies I observed high levels of OAS2 in the Ax LN in spite of the high viral load. The upregulation was lower in the CNS and a correlation with plasma or Ax LN viral loads was not observed. HIV has been shown to inhibit the RNAseL pathway by inducing the synthesis of an RNAse L inhibitor RLI [200]. It is therefore possible that although OAS2 is upregulated, the virus causes a block further down in the pathway thereby neutralizing any antiviral effects. HIV-1 Tat protein and TAR RNA has also been described to inhibit PKR, another important ISG molecule [200,215]. Therefore it is conceivable that SIV gene products can inhibit antiviral actions of ISGs and are therefore able to persist in the presence of IFN-α/β mediated immune response.

G1P3 is an ISG whose mode of action is not well understood. It has been found to be upregulated during Hepatitis C virus infection and has been shown to have some antiviral activities against HCV [198]. In related studies in our laboratory we have observed an upregulation of G1P3 in the lung tissue during SIV infection (Dr. D.H.Kim, unpublished observations). A study by Baca *et al.*, demonstrated that whereas OAS and MxA could be induced by both HIV and IFNα, G1P3 could be upregulated only by IFNα and not directly by HIV [217]. In our studies we observed upregulation of G1P3 in the CA particularly in the AIDS non-SIVE animals. In the Ax LN of two AcSIV animals and two AIDS animals, we observed high G1P3 mRNA levels that correlated with high levels of IFNα in these same animals (data not shown). However, no clear pattern was observed comparing Ax LN IFNα levels with CA G1P3 levels.

Comparing our observations with other studies it seems that the IFN-mediated immune response can be systemic, occurring when systemic viral loads are high, which can cause the cells in the CNS particularly those at the BBB to be affected. In accordance with this, we observed cells at that region, endothelial cells and perivascular MF, expressing high levels of MHCI mRNA, possibly as a marker for immune activation. In fact, MHCI has previously been found to be upregulated by IFNα, IFNβ, and IFNγ and described as an ISG [218,219]. In addition, we observed high levels of HLA-DR positive cells in the perivascular regions of the CNS suggesting they are in an activated state. The MHCI levels in the CNS were also found to correlate strongly with viral loads in plasma and Ax LN.

In summary, using SAGE and follow-up approaches, we have identified MHCI to be upregulated both in AcSIV and mSIVE brain tissues. We have further characterized MHCI to be expressed by endothelial cells irrespective of disease states but upregulated particularly during acute infection by MF/Mgl, neurons, astrocytes, and oligodendrocytes. These data suggest that

the CNS can be in a state of immune activation during the acute phase of infection even when local viral replication is absent or at low levels. These data also point toward a strong systemic interferon-mediated immune response early in infection can cause a persistent immune activation of the CNS resulting in local immune-mediated damage throughout the course of infection. In fact, a positive correlation has been described between the severity of the acute response and a more rapid progression to AIDS [220] and HAD [221] suggesting that while a strong early immune response can control the virus, it can cause a state of low level chronic immune activation that can lead towards faster and more severe CNS damage. These findings indicate that early, potent, suppression of viral replication throughout the body might potentially inhibit the development of virus-mediated neuropathology later on.

IV. Microarray analysis of differentially expressed genes in the CNS of SIV infected rhesus macaques

The following section contains data from microarray analyses of CNS tissues from the same macaque cohort infected with SIV/DeltaB670 studied by SAGE, and of MF and Mgl cells isolated from pigtailed macaques and co-infected *in vitro* with SIV 17E-Fr plus SIV/DeltaB670 (kindly provided by Dr. Joseph Mankowski, Department of Comparative Medicine, Johns Hopkins University). Follow-up studies involving stress-related genes found to be upregulated by microarray experiments are also included in this section.

The macaque cDNA microarray that was used for these experiments was developed by Dr. Todd Schaefer (at the time in Dr. Reinhart's laboratory).

A.   Preface

As a second approach to studying differential gene expression, I used an immunologically focused macaque sequence based microarray that was developed and validated in our laboratory. The following section describes data obtained from microarray hybridizations using SIV-infected CNS tissue RNA as well as *in vitro* infected MF and Mgl cell populations. In addition to confirmation of the SAGE data (MHCI upregulation) and the upregulation of RACE products (described in Section III E) the data obtained from microarray experiments further point toward immune activation of the CNS (upregulation of stress products, chemokines, and G1P3) during SIV infection.

B.   Abstract

DNA microarray technology permits the analysis of the expression levels of thousands of genes simultaneously. Although fast and efficient, a major limitation of this technology is that gene expression levels can only be assessed for the genes that are spotted on the array, that is, discovery of novel genes is not possible. To identify differentially expressed genes in the SIV infected rhesus macaque CNS, we used an immunologically focused microarray. Currently there are no macaque sequence specific microarrays that are commercially available but our laboratory has developed an immunologically focused custom microarray containing 256 macaque-specific genes. These genes included cytokines, chemokines and chemokine receptors all of which might have an important role to play in the SIV-associated disease process. The array also included macrophage, dendritic cell and lymphocyte related genes as well as genes involved in innate immunity and adhesion. we probed this array with both CNS tissue RNA from different disease states and RNA from *in vitro* infected primary MF and Mgl. Upregulated genes included chemokines MCP-1, 2, 3, and MIP1α, and ISG G1P3. Products amplified by RACE (described under section III E) included multiple stress-related genes, which were also upregulated. These genes could potentially play a role in the SIV induced pathology of the CNS.

C.   Introduction

DNA microarray technology allows the analysis of the expression levels of thousands of genes simultaneously [171,172]. The array consists of a highly ordered matrix of hundreds to thousands of different DNA sequences immobilized on a solid surface. In this method, a labeled cDNA target is hybridized to a DNA microarray and the gene expression levels assessed by quantifying hybridization intensities. Although results obtained from microarray hybridization experiments have been confirmed by other techniques [173] and the procedure is fast and efficient, commercially available arrays can be expensive and the bioinformatical analysis can be time consuming and complicated. A major limitation is that gene expression levels can be assessed only for the genes that are spotted on the array, that is, discovery of novel genes is not possible by this method. Also DNA arrays have been shown to lack the sensitivity to detect low abundance mRNAs particularly in complex tissues [174]. Furthermore, different protocols, reagents, and analyses used in different studies make it difficult to compare microarray data between laboratories.

Microarray technology has been used to study HIV/SIV infections and specifically, Roberts *et al*., has used this technology to study SIV infection of the CNS in acute phase and severe encephalitis [74,178]. However, all studies published so far have utilized commercially available human sequence based arrays.

To investigate differential gene expression in SIV infected macaques, we used an array that was spotted with 256 macaque cDNAs. This array was developed and validated in our laboratory and the cDNAs spotted on it consisted of genes involved in the immune response. We attempted to understand the SIV induced immune response by probing this small but functionally focused array with cDNAs synthesized from uninfected, SIV infected AcSIV, and mSIVE CNS

tissue RNA samples. We also used this array to investigate differential gene expression patterns in macaque MO and MF that were *in vitro* infected with SIV/17E-Cl or SIV/17E-Fr. In addition to the immunity-associated genes, 60 cDNAs that were amplified by the RACE method (described in Section III E,) were also spotted on this array.

In SIV infected CA tissue we found MHCI and B2M to be upregulated both in AcSIV and mSIVE relative to uninfected samples. In the *in vitro* infected cell populations, we found upregulation of chemokines MCP-1, MCP-2, MCP-3, and MIP1α, and ISG G1P3. Other upregulated genes included cDNAs that were amplified by RACE (Section III E) and spotted on the array. Many of the upregulated RACE products were stress-related genes with some belonging to the mitochondrial oxidative phosphorylation (OxPhos) pathway. In addition, RACE amplified cDNAs of unknown functions, for example, IMAGE clone 3856788 was also upregulated as a result of SIV infection. All the genes identified here could potentially play a role in SIV induced neuropathogenesis.

D. Materials and Methods

Animals and tissue processing

Animals and tissues used in this study are described under Section II D.

In vitro **infection of cells**

In vitro infected cells were received from Dr. Joseph Mankowski, Department of Comparative Medicine, Johns Hopkins University. Mgl were isolated from the CNS of pigtailed macaques (*Macaca nemestrina*), cultured *in vitro*, infected with SIV/17E-Fr or SIV/17E-Cl virus strains, and harvested on 7 dpi. MOs were isolated from the blood of pigtailed macaques and cultured and differentiated *in vitro*. These cells were infected with SIV/17E-Fr or SIV/17E-Cl virus strains, and harvested on 3 and 7 dpi.

Microarray hybridization

cDNA was reverse transcribed from cell culture total RNA using the array 350p random prime kit (Genisphere, Hatfield, PA) using 0.5 μg of DNA. Briefly, total RNA extracted from tissues using Trizol, was combined with random RT primer and nuclease free water to a final volume of 11μl on ice, heated at 80$^{\mathrm{o}}$C for 10 min, and then ice for 2 min. This reaction was then combined with 5X Superscript reaction buffer, dNTP mix, 0.1M DTT and Superscript II enzyme. Reverse transcription was performed at 42$^{\mathrm{o}}$C for 2 hrs. The reaction was stopped by adding 3.5μl of 0.5M NaOH/50mM EDTA and incubating at 65$^{\mathrm{o}}$C for 10 min. The reaction was then neutralized with 5μl of 1M Tris-HCl, pH 7.6. The cDNA synthesis was purified using the QIAQuick PCR Purification kit (Qiagen, Valencia, CA) and the cDNA was denatured at 90-95$^{\mathrm{o}}$C for 10 min,

then ice for 10 min. Cy5 (green) or Cy3 (red) were ligated onto cDNA using T4 DNA ligase. Ligation reactions were incubated for 2 hrs at room temperature and the reaction was stopped with 7μl of 0.5M EDTA and incubated at 65°C for 10 min. The ligation mixes were combined with 10μl of 10mM Tris-HCl (pH 8.0)/1mM EDTA, purified using an YM-30 column and centrifuged at 14,000 rpm for 2 min. A hybridization mixture including Cy3 and Cy5 capture reagents, CotI DNA and antifade hybridization buffer were incubated at 80°C for 10 min, 50°C for 20 min and the finally at 50°C for 3 hr. Washes were performed in graded SSC solutions for 12 min each. Microarray slides were then centrifuged in a 50 ml conical tube at 1,000rpm for 2 min to dry. Slides were scanned using the Affymetrix 417 array scanner on both the Cy3 and Cy5 wavelengths. Quantification of the pixels per spot in images for Cy3 and Cy5 was performed using the software package Imagene v5.0 (Biodiscovery, El Segundo, CA) and data normalization and manipulation was performed using Microsoft Excel. The data were statistically analyzed using one-way ANOVA and pairwise T test comparisons.

IHC

IHC was performed essentially as described in Section III D. Anti-Cyt C, (clone CTC05, Chemicon, Temecula, CA) and anti-HSP70 (rabbit Ig, Upstate, Lake Placid, NY) antibodies were used at 1:50 dilution. Retrievogen B (BD Pharmingen, San Jose, CA) was used for microwave antigen retrieval and tissues were blocked for 1 hr at room temperature in 1X PBS supplemented with 1.6% normal horse serum (Dako Corps, Carpinteria, CA). Antigen-positive cells were detected using the Super PicTure kit (Zymed, San Francisco, CA) using 3,3'-diaminobenzidine (DAB) as the substrate.

E.   Results

Microarray analyses of CA tissue

A total of 11 RNA samples (2 uninfected, 7 AcSIV, and 2 mSIVE) were extracted from the CA region of the macaque CNS. The macaque microarray was probed with RNA from 7 AcSIV and 2 mSIVE samples, each compared to a reference sample. The reference in each case comprised of a pool of the 2 uninfected RNA samples. A gene was defined as differentially expressed if it was found to be up- or down- regulated by at least 2-fold. The 2-fold cut off is standard for microarray analysis and has been well established.

Comparing AcSIV to uninfected CA, we found MHCI and B2M to be upregulated by 3.4-fold and 3.0-fold respectively. Another cDNA that was upregulated by 2.0-fold was a RACE product of unknown function (IMAGE Clone 3856788) (Table 8 A). In AcSIV, 5 genes were found to be upregulated by >2.0-fold relative to mSIVE. Three of these were MHCI, B2M, and IMAGE Clone 3856788, i.e. same genes that were upregulated in the AcSIV versus uninfected comparisons. When the sequence for IMAGE Clone 3856788 was BLAST searched, the most homologous gene of known identity was Malat-1 (metastasis associated in lung adenocarcinoma transcript 1) (86% homology). Malat-1, another RACE product, was also found to be upregulated by 2.2-fold (Table 8 A). Malat-1 is a non-coding RNA that is believed to act as a prognostic marker for metastasis in non-small cell lung cancer [222]. Expression of Malat-1 has been described in multiple tissue compartments including the CNS [222]. No genes were found to be upregulated more than 2 fold in mSIVE versus uninfected or mSIVE versus AcSIV groups.

Microarray analyses of in vitro SIV-infected cell populations

Mgl isolated from the CNS of two pigtailed macaques were infected with SIV strains 17E-Cl and 17E-Fr, and harvested at 3 and 7 dpi. MO were also isolated from the blood of these animals, cultured *in vitro*, and infected and harvested similar to the Mgl population. Total RNA isolated from these samples was used to probe the microarray. In the Mgl samples G1P3 was the only cellular gene that was found to be upregulated by greater than 2-fold in SIV/17E-Fr and SIV/17E-Cl infected cells relative to mock-infected cells (Table 8 B). As described in the previous section, G1P3 was found to be upregulated in the CNS and Ax LN possibly as a surrogate marker for IFNα-mediated immune response.

In the MF populations, multiple genes involved in immune function and stress-response pathways were found to be upregulated by greater than 2-fold (Table 8 C). These genes included MHCI, G1P3, calmodulin 1 and 2, chemokines such as MCP 1, MCP 2, MCP 3, MIP1α, and PARC (pulmonary and activation regulated chemokine), as well as stress-related genes such as mitochondrial dehydrogenase and Hsp70. Genes that were unknown or of undefined functions such as the IMAGE clone 3856788 and Malat-1, were also found to be upregulated. The cell population infected with the more virulent strain SIV/17E-Fr showed a larger number of genes that were upregulated by >2-fold compared to the population infected with the less virulent strain SIV/17E-Cl (Table 8 C).

Therefore, the results from the microarray experiments showed an upregulation of genes involved in immune activation, signal transduction, and stress. These genes are likely to play a role in development of neuropathology.

Table 8 Differentially expressed genes by microarray analyses

A

Genes upregulated in CA tissue[a]	AcSIV/mSIVE
IMAGE Clone 3856788[RACE]	2.5
B2M	2.4
Malat-1[RACE]	2.2
MHC I	2.2
Mtb 16S rRNA	2.0

Genes upregulated in CA tissue[a]	AcSIV/Uninfected
MHC I	3.4
B2M	3.0
IMAGE Clone 3856788[RACE]	2.0

B

Genes upregulated in Mgl[b]	17ECl Mgl/mock
SIV LTR	10.5
G1P3[RACE]	2.3

Genes upregulated in Mgl[b]	17EFr /Mgl/mock
SIV LTR	21.9
G1P3[RACE]	2.3

Genes upregulated in MF[c]	17EFr MF/mock
SIV LTR	17.4
α-Tubulin	3.1
Mitochondrial dehydrogenase[RACE]	3.1
MCP-1	3.0
MCP-3	3.0
MCP-2	2.9
Heat shock protein 70[RACE]	2.8
PARC	2.7
Mitochondrial genomic DNA[RACE]	2.7
G1P3[RACE]	2.6
GAPDH	2.6
Macrophage inhibitory factor	2.5
S100 Ca binding protein[RACE]	2.3
Bleomycin hydrolase[RACE]	2.2
IMAGE Clone 3856788[RACE]	2.2
Mtb 16S rRNA	2.2
Calmodulin-1	2.2
Eotaxin	2.2
MHC I	2.1
MIP-1α	2.1
FcER1-g	2.1
Calmodulin-2	2.0
CD16	2.0
Heat shock binding protein	2.0
Malat-1[RACE]	2.0
GAPDH 40	2.0

C

Genes upregulated in MF[c]	17ECl MF/mock
SIV LTR	13.0
Mitochondrial dehydrogenase[RACE]	2.5
Mtb 16S rRNA	2.3
α-Tubulin	2.3
MCP-1	2.3
Heat shock protein 70[RACE]	2.3
GAPDH	2.2
IMAGE Clone 3856788[RACE]	2.2
Bleomycin hydrolase[RACE]	2.2
MCP-3	2.1
MCP-2	2.1
MIP-1α	2.1
Macrophage inhibitory factor	2.0

[a] Genes upregulated >2-fold in CNS CA tissue infected with SIV/DeltaB670

[b] Genes upregulated >2-fold in Mgl *in vitro* infected with SIV 17E Cl and SIV 17E Fr

[c] Genes upregulated >2-fold in MF *in vitro* infected with SIV 17E Cl and SIV 17E Fr

[RACE] RACE products found to be upregulated by microarray

MHCI upregulation observed by microarray hybridizations

Since stress related products were upregulated *in vitro*, we investigated whether the upregulation of these products could also be observed *in vivo*. we performed IHC on SIV infected CNS tissues for detection of some of these products. From the microarray experiments we observed upregulation of stress related genes that belonged to the mitochondrial OxPhos pathway. These genes are listed in Table 5. Previously we had observed an upregulation of MHCI and ISGs in the CNS even with very low levels of local viral replication. In order to find out whether this immune activation was also characterized by mitochondrial damage, we performed immunostaining for Cyt C, a marker for mitochondrial leakage. We also stained for Hsp70, a stress related gene that was found to be upregulated by microarray. In SIVE tissues intense punctate Cyt C staining was observed at the perivascular as well as parenchymal regions. In comparison, non-SIVE tissues showed staining mostly restricted to the perivascular regions (Figure 21 i-ii). HSP70 expression was observed in both SIVE and non-SIVE tissues in the perivascular regions. The expression levels in this case were not significantly higher in SIVE compared to non-SIVE (Figure 21 iii-iv). For the Cyt C and Hsp70 IHC experiments, 2 SIVE and 2 non-SIVE animals were used. The tissues used were paraffin embedded sections obtained from Dr. Clayton Wiley. With our tissues, both cryopreserved and paraffin embedded, the Cyt C and Hsp70 antibodies did not work. This could have been due to the different tissue fixation protocols that are used by different laboratories. Unfortunately, as a result of this technical difficulty we were not able to compare the expression of these markers in our AcSIV tissues. Therefore, although evidence of stress was observed in SIVE versus non-SIVE tissues, whether low levels of stress was present in acute phase of infection could not be determined.
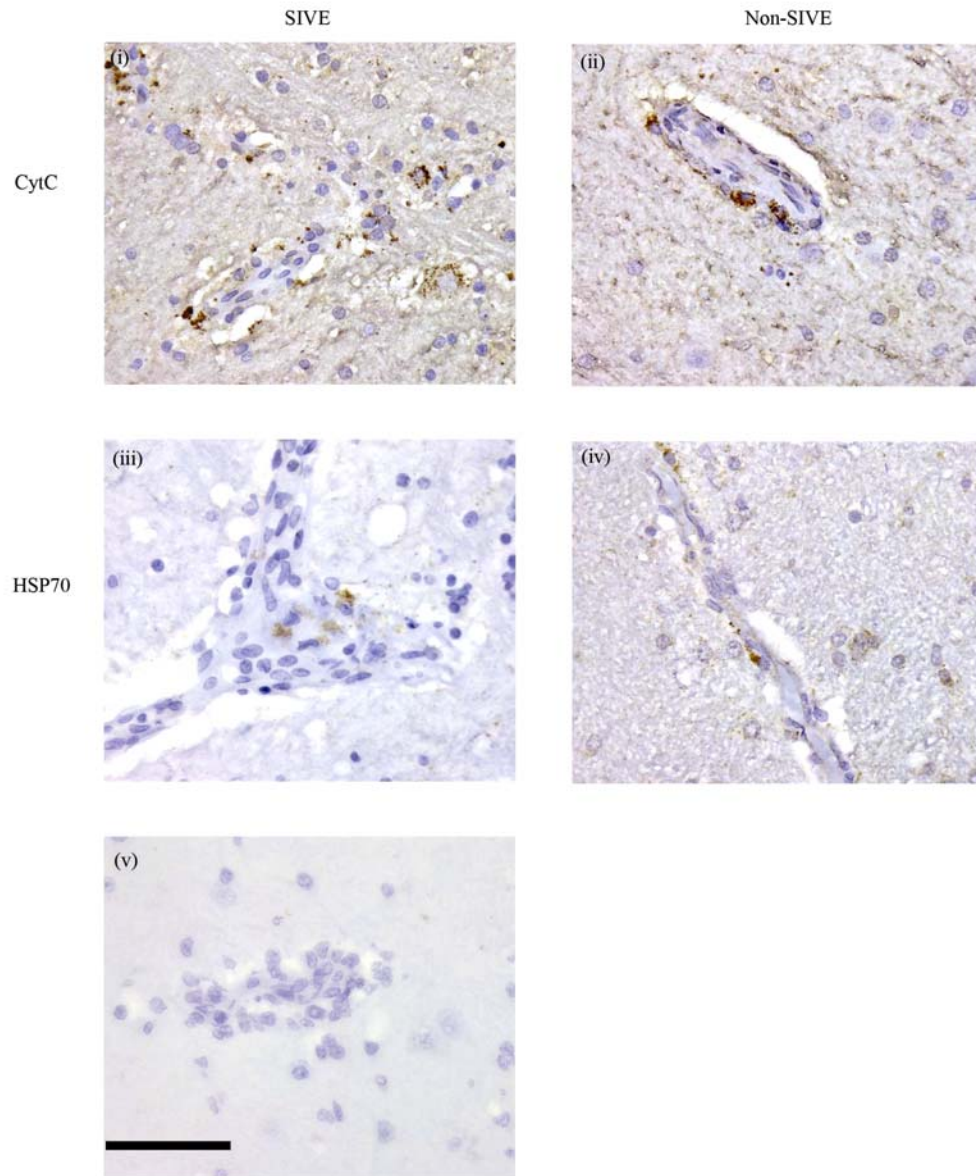
Figure 21 Expression of Cyt C and Hsp70 in SIVE and non-SIVE tissues

IHC was performed in SIVE and non-SIVE tissues using antibodies to CytC and Hsp70. CytC was found to be upregulated in the CNS of SIVE animals (i) compared to non-SIVE animals (ii). Expression of HSP70 was not elevated in SIVE (iii) compared to non-SIVE (iv) tissues. (v) shows tissue section stained with isotype control antibody. Size bar 50 μm. Original magnification 400x.

F.   Discussion

In this section we focused on using microarrays for studying differential gene expression in the CNS of SIV infected macaques. We used an immunologically focused macaque-specific microarray for these studies. The main objective of these studies was to identify differentially expressed genes in the CNS or CNS derived cells of SIV infected rhesus macaques. Another purpose was to confirm the data we had already obtained by SAGE. To this end, we found MHCI, the tag predicted to be upregulated by SAGE and then successfully identified by RACE, to be 2-fold or greater upregulated by microarray analysis in the CA tissue. In addition to the SAGE data confirmation, we attempted to determine whether the "mismatched" RACE products that were amplified using SAGE tag specific primers were indeed differentially expressed in these tissues. Some RACE products that were found to be upregulated in the CA tissue were stress related and belonged to the mitochondrial OxPhos pathway.

From the experiments with *in vitro* infected Mgl, a >2-fold upregulation was found only for G1P3. G1P3 is an ISG induced as part of an IFNα mediated immune response. We have found this gene to be upregulated both in the CNS and the Ax LN by real-time RT-PCR (described in Section III E). The microarray data lends confirmation to my previous findings.

In the MF population that were infected *in vitro* with SIV/17E-Fr, we found 27 genes that were upregulated by greater than 2-fold. These included MHCI, G1P3, calmodulin 1 and 2, chemokines, and mitochondrial stress-related products. The chemokines MCP-1, 2, 3, Mip1α were found to be upregulated in the MF population by >2-fold. Chemokines play an important role in HIV/SIV infection. Chemokine receptors and ligands CXCR4 and α-chemokines SDF-1α/β/γ, CCR5 and β-chemokines RANTES, MIP1α/β, MCP-1, and CX3CR1 and Fkn [223] have

been described to be important in HIVE/SIVE. In SIV infection, MCP-1 has been found to be upregulated both in CSF and within the brain parenchyma before encephalitic lesions appeared [37]. MF, Mgl, and astrocytes can secrete chemokines MIP1α and MIP1β, which are involved in stimulating MO/MF migration and retention [224] and therefore can play an important role in the development of HIV/SIV associated neuropathology.

The fact that MF showed more differentially expressed genes than the Mgl might not be unusual. Mgl are long-term residents of the CNS with a low turnover rate [86,149]. Mgl can be infected by HIV and SIV although, at least in the SIV model, perivascular MF are considered to be the central cell population that determines encephalitis [31]. MOs are cells that can get infected at the periphery traffic to the CNS and thus carry the virus into the CNS. Activated MFs produce proinflammatory cytokines, reactive oxygen species and neurotoxins, cause further dysregulation of the local cytokine chemokine balance, and can activate the resident Mgl [86]. Therefore it is possible that MF population will show a larger number of differentially expressed genes. However, the MF and Mgl are *in vitro* infected populations and the response of these cells to productive or non-productive infection *in vivo* might be different.

The microarrays probed with RNA extracted from CA tissue showed few genes that were upregulated >2-fold. Whereas tissue studies portray the *in vivo* disease process better, we also have to take into account that in a complex tissue of mixed cell populations, it might be more difficult to detect large changes in the expression levels of genes that might be taking place within a small population of cells within that tissue. In fact, in a complex heterogeneous environment like the CNS, genes with low abundance often have significant functions and even minute alterations in the gene expression levels can cause drastic changes in the CNS homeostatis[214]. Our microarray data are consistent with another study by Roberts *et al.*, in which

differential gene expression of the macaque CNS was addressed by microarray analysis [178]. This study also found similar levels of upregulation of MHCI and B2M in SIVE. Another study by the same group addressed the acute peak viremia period and again observed similar levels of MHCI upregulation [74]. Stress related genes were found to be upregulated in SIVE and a number of ISGs including G1P3 were found to be upregulated in both the acute phase and SIVE. Therefore our macaque microarray data agreed with other studies of neuroAIDS where human nucleotide sequence based arrays were used. This also indicates that elevated expression levels of immune associated molecules and stress markers are observed in other models of SIV encephalitis as well.

HIV-1 gp120 has been shown to cause oxidative stress in CNS cells [225,226]. Evidence of oxidative stress has also been noted in the CNS tissue and CSF of patients with HAD [96,227]. By microarray analysis we found stress related genes, particularly those belonging to the mitochondrial OxPhos pathway, to be upregulated. In tissues, mutations in mitochondrial DNA can cause an upregulation of the OxPhos pathways. OxPhos genes are believed to be upregulated in order to compensate for additional energy requirements that the cell might have as a consequence of coping with damage [228,229]. Dysregulation of Oxphos genes have been reported in mitochondrial myopathy, encephalopathy, lactic acidosis, and stroke-like episodes (MELAS). Mitochondrial damage can cause Cyt C release that eventually results in apoptosis [230 231]. In fact apoptotic pathways induced by HIV-1 have been shown to be associated with mitochondrial damage as measured by mitochondrial release of Cyt C [147,232-234]. Mitochondrial damage has also been reported to cause MHCI upregulation. These cells are then targeted by the immune system and destroyed [235]. Heat shock proteins are molecular chaperones that are produced by cells in response to stress. Hsp70 has been shown to act as an innate antiviral factor and diminish viral

replication in MFs [236]. In primary CNS cultures Hsp70 was shown to not be associated with protection against HIV gp120 mediated damage [237]. To assess oxidative stress and mitochondrial damage in SIV infected CNS tissues, we performed IHC using the markers Cyt C and Hsp70. These experiments were performed on 2 SIVE and 2 non-SIVE tissues where both sets were paraffin embedded and obtained from the laboratory of Dr. Clayton Wiley. However, the antibodies to CytC and Hsp70 could not be optimized to work in either cryopreserved or paraffin embedded sections obtained from our cohort of macaque. The reason for this could be the different protocols used by different laboratories to fix tissues post-necropsy. This technical hurdle prevented us from determining the expression levels of the stress-related genes in AcSIV animals with minimal viral replication where I have previously observed signs of immune activation. However, we found evidence of mitochondrial damage and leakage in SIVE compared to non-SIVE animals as determined by Cyt C IHC. The Hsp70 was less easily interpretable and it did not seem to indicate elevated expression levels in SIVE tissues relative to non-SIVE tissues. These data, in addition to confirmation of the microarray experiments, indicate that as in the case of HIV-1 infection, SIV infection of the CNS shows evidence of oxidative stress and mitochondrial damage.

V. Final Discussion

After more than 20 years since it was first described, HIV continues to be a raging epidemic worldwide with thousands of new people infected each day. A majority of HIV infected people develop some sort of neurological pathology although encephalitis and symptoms of dementia only develops in about 25-30% of those infected [1]. The focus of this body of work was the identification of differentially expressed genes in the CNS of SIV infected macaques in order to systematically characterize the CNS immune environment during such an infection.

The study of differential gene expression was approached by SAGE and microarray techniques. Although it was challenging to identify the macaque SAGE tags using human sequence databases, I identified MHCI as being differentially expressed by both techniques. The MHC class I molecule is an important component of the immune system particularly for antigen specific T cell lysis of target cells via interactions between the T cell receptor and a MHC class I peptide complex on the target cell. In the normal CNS MHCI expression is low but is upregulated during an inflammatory response. In the CNS, the potential candidates for MHCI expression are MF/Mgl, endothelial cells, astrocytes, oligodendrocytes, and neurons [203-206]. There are multiple reports of MHCI expression by brain MF/Mgl, particularly perivascular cells, in a variety of inflammatory conditions including HIV infection [207]. Both endothelial and perivascular cells are likely to be important for antigen presentation since they lie at the BBB interface through which both the virus and the immune cells must enter. In our studies I observed high levels of MHCI mRNA expression in the vascular/perivascular regions of the brain (Figure 9). Simultaneous ISH/IHC detection analyses for CD68 revealed approximately 2-fold higher proportion of MHCI$^+$/CD68$^+$ cells in AcSIV relative to uninfected, and a 4-fold higher

proportion in mSIVE relative to uninfected (Figure 12 and 13). Even in the inflammatory mSIVE condition MHCI+/CD68+ double positive cells accounted for approximately only 8% of total cells. Although 8% activated CD68+ cells could be of biological significance, this finding indicated that other CNS cell types were expressing much of the MHCI mRNA during SIV infection. ISH and IHC of subjacent sections showed that in uninfected tissues MHCI mRNA was being expressed by endothelial cells with the expression levels becoming elevated during disease (Figure 14). Astrocytes, oligodendrocytes, and neurons have all been previously reported to be capable of MHCI expression particularly in *in vitro* studies, but also in some *in vivo* studies [203,205,206,208]. In fact, in the CNS, the MHCI molecule has been described to play roles other than in the classically described antigen-presentation pathway. MHCI expression in certain subsets of neurons in both the developing and the mature brain can function in CNS remodeling and synaptic plasticity [210,211]. In addition, non-functional electrically silent neurons, such as those damaged by inflammation, have been shown to express MHCI, possibly to facilitate recognition by the immune system and subsequent elimination [206,212]. Therefore the elevated levels of MHCI that was observed in our study might have functions that are novel. In this study I observed an increase in the percentages of neurons, and oligodendrocytes expressing MHCI, particularly during the acute phase of infection when replicating virus was not detectable locally (Figure 15). The upregulation of MHCI in the CNS could not be attributed to a systemic upregulation of MHCI as no correlations between the two were observed (Figure 8 A, C). However systemic viral replication leading to increased plasma virus levels and immune factors could conceivably act on the CNS particularly at the vasculature where a lot of the MHCI expression was observed.

To define the CNS immune environment particularly in the absence of viral replication, we investigated the expression of cellular factors that might be upregulated either locally or

systematically as a result of SIV infection and also have an effect on the observed MHCI upregulation. Expressions of proinflammatory cytokines, (IL-6, IL-12, IL-2, TNFα) interferons (IFNα, IFNβ, IFNγ), and TLR2 were not detectable or the data were not interpretable, in the CNS CA. (Table 7) IL-1β mRNA was detectable but was not differentially expressed (Table 7). In contrast, TLR-4 showed a slight but statistically significant upregulation when comparing uninfected and AcSIV animals.(Table 7).

Type I interferons, IFNα and IFNβ, are antiviral molecules that are expressed early after infection. They activate innate and acute phase response immune molecules and can cause upregulation of MHCI [194]. Although we were unable to interpret the data for IFNα or IFNβ expression in the CNS, systemic upregulation of these molecules have been previously described for SIV infection. Other studies from our laboratory (Sanghavi SK and Reinhart TA, submitted for publication) have found high levels of systemic upregulation of IFNα during acute infection in the Ax LN of the same macaques that were used for this study. Published studies from other groups [74,215] have also found evidence of this phenomenon. In our study, we observed the upregulation of ISG mRNAs, G1P3, OAS2, and MxA, both in the CNS and the Ax LN during SIV infection. It is possible that although interferons might be below the levels of detection in the CNS, systemic upregulation IFNα as well as the specific ISGs was responsible for the local CNS upregulation of these ISGs and could be contributing to systemic interferon upregulation. In a study by Roberts *et.al*., the authors found no changes in the expression levels of IFNα/β in the CNS during acute infection but did detect a systemic upregulation of IFNα and attributed the changes in the CNS immune environment to systemic immune activation [74]. Since we also observed correlations between MHCI levels in the CNS and peripheral viral loads, it also seems possible that the virus carried by the blood could have been responsible for immune activation at

the CNS endothelium. In accordance to this we found MHCI mRNA to be expressed at high levels at the endothelium during the acute phase of infection when systemic viral loads are high yet no replicating virus was detected in the CNS. MHCI has also been described as an ISG and therefore systemic upregulation of IFNα could also have attributed to the MHCI upregulation particularly at the interface of the BBB [219]. In summary, the immune response that we observe in the CNS could be due to cellular mediators and ligands produced elsewhere in the body.

Previous studies by Abel *et al.* [215] and Bosinger *et al.* [216] have found systemic upregulation of MxA in acute and chronic disease without reduction in viral load. In our system we also observed upregulation of MxA and OAS2 in Ax LN during acute phase of infection in the presence of high viral loads suggesting that neither of these molecules were able control viral replication. HIV-1 has previously been described to have developed evasion strategies against certain ISGs [200]. HIV-1 has been shown to inhibit the RNAseL pathway by inducing the synthesis of an RNAse L inhibitor RLI [200]. HIV-1 Tat protein and TAR RNA has also been described to inhibit PKR, another important ISG molecule [200,215]. Therefore it is conceivable that SIV gene products can inhibit antiviral actions of ISGs and are therefore able to persist in the presence of IFN-α/β mediated immune response.

CNS damage in the presence and absence of local viral replication

Based on the collective data presented in this dissertation, I present a potential model of CNS damage during early SIV infection. During acute SIV infection, viral loads are high in plasma and Ax LN. As an early antiviral immune response, IFNα levels are highly elevated in the periphery (blood and/or Ax LN) inducing the expression of ISGs specifically G1P3, MxA, and OAS2. Virus carried by infected MO enters the CNS at the BBB and causes a local inflammatory

response. During this stage, viral load and IFNα levels in the blood are also very high. At the CNS vasculature, the endothelial cells begin to express high levels of MHCI mRNA. Perivascular MO/MF also located around the vasculature get activated, expressing HLA-DR and high levels of MHCI. Although neurons, astrocytes, and oligodendrocytes are not efficiently infected by SIV or HIV, they can be activated by the ongoing local immune response or by non-productive infection. The activation could be caused directly by the virus or viral products (shed gp120, Tat) or indirectly by products from activated MF/Mgl (pro-inflammatory cytokines, NO, PAF). As a result of this they might upregulate MHCI on their cell surfaces. Although there is evidence that the virus enters the CNS early by 7 dpi, even by 14 dpi, only minimal productive infection can be observed. This is assumed to be due to a robust immune response at the periphery and possibly at the BBB as well. Although we did not observed many T cells within the CNS of these animals, it is conceivable that due to virus interactions with endothelial cells at the point of viral entry at the endothelium, T cell mediated lysis of cells infected with SIV can occur leading to low level but ongoing disruption of the BBB. In summary, in this early stage of infection, virus entry into the CNS as well as high levels of virus and interferons in the blood can cause a local immune response. This response can be defined by an upregulation of G1P3, MxA, and OAS2 in the CNS. In addition, the elevated levels of MHCI that is observed might be a surrogate ISG marker for the massive interferon-mediated immune response.

In the late stages of disease, immune control from the periphery is lost and infected MO/MFs enter the CNS and re-seed it with virus. The low level persistent immune activation is not enough to control this onslaught. Activated MO/MFs express toxic products that directly act on the resident CNS cells causing massive gliosis and neuronal apoptosis. Oxidative stress is also
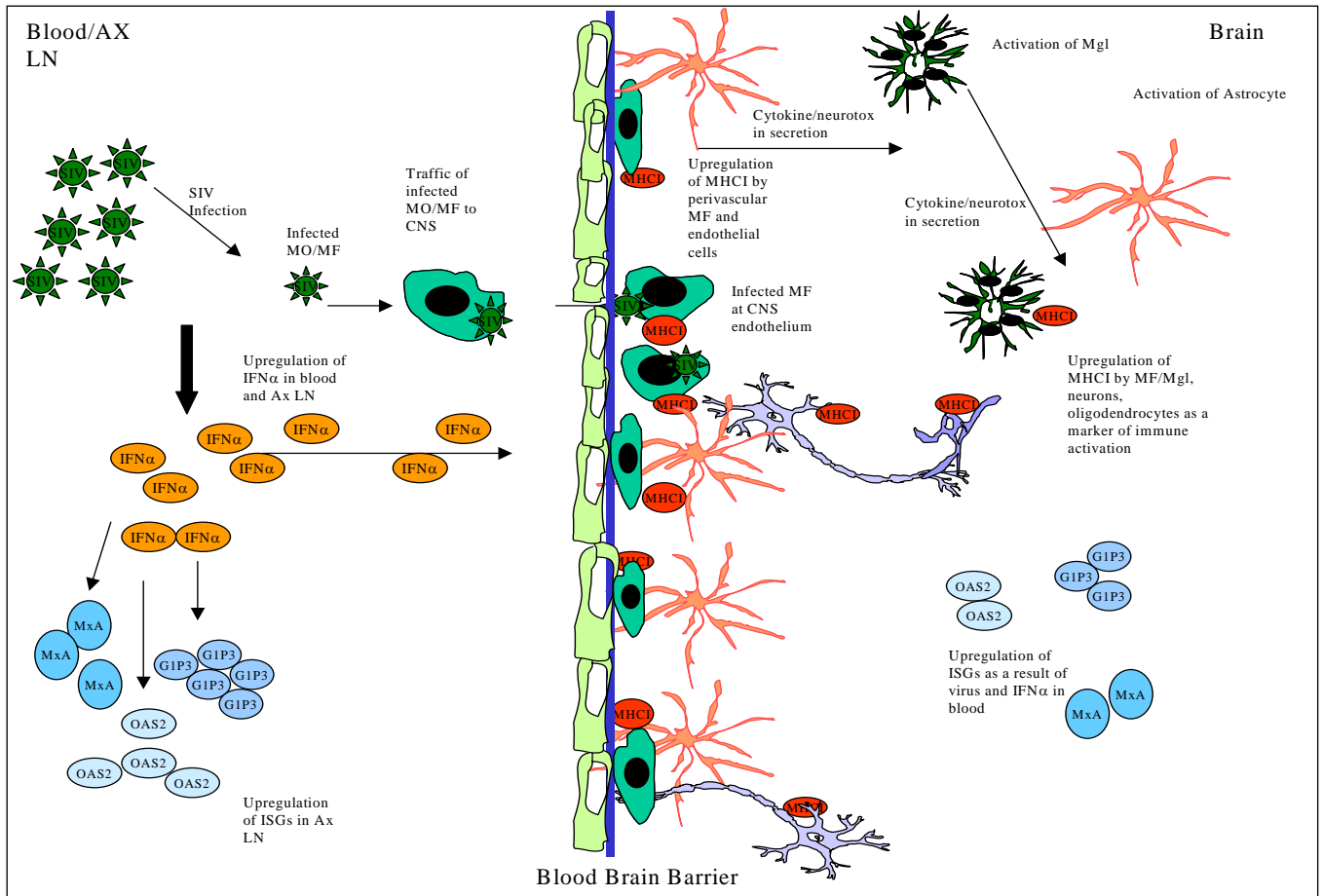
Figure 22 Immune response associated with early SIV infection of the CNS

In acute infection viral load is high in the periphery. Infected MO carry virus into the CNS where the infection is cleared rapidly. IFNα mediated systemic immune response and high plasma viral loads cause an upregulation of MHCI at the CNS endothelium. Other CNS cells such as MF/Mgl, astrocytes, neurons, and oligodendrocytes, also express MHCI mRNA during this time even in the absence of local viral replication. MHCI and ISGs G1P3, MxA, and OAS2, are upregulated in the CNS possibly acting as surrogate markers for interferon-mediated immune response.

present at this time as observed by the elevated expression of CytC indicating mitochondrial damage and leakage. In the periphery, IFNα and ISGs remain in high levels unable to control viral replication. At the CNS, MxA, and OAS2 remain at high levels as well and are not able to control viral replication locally. G1P3 levels, however, actually decrease in the CNS when viral levels are high. The reason for this is not clear, but since HIV has been described to have

developed immune evasion strategies against other ISGs, it is conceivable that there is a mechanism by which SIV can render G1P3 ineffective.

In summary, this model (Figure 21) suggests that during early infection, there is a robust innate immune response mediated by IFNα. The presence of infected MO in the CNS as well as systemic upregulation of IFNα results in upregulation of ISGs including MHCI in the CNS particularly at the endothelium situated at the junction of the BBB. Although the virus that enters the CNS during early infection is controlled rapidly, the state of immune activation persists in a chronic manner. A positive correlation has been described between the severity of the acute response and a more rapid progression to AIDS [220] and HAD [221] suggesting that while a strong early immune response can control the virus, it can cause a state of low level chronic immune activation that can lead towards faster and more severe CNS damage. During encephalitis when peripheral immune control is lost, infected and activated MO/MFs enter the CNS re-seed it with virus, and can cause massive inflammation. At this stage stress markers are also expressed and neuronal apoptosis occurs mostly caused by the toxic products secreted by activated MF/Mgl. Pathologically, this state of massive inflammation results in encephalitis and the actual loss or dysfunction of neurons gives rise to symptoms leading to dementia.

With the advent of HAART, the incidence of HAD has decreased, however, the cumulative prevalence of HAD has increased possibly because of the increased lengths of survival in AIDS patients [53,64]. The data presented here indicate that after the early viral invasion of the CNS, a persistent immune activation might occur which can affect the development of HIV/SIV associated neuropathogenesis later on. Therefore, if vigorous therapy and treatment is assumed very early during infection, the severity of neuropathological developments might be

reduced. From the perspective of public health, early detection and intervention strategies might

be effective in reducing the incidence of HAD.

VI. Future Experiments

In this dissertation I have expanded our understanding of the CNS during SIV infection particularly early during infection in the absence of local viral replication. Through this process many questions arose that were not addressed in the interests of time. The following section discusses some questions that remain unresolved but could add valuable information to the field of SIV and HIV neuropathology, if addressed.

Expression of cytokines, interferons, ISGs: Expansion of study and inclusion of other models of SIV encephalitis

I investigated the expression patterns of cytokines, interferons, and ISGs only in our model of rhesus macaques infected with SIV/DeltaB670. Although I could investigate the early acute phase of infection using this system, the system did not prove to be successful for studying aspects of encephalitis. Out of two different cohorts consisting of 12 animals each, only two developed mild encephalitis. Since I was using genetically distinct out-bred macaques, the study needed the addition of more animals per disease group, particularly for the mSIVE group. Also, it would have been useful to compare the data we obtained from our model to other successful models of SIV encephalitis. I had obtained samples from two such models that I used to compare MHCI upregulation across disease states. I believe that comparing the expressions of cytokines, interferons, and ISGs in these other models would provide valuable information.

Systematic analysis of ISGs

In my studies, I only focused on eight ISGs and followed up with three of those. ISGs are being recognized to be increasingly relevant in the SIV/HIV associated disease process. Therefore I believe that a more systematic analysis of the ISGs would be valuable particularly focusing on those (for example, PKR) that have already been described to be affected by HIV or SIV. Another important aspect would be to identify the cell types that are expressing these ISGs particularly in the CNS both during the presence and absence of local virus replication. This information would enable us to better understand how the initial virus infection in the CNS is controlled, which cells are responsible for maintaining the chronic immune activation status in the absence of viral replication and which cells are responsible for expressing the ISGs during encephalitis.

***In vitro* assay to determine stress related damage by mitochondrial leakage**

In my attempts to identify SAGE tags by RACE we amplified a number of genes that were mismatched at the tag region. A number of these genes were stress related, particularly related to mitochondrial OxPhos pathways and were shown to be upregulated by use of a microarray. In this dissertation I have attempted a small-scale study to observe the upregulation of stress markers. Although I found some upregulation of these markers in SIVE when compared to non-SIVE, technical difficulties prevented me from studying the expression of these markers in all the disease states.

I found the Cyt C gene to be upregulated by both microarray and IHC. An overexpression of this gene denotes mitochondrial damage or leakage as signs of stress and pre-requisites to

apoptosis. The mitochondrial damage could be better studied by the use of *in vitro* assay systems. In a cell culture treated with stress inducing agents i.e. virus, a time course for mitochondrial leakage could be plotted using the Mitotracker dyes. These fluorescent dyes specifically bind to the mitochondrial membranes and change color when the membrane is damaged and leaky. The study of oxidative stress in the HIV/SIV field is relatively new and I believe information on how the mitochondria are affected by viral infection could be valuable to the field of SIV/HIV neuropathology.

Comparison to the human system

All the work described here was conducted using the macaque model system. Although, the SIV system closely mimics the HIV infection and disease progression, ultimately, all data obtained by using the macaque system must be tested in the human system because. The limitation of the human system is the availability of early time points of infection. However, I could still compare the expressions of the immune molecules that we found to be important in macaques, to HIVE and non-HIVE human CNS tissues.

As previously mentioned, the questions discussed in the sections above if addressed could provide useful information regarding the early immune environment of the CNS during SIV/HIV infection and the role of specific molecules such as MHCI and ISGs in the maintenance of chronic immune activation and the development of encephalitis.

BIBLIOGRAPHY

1. http://worldaidsday.nih.gov/worldaidsday/december1.htm. NIH . 2004.
   Ref Type: Electronic Citation

2. AIDS Epidemic Update. UNAIDS . 2004.
   Ref Type: Electronic Citation

3. 1997. Retroviruses. Cold Spring Harbor Laboratory Press.

4. **Korber, B. T., S. Osmanov, J. Esparza, and G. Myers**. 1994. The World Health Organization Global Programme on AIDS proposal for standardization of HIV sequence nomenclature. WHO Network for HIV Isolation and Characterization. AIDS Res. Hum. Retroviruses **10**:1355-1358.

5. **Nathanson, N., K. A. McGann, J. Wilesmith, R. C. Desrosiers, and R. Brookmeyer**. 1993. The evolution of virus diseases: their emergence, epidemicity, and control. Virus Res. **29**:3-20.

6. **Desrosiers, R. C.** 1990. HIV-1 origins. A finger on the missing link. Nature **345**:288-289.

7. **Huet, T., R. Cheynier, A. Meyerhans, G. Roelants, and S. Wain-Hobson**. 1990. Genetic organization of a chimpanzee lentivirus related to HIV-1. Nature **345**:356-359.

8. **Fauci AS.** 1993. Multifactorial nature of human immunodeficiency virus disease: implications for therapy. Science **262**:1011-1018.

9. **Feng, Y., C. C. Broder, P. E. Kennedy, and E. A. Berger**. 1996. HIV-1 entry cofactor: functional cDNA cloning of a seven-transmembrane, G protein-coupled receptor. Science **272**:872-877.

10. **Dragic, T., V. Litwin, G. P. Allaway, S. R. Martin, Y. Huang, K. A. Nagashima, C. Cayanan, P. J. Maddon, R. A. Koup, J. P. Moore, and W. A. Paxton**. 1996. HIV-1 entry into CD4+ cells is mediated by the chemokine receptor CC-CKR-5. Nature **381**:667-673.

11. **Clapham, P. R. and A. McKnight**. 2002. Cell surface receptors, virus entry and tropism of primate lentiviruses. J. Gen. Virol. **83**:1809-1829.

12. **Mennicken, F., R. Maki, E. B. de Souza, and R. Quirion**. 1999. Chemokines and chemokine receptors in the CNS: a possible role in neuroinflammation and patterning. Trends Pharmacol. Sci. **20**:73-78.

13. **Clark, S. J., M. S. Saag, W. D. Decker, S. Campbell-Hill, J. L. Roberson, P. J. Veldkamp, J. C. Kappes, B. H. Hahn, and G. M. Shaw**. 1991. High titers of cytopathic

virus in plasma of patients with symptomatic primary HIV-1 infection. N. Engl. J. Med. **324**:954-960.

14. **Gaines, H., M. A. von Sydow, L. V. von Stedingk, G. Biberfeld, B. Bottiger, L. O. Hansson, P. Lundbergh, A. B. Sonnerborg, J. Wasserman, and O. O. Strannegaard**. 1990. Immunological changes in primary HIV-1 infection. AIDS **4**:995-999.

15. **Ho, D. D., T. R. Rota, and M. S. Hirsch**. 1985. Antibody to lymphadenopathy-associated virus in AIDS. N. Engl. J. Med. **312**:649-650.

16. **Gaines, H., M. von Sydow, A. Sonnerborg, J. Albert, J. Czajkowski, P. O. Pehrson, F. Chiodi, L. Moberg, E. M. Fenyo, B. Asjo, and .** 1987. Antibody response in primary human immunodeficiency virus infection. Lancet **1**:1249-1253.

17. **Moss, A. R. and P. Bacchetti**. 1989. Natural history of HIV infection. AIDS **3**:55-61.

18. **Coffin, J. M.** 1995. HIV population dynamics in vivo: implications for genetic variation, pathogenesis, and therapy. Science **267**:483-489.

19. **Mellors, J. W., C. R. Rinaldo, Jr., P. Gupta, R. M. White, J. A. Todd, and L. A. Kingsley**. 1996. Prognosis in HIV-1 infection predicted by the quantity of virus in plasma. Science **272**:1167-1170.

20. **Mellors, J. W., A. Munoz, J. V. Giorgi, J. B. Margolick, C. J. Tassoni, P. Gupta, L. A. Kingsley, J. A. Todd, A. J. Saah, R. Detels, J. P. Phair, and C. R. Rinaldo, Jr.** 1997. Plasma viral load and CD4+ lymphocytes as prognostic markers of HIV-1 infection. Ann. Intern. Med. **126**:946-954.

21. **Kirchhoff, F., T. C. Greenough, D. B. Brettler, J. L. Sullivan, and R. C. Desrosiers**. 1995. Brief report: absence of intact nef sequences in a long-term survivor with nonprogressive HIV-1 infection. N. Engl. J. Med. **332**:228-232.

22. **Daniel, M. D., F. Kirchhoff, S. C. Czajak, P. K. Sehgal, and R. C. Desrosiers**. 1992. Protective effects of a live attenuated SIV vaccine with a deletion in the nef gene. Science **258**:1938-1941.

23. **Levy, J. A.** 1993. HIV pathogenesis and long-term survival. AIDS **7**:1401-1410.

24. **Dean, M., M. Carrington, C. Winkler, G. A. Huttley, M. W. Smith, R. Allikmets, J. J. Goedert, S. P. Buchbinder, E. Vittinghoff, E. Gomperts, S. Donfield, D. Vlahov, R. Kaslow, A. Saah, C. Rinaldo, R. Detels, and S. J. O'Brien**. 1996. Genetic restriction of HIV-1 infection and progression to AIDS by a deletion allele of the CKR5 structural gene. Hemophilia Growth and Development Study, Multicenter AIDS Cohort Study, Multicenter Hemophilia Cohort Study, San Francisco City Cohort, ALIVE Study. Science **273**:1856-1862.

25. **Huang, Y., W. A. Paxton, S. M. Wolinsky, A. U. Neumann, L. Zhang, T. He, S. Kang, D. Ceradini, Z. Jin, K. Yazdanbakhsh, K. Kunstman, D. Erickson, E. Dragon,**

N. R. Landau, J. Phair, D. D. Ho, and R. A. Koup. 1996. The role of a mutant CCR5 allele in HIV-1 transmission and disease progression. Nat. Med. **2**:1240-1243.

26. **Rausch, D. M., E. A. Murray, and L. E. Eiden**. 1999. The SIV-infected rhesus monkey model for HIV-associated dementia and implications for neurological diseases. J. Leukoc. Biol. **65**:466-474.

27. **Clements, J. E., M. G. Anderson, M. C. Zink, S. V. Joag, and O. Narayan**. 1994. The SIV model of AIDS encephalopathy. Role of neurotropic viruses in diseases. Res. Publ. Assoc. Res. Nerv. Ment. Dis. **72**:147-157.

28. **Sopper, S., E. Koutsilieri, C. Scheller, S. Czub, P. Riederer, and M. ter, V**. 2002. Macaque animal model for HIV-induced neurological disease. J. Neural Transm. **109**:747-766.

29. **Fox, H. S., L. H. Gold, S. J. Henriksen, and F. E. Bloom**. 1997. Simian immunodeficiency virus: a model for neuroAIDS. Neurobiol. Dis. **4**:265-274.

30. **Chakrabarti, L., M. Hurtrel, M. A. Maire, R. Vazeux, D. Dormont, L. Montagnier, and B. Hurtrel**. 1991. Early viral replication in the brain of SIV-infected rhesus monkeys. Am. J. Pathol. **139**:1273-1280.

31. **Williams, K. C., S. Corey, S. V. Westmoreland, D. Pauley, H. Knight, C. deBakker, X. Alvarez, and A. A. Lackner**. 2001. Perivascular macrophages are the primary cell type productively infected by simian immunodeficiency virus in the brains of macaques: implications for the neuropathogenesis of AIDS. J. Exp. Med. **193**:905-915.

32. **Rausch, D. M., M. P. Heyes, E. A. Murray, J. Lendvay, L. R. Sharer, J. M. Ward, S. Rehm, D. Nohr, E. Weihe, and L. E. Eiden**. 1994. Cytopathologic and neurochemical correlates of progression to motor/cognitive impairment in SIV-infected rhesus monkeys. J. Neuropathol. Exp. Neurol. **53**:165-175.

33. **Marcondes, M. C., E. M. Burudi, S. Huitron-Resendiz, M. Sanchez-Alavez, D. Watry, M. Zandonatti, S. J. Henriksen, and H. S. Fox**. 2001. Highly activated CD8(+) T cells in the brain correlate with early central nervous system dysfunction in simian immunodeficiency virus infection. J. Immunol. **167**:5429-5438.

34. **Adamson, D. C., T. M. Dawson, M. C. Zink, J. E. Clements, and V. L. Dawson**. 1996. Neurovirulent simian immunodeficiency virus infection induces neuronal, endothelial, and glial apoptosis. Mol. Med. **2**:417-428.

35. **Sopper, S., M. Demuth, C. Stahl-Hennig, G. Hunsmann, R. Plesker, C. Coulibaly, S. Czub, M. Ceska, E. Koutsilieri, P. Riederer, R. Brinkmann, M. Katz, and M. ter, V**. 1996. The effect of simian immunodeficiency virus infection in vitro and in vivo on the cytokine production of isolated microglia and peripheral macrophages from rhesus monkey. Virology **220**:320-329.

36. **Lane, J. H., V. G. Sasseville, M. O. Smith, P. Vogel, D. R. Pauley, M. P. Heyes, and A. A. Lackner**. 1996. Neuroinvasion by simian immunodeficiency virus coincides with increased numbers of perivascular macrophages/microglia and intrathecal immune activation. J. Neurovirol. **2**:423-432.

37. **Zink, M. C., G. D. Coleman, J. L. Mankowski, R. J. Adams, P. M. Tarwater, K. Fox, and J. E. Clements**. 2001. Increased macrophage chemoattractant protein-1 in cerebrospinal fluid precedes and predicts simian immunodeficiency virus encephalitis. J. Infect. Dis. **184**:1015-1021.

38. **Baskin, G. B., M. Murphey-Corb, E. D. Roberts, P. J. Didier, and L. N. Martin**. 1992. Correlates of SIV encephalitis in rhesus monkeys. J. Med. Primatol. **21**:59-63.

39. **Lackner, A. A., M. O. Smith, R. J. Munn, D. J. Martfeld, M. B. Gardner, P. A. Marx, and S. Dandekar**. 1991. Localization of simian immunodeficiency virus in the central nervous system of rhesus monkeys. Am. J. Pathol. **139**:609-621.

40. **Zink, M. C., A. M. Amedee, J. L. Mankowski, L. Craig, P. Didier, D. L. Carter, A. Munoz, M. Murphey-Corb, and J. E. Clements**. 1997. Pathogenesis of SIV encephalitis. Selection and replication of neurovirulent SIV. Am. J. Pathol. **151**:793-803.

41. **Demuth, M., S. Czub, U. Sauer, E. Koutsilieri, P. Haaft, J. Heeney, C. Stahl-Hennig, M. ter, V, and S. Sopper**. 2000. Relationship between viral load in blood, cerebrospinal fluid, brain tissue and isolated microglia with neurological disease in macaques infected with different strains of SIV. J. Neurovirol. **6**:187-201.

42. **Schmitz, J. E., M. J. Kuroda, S. Santra, V. G. Sasseville, M. A. Simon, M. A. Lifton, P. Racz, K. Tenner-Racz, M. Dalesandro, B. J. Scallon, J. Ghrayeb, M. A. Forman, D. C. Montefiori, E. P. Rieber, N. L. Letvin, and K. A. Reimann**. 1999. Control of viremia in simian immunodeficiency virus infection by CD8+ lymphocytes. Science **283**:857-860.

43. **Mankowski, J. L., J. E. Clements, and M. C. Zink**. 2002. Searching for clues: tracking the pathogenesis of human immunodeficiency virus central nervous system disease by use of an accelerated, consistent simian immunodeficiency virus macaque model. J. Infect. Dis. **186 Suppl 2**:S199-S208.

44. **Zink, M. C. and J. E. Clements**. 2002. A novel simian immunodeficiency virus model that provides insight into mechanisms of human immunodeficiency virus central nervous system disease. J. Neurovirol. **8 Suppl 2**:42-48.

45. **Buch, S. J., F. Villinger, D. Pinson, Y. Hou, I. Adany, Z. Li, R. Dalal, R. Raghavan, A. Kumar, and O. Narayan**. 2002. Innate differences between simian-human immunodeficiency virus (SHIV)(KU-2)-infected rhesus and pig-tailed macaques in development of neurological disease. Virology **295**:54-62.

46. **Tyor, W. R., C. Power, H. E. Gendelman, and R. B. Markham**. 1993. A model of human immunodeficiency virus encephalitis in scid mice. Proc. Natl. Acad. Sci. U. S. A **90**:8658-8662.

47. **Persidsky, Y. and H. E. Gendelman**. 1997. Development of laboratory and animal model systems for HIV-1 encephalitis and its associated dementia. J. Leukoc. Biol. **62**:100-106.

48. **Persidsky, Y., M. Buttini, J. Limoges, P. Bock, and H. E. Gendelman**. 1997. An analysis of HIV-1-associated inflammatory products in brain tissue of humans and SCID mice with HIV-1 encephalitis. J. Neurovirol. **3**:401-416.

49. **Avgeropoulos, N., B. Kelley, L. Middaugh, S. Arrigo, Y. Persidsky, H. E. Gendelman, and W. R. Tyor**. 1998. SCID mice with HIV encephalitis develop behavioral abnormalities. J. Acquir. Immune. Defic. Syndr. Hum. Retrovirol. **18**:13-20.

50. **Toggas, S. M., E. Masliah, E. M. Rockenstein, G. F. Rall, C. R. Abraham, and L. Mucke**. 1994. Central nervous system damage produced by expression of the HIV-1 coat protein gp120 in transgenic mice. Nature **367**:188-193.

51. **Toneatto, S., O. Finco, P. H. van der, S. Abrignani, and P. Annunziata**. 1999. Evidence of blood-brain barrier alteration and activation in HIV-1 gp120 transgenic mice. AIDS **13**:2343-2348.

52. **Hanna, Z., D. G. Kay, M. Cool, S. Jothy, N. Rebai, and P. Jolicoeur**. 1998. Transgenic mice expressing human immunodeficiency virus type 1 in immune cells develop a severe AIDS-like disease. J. Virol. **72**:121-132.

53. **McArthur, J. C., N. Haughey, S. Gartner, K. Conant, C. Pardo, A. Nath, and N. Sacktor**. 2003. Human immunodeficiency virus-associated dementia: an evolving disease. J. Neurovirol. **9**:205-221.

54. **Krebs, F. C., H. Ross, J. McAllister, and B. Wigdahl**. 2000. HIV-1-associated central nervous system dysfunction. Adv. Pharmacol. **49**:315-385.

55. **Glass, J. D., H. Fedor, S. L. Wesselingh, and J. C. McArthur**. 1995. Immunocytochemical quantitation of human immunodeficiency virus in the brain: correlations with dementia. Ann. Neurol. **38**:755-762.

56. **Wiley, C. A., V. Soontornniyomkij, L. Radhakrishnan, E. Masliah, J. Mellors, S. A. Hermann, P. Dailey, and C. L. Achim**. 1998. Distribution of brain HIV load in AIDS. Brain Pathol. **8**:277-284.

57. **Masliah, E., C. E. Westland, E. M. Rockenstein, C. R. Abraham, M. Mallory, I. Veinberg, E. Sheldon, and L. Mucke**. 1997. Amyloid precursor proteins protect neurons of transgenic mice against acute and chronic excitotoxic injuries in vivo. Neuroscience **78**:135-146.

58. **Achim, C. L., R. D. Schrier, and C. A. Wiley**. 1991. Immunopathogenesis of HIV encephalitis. Brain Pathol. **1**:177-184.

59. **Adle-Biassette, H., Y. Levy, M. Colombel, F. Poron, S. Natchev, C. Keohane, and F. Gray**. 1995. Neuronal apoptosis in HIV infection in adults. Neuropathol. Appl. Neurobiol. **21**:218-227.

60. **Gelbard, H. A., H. J. James, L. R. Sharer, S. W. Perry, Y. Saito, A. M. Kazee, B. M. Blumberg, and L. G. Epstein**. 1995. Apoptotic neurons in brains from paediatric patients with HIV-1 encephalitis and progressive encephalopathy. Neuropathol. Appl. Neurobiol. **21**:208-217.

61. **Petito, C. K.** 1995. Mechanisms of cell death in brains of patients with AIDS. J. Neuropathol. Exp. Neurol. **54**:404.

62. **Zink, M. C., K. Suryanarayana, J. L. Mankowski, A. Shen, M. Piatak, Jr., J. P. Spelman, D. L. Carter, R. J. Adams, J. D. Lifson, and J. E. Clements**. 1999. High viral load in the cerebrospinal fluid and brain correlates with severity of simian immunodeficiency virus encephalitis. J. Virol. **73**:10480-10488.

63. **Gartner, S.** 2000. HIV infection and dementia. Science **287**:602-604.

64. **Suarez, S., L. Baril, B. Stankoff, M. Khellaf, B. Dubois, C. Lubetzki, F. Bricaire, and J. J. Hauw**. 2001. Outcome of patients with HIV-1-related cognitive impairment on highly active antiretroviral therapy. AIDS **15**:195-200.

65. **Corder, E. H., K. Robertson, L. Lannfelt, N. Bogdanovic, G. Eggertsen, J. Wilkins, and C. Hall**. 1998. HIV-infected subjects with the E4 allele for APOE have excess dementia and peripheral neuropathy. Nat. Med. **4**:1182-1184.

66. **Gonzalez, E., B. H. Rovin, L. Sen, G. Cooke, R. Dhanda, S. Mummidi, H. Kulkarni, M. J. Bamshad, V. Telles, S. A. Anderson, E. A. Walter, K. T. Stephan, M. Deucher, A. Mangano, R. Bologna, S. S. Ahuja, M. J. Dolan, and S. K. Ahuja**. 2002. HIV-1 infection and AIDS dementia are influenced by a mutant MCP-1 allele linked to increased monocyte infiltration of tissues and MCP-1 levels. Proc. Natl. Acad. Sci. U. S. A **99**:13795-13800.

67. **He, J., Y. Chen, M. Farzan, H. Choe, A. Ohagen, S. Gartner, J. Busciglio, X. Yang, W. Hofmann, W. Newman, C. R. Mackay, J. Sodroski, and D. Gabuzda**. 1997. CCR3 and CCR5 are co-receptors for HIV-1 infection of microglia. Nature **385**:645-649.

68. **Albright, A. V., J. T. Shieh, M. J. O'Connor, and F. Gonzalez-Scarano**. 2000. Characterization of cultured microglia that can be infected by HIV-1. J. Neurovirol. **6 Suppl 1**:S53-S60.

69. **Boche, D., F. Gray, L. Chakrabarti, M. Hurtrel, L. Montagnier, and B. Hurtrel**. 1995. Low susceptibility of resident microglia to simian immunodeficiency virus

replication during the early stages of infection. Neuropathol. Appl. Neurobiol. **21**:535-539.

70. **Cosenza, M. A., M. L. Zhao, Q. Si, and S. C. Lee**. 2002. Human brain parenchymal microglia express CD14 and CD45 and are productively infected by HIV-1 in HIV-1 encephalitis. Brain Pathol. **12**:442-455.

71. **Boche, D., E. Khatissian, F. Gray, P. Falanga, L. Montagnier, and B. Hurtrel**. 1999. Viral load and neuropathology in the SIV model. J. Neurovirol. **5**:232-240.

72. **Gonzalez, R. G., L. L. Cheng, S. V. Westmoreland, K. E. Sakaie, L. R. Becerra, P. L. Lee, E. Masliah, and A. A. Lackner**. 2000. Early brain injury in the SIV-macaque model of AIDS. AIDS **14**:2841-2849.

73. **Sasseville, V. G., J. H. Lane, D. Walsh, D. J. Ringler, and A. A. Lackner**. 1995. VCAM-1 expression and leukocyte trafficking to the CNS occur early in infection with pathogenic isolates of SIV. J. Med. Primatol. **24**:123-131.

74. **Roberts, E. S., E. M. Burudi, C. Flynn, L. J. Madden, K. L. Roinick, D. D. Watry, M. A. Zandonatti, M. A. Taffe, and H. S. Fox**. 2004. Acute SIV infection of the brain leads to upregulation of IL6 and interferon-regulated genes: expression patterns throughout disease progression and impact on neuroAIDS. J. Neuroimmunol. **157**:81-92.

75. **Horn, T. F., S. Huitron-Resendiz, M. R. Weed, S. J. Henriksen, and H. S. Fox**. 1998. Early physiological abnormalities after simian immunodeficiency virus infection. Proc. Natl. Acad. Sci. U. S. A **95**:15072-15077.

76. **Koutsilieri, E., S. Czub, C. Scheller, S. Sopper, T. Tatschner, C. Stahl-Hennig, M. ter, V, and P. Riederer**. 2000. Brain choline acetyltransferase reduction in SIV infection. An index of early dementia? Neuroreport **11**:2391-2393.

77. **Koutsilieri, E., C. Scheller, S. Sopper, M. E. Gotz, M. Gerlach, V. Meulen, and P. Riederer**. 2001. Selegiline completely restores choline acetyltransferase activity deficits in simian immunodeficiency infection. Eur. J. Pharmacol. **411**:R1-R2.

78. **Czub, S., E. Koutsilieri, S. Sopper, M. Czub, C. Stahl-Hennig, J. G. Muller, V. Pedersen, W. Gsell, J. L. Heeney, M. Gerlach, G. Gosztonyi, P. Riederer, and M. ter, V**. 2001. Enhancement of central nervous system pathology in early simian immunodeficiency virus infection by dopaminergic drugs. Acta Neuropathol. (Berl) **101**:85-91.

79. **Clements, J. E., T. Babas, J. L. Mankowski, K. Suryanarayana, M. Piatak, Jr., P. M. Tarwater, J. D. Lifson, and M. C. Zink**. 2002. The central nervous system as a reservoir for simian immunodeficiency virus (SIV): steady-state levels of SIV DNA in brain from acute through asymptomatic infection. J. Infect. Dis. **186**:905-913.

80. **Gold, L. H., H. S. Fox, S. J. Henriksen, M. J. Buchmeier, M. R. Weed, M. A. Taffe, S. Huitron-Resendiz, T. F. Horn, and F. E. Bloom**. 1998. Longitudinal analysis of

behavioral, neurophysiological, viral and immunological effects of SIV infection in rhesus monkeys. J. Med. Primatol. **27**:104-112.

81. **Koutsilieri, E., S. Sopper, T. Heinemann, C. Scheller, J. Lan, C. Stahl-Hennig, M. ter, V, P. Riederer, and M. Gerlach**. 1999. Involvement of microglia in cerebrospinal fluid glutamate increase in SIV-infected rhesus monkeys (Macaca mulatta). AIDS Res. Hum. Retroviruses **15**:471-477.

82. **Griffin, D. E., J. C. McArthur, and D. R. Cornblath**. 1991. Neopterin and interferon-gamma in serum and cerebrospinal fluid of patients with HIV-associated neurologic disease. Neurology **41**:69-74.

83. **Achim, C. L., M. P. Heyes, and C. A. Wiley**. 1993. Quantitation of human immunodeficiency virus, immune activation factors, and quinolinic acid in AIDS brains. J. Clin. Invest **91**:2769-2775.

84. **Gelbard, H. A., H. S. Nottet, S. Swindells, M. Jett, K. A. Dzenko, P. Genis, R. White, L. Wang, Y. B. Choi, D. Zhang, and .** 1994. Platelet-activating factor: a candidate human immunodeficiency virus type 1-induced neurotoxin. J. Virol. **68**:4628-4635.

85. **Kaul, M., G. A. Garden, and S. A. Lipton**. 2001. Pathways to neuronal injury and apoptosis in HIV-associated dementia. Nature **410**:988-994.

86. **Williams, K. C. and W. F. Hickey**. 2002. Central nervous system damage, monocytes and macrophages, and neurological disorders in AIDS. Annu. Rev. Neurosci. **25**:537-562.

87. **Danbolt, N. C.** 2001. Glutamate uptake. Prog. Neurobiol. **65**:1-105.

88. **Giulian, D., K. Vaca, and C. A. Noonan**. 1990. Secretion of neurotoxins by mononuclear phagocytes infected with HIV-1. Science **250**:1593-1596.

89. **Lipton, S. A.** 1994. HIV-related neuronal injury. Potential therapeutic intervention with calcium channel antagonists and NMDA antagonists. Mol. Neurobiol. **8**:181-196.

90. **Kaiser, P. K., J. T. Offermann, and S. A. Lipton**. 1990. Neuronal injury due to HIV-1 envelope protein is blocked by anti-gp120 antibodies but not by anti-CD4 antibodies. Neurology **40**:1757-1761.

91. **Pulliam, L., D. West, N. Haigwood, and R. A. Swanson**. 1993. HIV-1 envelope gp120 alters astrocytes in human brain cultures. AIDS Res. Hum. Retroviruses **9**:439-444.

92. **Rappaport, J., J. Joseph, S. Croul, G. Alexander, L. Del Valle, S. Amini, and K. Khalili**. 1999. Molecular pathway involved in HIV-1-induced CNS pathology: role of viral regulatory protein, Tat. J. Leukoc. Biol. **65**:458-465.

93. **Hofman, F. M., M. M. Dohadwala, A. D. Wright, D. R. Hinton, and S. M. Walker**. 1994. Exogenous tat protein activates central nervous system-derived endothelial cells. J. Neuroimmunol. **54**:19-28.

94. **Zidovetzki, R., J. L. Wang, P. Chen, R. Jeyaseelan, and F. Hofman**. 1998. Human immunodeficiency virus Tat protein induces interleukin 6 mRNA expression in human brain endothelial cells via protein kinase C- and cAMP-dependent protein kinase pathways. AIDS Res. Hum. Retroviruses **14**:825-833.

95. **Boven, L. A., L. Gomes, C. Hery, F. Gray, J. Verhoef, P. Portegies, M. Tardieu, and H. S. Nottet**. 1999. Increased peroxynitrite activity in AIDS dementia complex: implications for the neuropathogenesis of HIV-1 infection. J. Immunol. **162**:4319-4327.

96. **Turchan, J., C. B. Pocernich, C. Gairola, A. Chauhan, G. Schifitto, D. A. Butterfield, S. Buch, O. Narayan, A. Sinai, J. Geiger, J. R. Berger, H. Elford, and A. Nath**. 2003. Oxidative stress in HIV demented patients and protection ex vivo with novel antioxidants. Neurology **60**:307-314.

97. **Hughes, E. S., J. E. Bell, and P. Simmonds**. 1997. Investigation of the dynamics of the spread of human immunodeficiency virus to brain and other tissues by evolutionary analysis of sequences from the p17gag and env genes. J. Virol. **71**:1272-1280.

98. **Strizki, J. M., A. V. Albright, H. Sheng, M. O'Connor, L. Perrin, and F. Gonzalez-Scarano**. 1996. Infection of primary human microglia and monocyte-derived macrophages with human immunodeficiency virus type 1 isolates: evidence of differential tropism. J. Virol. **70**:7654-7662.

99. **Chen, H., C. Wood, and C. K. Petito**. 2000. Comparisons of HIV-1 viral sequences in brain, choroid plexus and spleen: potential role of choroid plexus in the pathogenesis of HIV encephalitis. J. Neurovirol. **6**:498-506.

100. **Mankowski, J. L., M. T. Flaherty, J. P. Spelman, D. A. Hauer, P. J. Didier, A. M. Amedee, M. Murphey-Corb, L. M. Kirstein, A. Munoz, J. E. Clements, and M. C. Zink**. 1997. Pathogenesis of simian immunodeficiency virus encephalitis: viral determinants of neurovirulence. J. Virol. **71**:6055-6060.

101. **Power, C., J. C. McArthur, R. T. Johnson, D. E. Griffin, J. D. Glass, S. Perryman, and B. Chesebro**. 1994. Demented and nondemented patients with AIDS differ in brain-derived human immunodeficiency virus type 1 envelope sequences. J. Virol. **68**:4643-4649.

102. **Liu, Y., X. P. Tang, J. C. McArthur, J. Scott, and S. Gartner**. 2000. Analysis of human immunodeficiency virus type 1 gp160 sequences from a patient with HIV dementia: evidence for monocyte trafficking into brain. J. Neurovirol. **6 Suppl 1**:S70-S81.

103. **Gorry, P. R., G. Bristol, J. A. Zack, K. Ritola, R. Swanstrom, C. J. Birch, J. E. Bell, N. Bannert, K. Crawford, H. Wang, D. Schols, E. De Clercq, K. Kunstman, S. M. Wolinsky, and D. Gabuzda**. 2001. Macrophage tropism of human immunodeficiency virus type 1 isolates from brain and lymphoid tissues predicts neurotropism independent of coreceptor specificity. J. Virol. **75**:10073-10089.

104. **Petito, C. K., B. Adkins, M. McCarthy, B. Roberts, and I. Khamis**. 2003. CD4+ and CD8+ cells accumulate in the brains of acquired immunodeficiency syndrome patients with human immunodeficiency virus encephalitis. J. Neurovirol. **9**:36-44.

105. **von Herrath, M., M. B. Oldstone, and H. S. Fox**. 1995. Simian immunodeficiency virus (SIV)-specific CTL in cerebrospinal fluid and brains of SIV-infected rhesus macaques. J. Immunol. **154**:5582-5589.

106. **Walker, B. D., S. Chakrabarti, B. Moss, T. J. Paradis, T. Flynn, A. G. Durno, R. S. Blumberg, J. C. Kaplan, M. S. Hirsch, and R. T. Schooley**. 1987. HIV-specific cytotoxic T lymphocytes in seropositive individuals. Nature **328**:345-348.

107. **Weidenheim, K. M., I. Epshteyn, and W. D. Lyman**. 1993. Immunocytochemical identification of T-cells in HIV-1 encephalitis: implications for pathogenesis of CNS disease. Mod. Pathol. **6**:167-174.

108. **Lokensgard, J. R., G. Gekker, S. Hu, C. C. Chao, M. Simpson, R. L. Schut, and P. K. Peterson**. 1999. CD8+ lymphocyte-mediated suppression of human immunodeficiency virus type 1 expression in human brain cells. Immunol. Lett. **67**:257-261.

109. **Kim, W. K., S. Corey, G. Chesney, H. Knight, S. Klumpp, C. Wuthrich, N. Letvin, I. Koralnik, A. Lackner, R. Veasey, and K. Williams**. 2004. Identification of T lymphocytes in simian immunodeficiency virus encephalitis: distribution of CD8+ T cells in association with central nervous system vessels and virus. J. Neurovirol. **10**:315-325.

110. **Jassoy, C., R. P. Johnson, B. A. Navia, J. Worth, and B. D. Walker**. 1992. Detection of a vigorous HIV-1-specific cytotoxic T lymphocyte response in cerebrospinal fluid from infected persons with AIDS dementia complex. J. Immunol. **149**:3113-3119.

111. **Kato, T., H. M. Dembitzer, A. Hirano, and J. F. Llena**. 1987. HTLV-III-like particles within a cell process surrounded by a myelin sheath in an AIDS brain. Acta Neuropathol. (Berl) **73**:306-308.

112. **Albright, A. V., J. Strizki, J. M. Harouse, E. Lavi, M. O'Connor, and F. Gonzalez-Scarano**. 1996. HIV-1 infection of cultured human adult oligodendrocytes. Virology **217**:211-219.

113. **Sharpless, N., D. Gilbert, B. Vandercam, J. M. Zhou, E. Verdin, G. Ronnett, E. Friedman, and M. Dubois-Dalcq**. 1992. The restricted nature of HIV-1 tropism for cultured neural cells. Virology **191**:813-825.

114. **Rottman, J. B., K. P. Ganley, K. Williams, L. Wu, C. R. Mackay, and D. J. Ringler**. 1997. Cellular localization of the chemokine receptor CCR5. Correlation to cellular targets of HIV-1 infection. Am. J. Pathol. **151**:1341-1351.

115. **Sanders, V. J., C. A. Pittman, M. G. White, G. Wang, C. A. Wiley, and C. L. Achim**. 1998. Chemokines and receptors in HIV encephalitis. AIDS **12**:1021-1026.

116. **Willey, S. J., J. D. Reeves, R. Hudson, K. Miyake, N. Dejucq, D. Schols, E. De Clercq, J. Bell, A. McKnight, and P. R. Clapham**. 2003. Identification of a subset of human immunodeficiency virus type 1 (HIV-1), HIV-2, and simian immunodeficiency virus strains able to exploit an alternative coreceptor on untransformed human brain and lymphoid cells. J. Virol. **77**:6138-6152.

117. **Mukhtar, M., S. Harley, P. Chen, M. BouHamdan, C. Patel, E. Acheampong, and R. J. Pomerantz**. 2002. Primary isolated human brain microvascular endothelial cells express diverse HIV/SIV-associated chemokine coreceptors and DC-SIGN and L-SIGN. Virology **297**:78-88.

118. **Stins, M. F., Y. Shen, S. H. Huang, F. Gilles, V. K. Kalra, and K. S. Kim**. 2001. Gp120 activates children's brain endothelial cells via CD4. J. Neurovirol. **7**:125-134.

119. **Poland, S. D., G. P. Rice, and G. A. Dekaban**. 1995. HIV-1 infection of human brain-derived microvascular endothelial cells in vitro. J. Acquir. Immune. Defic. Syndr. Hum. Retrovirol. **8**:437-445.

120. **Gilles, P. N., J. L. Lathey, and S. A. Spector**. 1995. Replication of macrophage-tropic and T-cell-tropic strains of human immunodeficiency virus type 1 is augmented by macrophage-endothelial cell contact. J. Virol. **69**:2133-2139.

121. **Klein, R. S., K. C. Williams, X. Alvarez-Hernandez, S. Westmoreland, T. Force, A. A. Lackner, and A. D. Luster**. 1999. Chemokine receptor expression and signaling in macaque and human fetal neurons and astrocytes: implications for the neuropathogenesis of AIDS. J. Immunol. **163**:1636-1646.

122. **Funke, I., A. Hahn, E. P. Rieber, E. Weiss, and G. Riethmuller**. 1987. The cellular receptor (CD4) of the human immunodeficiency virus is expressed on neurons and glial cells in human brain. J. Exp. Med. **165**:1230-1235.

123. **Li XL, M. T. V. H. H. D.** 1990. CD4-independent, productive infection of a neuronal cell line by human immunodeficiency virus type 1. J Virol. **64**:1383-1387.

124. **Petito, C. K.** 2004. Human immunodeficiency virus type 1 compartmentalization in the central nervous system. J. Neurovirol. **10 Suppl 1**:21-24.

125. **Speck, R. F., U. Esser, M. L. Penn, D. A. Eckstein, L. Pulliam, S. Y. Chan, and M. A. Goldsmith**. 1999. A trans-receptor mechanism for infection of CD4-negative cells by human immunodeficiency virus type 1. Curr. Biol. **9**:547-550.

126. **Shapshak, P., N. C. Sun, L. Resnick, J. T. Thornthwaite, P. Schiller, M. Yoshioka, A. Svenningsson, W. W. Tourtellotte, and D. T. Imagawa**. 1991. HIV-1 propagates in human neuroblastoma cells. J. Acquir. Immune. Defic. Syndr. **4**:228-237.

127. **Overholser, E. D., G. D. Coleman, J. L. Bennett, R. J. Casaday, M. C. Zink, S. A. Barber, and J. E. Clements**. 2003. Expression of simian immunodeficiency virus (SIV)

nef in astrocytes during acute and terminal infection and requirement of nef for optimal replication of neurovirulent SIV in vitro. J. Virol. **77**:6855-6866.

128. **Saito, Y., L. R. Sharer, L. G. Epstein, J. Michaels, M. Mintz, M. Louder, K. Golding, T. A. Cvetkovich, and B. M. Blumberg**. 1994. Overexpression of nef as a marker for restricted HIV-1 infection of astrocytes in postmortem pediatric central nervous tissues. Neurology **44**:474-481.

129. **Nath, A., V. Hartloper, M. Furer, and K. R. Fowke**. 1995. Infection of human fetal astrocytes with HIV-1: viral tropism and the role of cell to cell contact in viral transmission. J. Neuropathol. Exp. Neurol. **54**:320-330.

130. **Di Rienzo, A. M., F. Aloisi, A. C. Santarcangelo, C. Palladino, E. Olivetta, D. Genovese, P. Verani, and G. Levi**. 1998. Virological and molecular parameters of HIV-1 infection of human embryonic astrocytes. Arch. Virol. **143**:1599-1615.

131. **Sabri, F., E. Tresoldi, M. Di Stefano, S. Polo, M. C. Monaco, A. Verani, J. R. Fiore, P. Lusso, E. Major, F. Chiodi, and G. Scarlatti**. 1999. Nonproductive human immunodeficiency virus type 1 infection of human fetal astrocytes: independence from CD4 and major chemokine receptors. Virology **264**:370-384.

132. **Williams, K., X. Alvarez, and A. A. Lackner**. 2001. Central nervous system perivascular cells are immunoregulatory cells that connect the CNS with the peripheral immune system. Glia **36**:156-164.

133. **Power, C., P. A. Kong, T. O. Crawford, S. Wesselingh, J. D. Glass, J. C. McArthur, and B. D. Trapp**. 1993. Cerebral white matter changes in acquired immunodeficiency syndrome dementia: alterations of the blood-brain barrier. Ann. Neurol. **34**:339-350.

134. **Petito, C. K. and K. S. Cash**. 1992. Blood-brain barrier abnormalities in the acquired immunodeficiency syndrome: immunohistochemical localization of serum proteins in postmortem brain. Ann. Neurol. **32**:658-666.

135. **Dallasta, L. M., L. A. Pisarov, J. E. Esplen, J. V. Werley, A. V. Moses, J. A. Nelson, and C. L. Achim**. 1999. Blood-brain barrier tight junction disruption in human immunodeficiency virus-1 encephalitis. Am. J. Pathol. **155**:1915-1927.

136. **Nottet, H. S., Y. Persidsky, V. G. Sasseville, A. N. Nukuna, P. Bock, Q. H. Zhai, L. R. Sharer, R. D. McComb, S. Swindells, C. Soderland, and H. E. Gendelman**. 1996. Mechanisms for the transendothelial migration of HIV-1-infected monocytes into brain. J. Immunol. **156**:1284-1295.

137. **Sasseville, V. G., W. Newman, S. J. Brodie, P. Hesterberg, D. Pauley, and D. J. Ringler**. 1994. Monocyte adhesion to endothelium in simian immunodeficiency virus-induced AIDS encephalitis is mediated by vascular cell adhesion molecule-1/alpha 4 beta 1 integrin interactions. Am. J. Pathol. **144**:27-40.

138. **Ghorpade, A., R. Persidskaia, R. Suryadevara, M. Che, X. J. Liu, Y. Persidsky, and H. E. Gendelman**. 2001. Mononuclear phagocyte differentiation, activation, and viral infection regulate matrix metalloproteinase expression: implications for human immunodeficiency virus type 1-associated dementia. J. Virol. **75**:6572-6583.

139. **Dhawan, S., B. S. Weeks, C. Soderland, H. W. Schnaper, L. A. Toro, S. P. Asthana, I. K. Hewlett, W. G. Stetler-Stevenson, S. S. Yamada, K. M. Yamada, and .** 1995. HIV-1 infection alters monocyte interactions with human microvascular endothelial cells. J. Immunol. **154**:422-432.

140. **Boven, L. A., J. Middel, J. Verhoef, C. J. De Groot, and H. S. Nottet**. 2000. Monocyte infiltration is highly associated with loss of the tight junction protein zonula occludens in HIV-1-associated dementia. Neuropathol. Appl. Neurobiol. **26**:356-360.

141. **Wiley, C. A., E. Masliah, and C. L. Achim**. 1994. Measurement of CNS HIV burden and its association with neurologic damage. Adv. Neuroimmunol. **4**:319-325.

142. **Cherner, M., E. Masliah, R. J. Ellis, T. D. Marcotte, D. J. Moore, I. Grant, and R. K. Heaton**. 2002. Neurocognitive dysfunction predicts postmortem findings of HIV encephalitis. Neurology **59**:1563-1567.

143. **Nuovo, G. J., F. Gallery, P. MacConnell, and A. Braun**. 1994. In situ detection of polymerase chain reaction-amplified HIV-1 nucleic acids and tumor necrosis factor-alpha RNA in the central nervous system. Am. J. Pathol. **144**:659-666.

144. **Bagasra, O., E. Lavi, L. Bobroski, K. Khalili, J. P. Pestaner, R. Tawadros, and R. J. Pomerantz**. 1996. Cellular reservoirs of HIV-1 in the central nervous system of infected individuals: identification by the combination of in situ polymerase chain reaction and immunohistochemistry. AIDS **10**:573-585.

145. **Bissel, S. J. and C. A. Wiley**. 2004. Human immunodeficiency virus infection of the brain: pitfalls in evaluating infected/affected cell populations. Brain Pathol. **14**:97-108.

146. **Sanders, V. J., C. A. Wiley, and R. L. Hamilton**. 2001. The mechanisms of neuronal damage in retroviral infections of the nervous system. Curr. Top. Microbiol. Immunol. **253**:179-201.

147. **Garden, G. A., S. L. Budd, E. Tsai, L. Hanson, M. Kaul, D. M. D'Emilia, R. M. Friedlander, J. Yuan, E. Masliah, and S. A. Lipton**. 2002. Caspase cascades in human immunodeficiency virus-associated neurodegeneration. J. Neurosci. **22**:4015-4024.

148. **Gartner, S. and Y. Liu**. 2002. Insights into the role of immune activation in HIV neuropathogenesis. J. Neurovirol. **8**:69-75.

149. **Kim, W. K., S. Corey, X. Alvarez, and K. Williams**. 2003. Monocyte/macrophage traffic in HIV and SIV encephalitis. J. Leukoc. Biol.

150. **Velculescu, V. E., L. Zhang, B. Vogelstein, and K. W. Kinzler**. 1995. Serial analysis of gene expression. Science **270**:484-487.

151. **Yamamoto, M., T. Wakatsuki, A. Hada, and A. Ryo**. 2001. Use of serial analysis of gene expression (SAGE) technology. J. Immunol. Methods **250**:45-66.

152. **Feldker, D. E., E. R. De Kloet, M. R. Kruk, and N. A. Datson**. 2003. Large-scale gene expression profiling of discrete brain regions: potential, limitations, and application in genetics of aggressive behavior. Behav. Genet. **33**:537-548.

153. **Chrast, R., H. S. Scott, M. P. Papasavvas, C. Rossier, E. S. Antonarakis, C. Barras, M. T. Davisson, C. Schmidt, X. Estivill, M. Dierssen, M. Pritchard, and S. E. Antonarakis**. 2000. The mouse brain transcriptome by SAGE: differences in gene expression between P30 brains of the partial trisomy 16 mouse model of Down syndrome (Ts65Dn) and normals. Genome Res. **10**:2006-2021.

154. **Hashimoto, S. I., T. Suzuki, S. Nagai, T. Yamashita, N. Toyoda, and K. Matsushima**. 2000. Identification of genes specifically expressed in human activated and mature dendritic cells through serial analysis of gene expression. Blood **96**:2206-2214.

155. **Feldker, D. E., N. A. Datson, A. H. Veenema, E. Meulmeester, E. R. De Kloet, and E. Vreugdenhil**. 2003. Serial analysis of gene expression predicts structural differences in hippocampus of long attack latency and short attack latency mice. Eur. J Neurosci. **17**:379-387.

156. **Ishii, M., S. Hashimoto, S. Tsutsumi, Y. Wada, K. Matsushima, T. Kodama, and H. Aburatani**. 2000. Direct comparison of GeneChip and SAGE on the quantitative accuracy in transcript profiling analysis. Genomics **68**:136-143.

157. **Velculescu, V. E., B. Vogelstein, and K. W. Kinzler**. 2000. Analysing uncharted transcriptomes with SAGE. Trends Genet. **16**:423-425.

158. **Datson, N. A., van der Perk-de Jong, M. P. van den Berg, E. R. De Kloet, and E. Vreugdenhil**. 1999. MicroSAGE: a modified procedure for serial analysis of gene expression in limited amounts of tissue. Nucleic Acids Res. **27**:1300-1307.

159. **Peters, D. G., A. B. Kassam, H. Yonas, E. H. O'Hare, R. E. Ferrell, and A. M. Brufsky**. 1999. Comprehensive transcript analysis in small quantities of mRNA by SAGE-lite. Nucleic Acids Res. **27**:e39.

160. **Neilson, L., A. Andalibi, D. Kang, C. Coutifaris, J. F. Strauss, III, J. A. Stanton, and D. P. Green**. 2000. Molecular phenotype of the human oocyte by PCR-SAGE. Genomics **63**:13-24.

161. **Ye, S. Q., L. Q. Zhang, F. Zheng, D. Virgil, and P. O. Kwiterovich**. 2000. miniSAGE: gene expression profiling using serial analysis of gene expression from 1 microg total RNA. Anal. Biochem. **287**:144-152.

162. **van den, B. A., L. J. van der, and S. Poppema**. 1999. Serial analysis of gene expression: rapid RT-PCR analysis of unknown SAGE tags. Nucleic Acids Res. **27**:e17.

163. **Chen, J. J., J. D. Rowley, and S. M. Wang**. 2000. Generation of longer cDNA fragments from serial analysis of gene expression tags for gene identification. Proc. Natl. Acad. Sci. U. S. A **97**:349-353.

164. **Weeraratna, A. T.** 2003. Serial Analysis of Gene Expression (SAGE): Advances, Analysis and Applications to Pigment Cell Research. Pigment Cell Res. **16**:183-189.

165. **Pleasance, E. D., M. A. Marra, and S. J. Jones**. 2003. Assessment of SAGE in transcript identification. Genome Res. **13**:1203-1215.

166. **Riggins, G. J.** 2001. Using Serial Analysis of Gene Expression to identify tumor markers and antigens. Dis. Markers **17**:41-48.

167. **Hermeking, H.** 2003. Serial analysis of gene expression and cancer. Curr. Opin. Oncol. **15**:44-49.

168. **Hashimoto, S., T. Suzuki, H. Y. Dong, S. Nagai, N. Yamazaki, and K. Matsushima**. 1999. Serial analysis of gene expression in human monocyte-derived dendritic cells. Blood **94**:845-852.

169. **Arai, M., S. Amano, A. Ryo, A. Hada, T. Wakatsuki, M. Shuda, N. Kondoh, and M. Yamamoto**. 2003. Identification of epilepsy-related genes by gene expression profiling in the hippocampus of genetically epileptic rat. Brain Res. Mol. Brain Res. **118**:147-151.

170. **Ryo, A., Y. Suzuki, K. Ichiyama, T. Wakatsuki, N. Kondoh, A. Hada, M. Yamamoto, and N. Yamamoto**. 1999. Serial analysis of gene expression in HIV-1-infected T cell lines. FEBS Lett. **462**:182-186.

171. **Schena, M., D. Shalon, R. W. Davis, and P. O. Brown**. 1995. Quantitative monitoring of gene expression patterns with a complementary DNA microarray. Science **270**:467-470.

172. **Schena, M., R. A. Heller, T. P. Theriault, K. Konrad, E. Lachenmeier, and R. W. Davis**. 1998. Microarrays: biotechnology's discovery platform for functional genomics. Trends Biotechnol. **16**:301-306.

173. **Zhao, X., E. S. Lein, A. He, S. C. Smith, C. Aston, and F. H. Gage**. 2001. Transcriptional profiling reveals strict boundaries between hippocampal subregions. J. Comp Neurol. **441**:187-196.

174. **Evans, S. J., N. A. Datson, M. Kabbaj, R. C. Thompson, E. Vreugdenhil, E. R. De Kloet, S. J. Watson, and H. Akil**. 2002. Evaluation of Affymetrix Gene Chip sensitivity in rat hippocampal tissue using SAGE analysis. Serial Analysis of Gene Expression. Eur. J. Neurosci. **16**:409-413.

175. **Sawiris, G. P., C. A. Sherman-Baust, K. G. Becker, C. Cheadle, D. Teichberg, and P. J. Morin**. 2002. Development of a highly specialized cDNA array for the study and diagnosis of epithelial ovarian cancer. Cancer Res. **62**:2923-2928.

176. **Keime, C., F. Damiola, D. Mouchiroud, L. Duret, and O. Gandrillon**. 2004. Identitag, a relational database for SAGE tag identification and interspecies comparison of SAGE libraries. BMC. Bioinformatics. **5**:143.

177. **Brew, B. J., M. Rosenblum, K. Cronin, and R. W. Price**. 1995. AIDS dementia complex and HIV-1 brain infection: clinical-virological correlations. Ann. Neurol. **38**:563-570.

178. **Roberts, E. S., M. A. Zandonatti, D. D. Watry, L. J. Madden, S. J. Henriksen, M. A. Taffe, and H. S. Fox**. 2003. Induction of pathogenic sets of genes in macrophages and neurons in NeuroAIDS. Am. J. Pathol. **162**:2041-2057.

179. **Kaul, M. and S. A. Lipton**. 1999. Chemokines and activated macrophages in HIV gp120-induced neuronal apoptosis. Proc. Natl. Acad. Sci. U. S. A **96**:8212-8216.

180. **Bissel, S. J., G. Wang, M. Ghosh, T. A. Reinhart, S. Capuano, III, C. K. Stefano, M. Murphey-Corb, J. M. Piatak, Jr., J. D. Lifson, and C. A. Wiley**. 2002. Macrophages relate presynaptic and postsynaptic damage in simian immunodeficiency virus encephalitis. Am. J. Pathol. **160**:927-941.

181. **Sharer, L. R.** 1992. Pathology of HIV-1 infection of the central nervous system. A review. J. Neuropathol. Exp. Neurol. **51**:3-11.

182. **Reinhart, T. A., B. A. Fallert, M. E. Pfeifer, S. Sanghavi, S. Capuano, III, P. Rajakumar, M. Murphey-Corb, R. Day, C. L. Fuller, and T. M. Schaefer**. 2002. Increased expression of the inflammatory chemokine CXC chemokine ligand 9/monokine induced by interferon-gamma in lymphoid tissues of rhesus macaques during simian immunodeficiency virus infection and acquired immunodeficiency syndrome. Blood **99**:3119-3128.

183. **Choi, Y. K., K. M. Whelton, B. Mlechick, M. A. Murphey-Corb, and T. A. Reinhart**. 2003. Productive infection of dendritic cells by simian immunodeficiency virus in macaque intestinal tissues. J Pathol. **201**:616-628.

184. **Fuller, C. L., Y. K. Choi, B. A. Fallert, S. Capuano, III, P. Rajakumar, M. Murphey-Corb, and T. A. Reinhart**. 2002. Restricted SIV replication in rhesus macaque lung tissues during the acute phase of infection. Am. J Pathol. **161**:969-978.

185. **Fallert, B. A. and T. A. Reinhart**. 2002. Improved detection of simian immunodeficiency virus RNA by in situ hybridization in fixed tissue sections: combined effects of temperatures for tissue fixation and probe hybridization. J. Virol. Methods **99**:23-32.

186. **Aldape, K., D. G. Ginzinger, and T. E. Godfrey**. 2002. Real-time quantitative polymerase chain reaction: a potential tool for genetic analysis in neuropathology. Brain Pathol. **12**:54-66.

187. **Godfrey, T. E. and L. A. Kelly**. 2004. Development of quantitative reverse transcriptase PCR assays for measuring gene expression. Methods Mol. Biol. **291**:423-446.

188. **Li, H. Y., J. F. Li, and G. W. Lu**. 2003. [Neurogranin: a brain-specific protein]. Sheng Li Ke. Xue. Jin. Zhan. **34**:111-115.

189. **Represa, A., J. C. Deloulme, M. Sensenbrenner, Y. Ben Ari, and J. Baudier**. 1990. Neurogranin: immunocytochemical localization of a brain-specific protein kinase C substrate. J. Neurosci. **10**:3782-3792.

190. **Siu, I. M., A. Lal, and G. J. Riggins**. 2001. A database for regional gene expression in the human brain. Gene Expr. Patterns. **1**:33-38.

191. **Elmquist, J. K., T. E. Scammell, and C. B. Saper**. 1997. Mechanisms of CNS response to systemic immune challenge: the febrile response. Trends Neurosci. **20**:565-570.

192. **Ensoli, F., V. Fiorelli, M. De Cristofaro, D. S. Muratori, A. Novi, A. Isgro, and F. Aiuti**. 2000. Role of immune-derived diffusible mediators in AIDS-associated neurological disorders. Arch. Immunol. Ther. Exp. (Warsz.) **48**:259-266.

193. **Ferencik, M. and V. Stvrtinova**. 1997. [Is the immune system our sixth sense? Relation between the immune and neuroendocrine systems]. Bratisl. Lek. Listy **98**:187-198.

194. **Milner, R. and I. L. Campbell**. 2003. The extracellular matrix and cytokines regulate microglial integrin expression and activation. J. Immunol. **170**:3850-3858.

195. **Martensen, P. M. and J. Justesen**. 2004. Small ISGs coming forward. J. Interferon Cytokine Res. **24**:1-19.

196. **Bottcher, T., M. von Mering, S. Ebert, U. Meyding-Lamade, U. Kuhnt, J. Gerber, and R. Nau**. 2003. Differential regulation of Toll-like receptor mRNAs in experimental murine central nervous system infections. Neurosci. Lett. **344**:17-20.

197. **Kurt-Jones, E. A., L. Popova, L. Kwinn, L. M. Haynes, L. P. Jones, R. A. Tripp, E. E. Walsh, M. W. Freeman, D. T. Golenbock, L. J. Anderson, and R. W. Finberg**. 2000. Pattern recognition receptors TLR4 and CD14 mediate response to respiratory syncytial virus. Nat. Immunol. **1**:398-401.

198. **Zhu, H., H. Zhao, C. D. Collins, S. E. Eckenrode, Q. Run, R. A. McIndoe, J. M. Crawford, D. R. Nelson, J. X. She, and C. Liu**. 2003. Gene expression associated with interferon alfa antiviral activity in an HCV replicon cell line. Hepatology **37**:1180-1188.

199. **Haller, O. and G. Kochs**. 2002. Interferon-induced mx proteins: dynamin-like GTPases with antiviral activity. Traffic. **3**:710-717.

200. **Weber, F., G. Kochs, and O. Haller**. 2004. Inverse interference: how viruses fight the interferon system. Viral Immunol. **17**:498-515.

201. **Rebouillat, D. and A. G. Hovanessian**. 1999. The human 2',5'-oligoadenylate synthetase family: interferon-induced proteins with unique enzymatic properties. J. Interferon Cytokine Res. **19**:295-308.

202. **Chen, J., S. Lee, G. Zhou, and S. M. Wang**. 2002. High-throughput GLGI procedure for converting a large number of serial analysis of gene expression tag sequences into 3' complementary DNAs. Genes Chromosomes. Cancer **33**:252-261.

203. **Gilmore, W., J. Correale, and L. P. Weiner**. 1994. Coronavirus induction of class I major histocompatibility complex expression in murine astrocytes is virus strain specific. J. Exp. Med. **180**:1013-1023.

204. **Foster, J. A., N. Quan, E. L. Stern, K. Kristensson, and M. Herkenham**. 2002. Induced neuronal expression of class I major histocompatibility complex mRNA in acute and chronic inflammation models. J. Neuroimmunol. **131**:83-91.

205. **Redwine, J. M., M. J. Buchmeier, and C. F. Evans**. 2001. In vivo expression of major histocompatibility complex molecules on oligodendrocytes and neurons during viral infection. Am. J. Pathol. **159**:1219-1224.

206. **Neumann, H., H. Schmidt, A. Cavalie, D. Jenne, and H. Wekerle**. 1997. Major histocompatibility complex (MHC) class I gene expression in single neurons of the central nervous system: differential regulation by interferon (IFN)-gamma and tumor necrosis factor (TNF)-alpha. J. Exp. Med. **185**:305-316.

207. **Achim, C. L., M. K. Morey, and C. A. Wiley**. 1991. Expression of major histocompatibility complex and HIV antigens within the brains of AIDS patients. AIDS **5**:535-541.

208. **Turnley, A. M., J. F. Miller, and P. F. Bartlett**. 1991. Regulation of MHC molecules on MBP positive oligodendrocytes in mice by IFN-gamma and TNF-alpha. Neurosci. Lett. **123**:45-48.

209. **Joly, E. and M. B. Oldstone**. 1992. Neuronal cells are deficient in loading peptides onto MHC class I molecules. Neuron **8**:1185-1190.

210. **Huh, G. S., L. M. Boulanger, H. Du, P. A. Riquelme, T. M. Brotz, and C. J. Shatz**. 2000. Functional requirement for class I MHC in CNS development and plasticity. Science **290**:2155-2159.

211. **Corriveau, R. A., G. S. Huh, and C. J. Shatz**. 1998. Regulation of class I MHC gene expression in the developing and mature CNS by neural activity. Neuron **21**:505-520.

212. **Neumann, H., A. Cavalie, D. E. Jenne, and H. Wekerle**. 1995. Induction of MHC class I genes in neurons. Science **269**:549-552.

213. **Lu, J., A. Lal, B. Merriman, S. Nelson, and G. Riggins**. 2004. A comparison of gene expression profiles produced by SAGE, long SAGE, and oligonucleotide chips. Genomics **84**:631-636.

214. **Nisenbaum, L. K.** 2002. The ultimate chip shot: can microarray technology deliver for neuroscience? Genes Brain Behav. **1**:27-34.

215. **Abel, K., M. J. Alegria-Hartman, K. Rothaeusler, M. Marthas, and C. J. Miller**. 2002. The relationship between simian immunodeficiency virus RNA levels and the mRNA levels of alpha/beta interferons (IFN-alpha/beta) and IFN-alpha/beta-inducible Mx in lymphoid tissues of rhesus macaques during acute and chronic infection. J. Virol. **76**:8433-8445.

216. **Bosinger, S. E., K. A. Hosiawa, M. J. Cameron, D. Persad, L. Ran, L. Xu, M. R. Boulassel, M. Parenteau, J. Fournier, E. W. Rud, and D. J. Kelvin**. 2004. Gene expression profiling of host response in models of acute HIV infection. J. Immunol. **173**:6858-6863.

217. **Baca, L. M., P. Genis, D. Kalvakolanu, G. Sen, M. S. Meltzer, A. Zhou, R. Silverman, and H. E. Gendelman**. 1994. Regulation of interferon-alpha-inducible cellular genes in human immunodeficiency virus-infected monocytes. J. Leukoc. Biol. **55**:299-309.

218. **Schiller, J. H., B. Storer, D. M. Paulnock, R. R. Brown, S. P. Datta, P. L. Witt, and E. C. Borden**. 1990. A direct comparison of biological response modulation and clinical side effects by interferon-beta ser, interferon-gamma, or the combination of interferons beta ser and gamma in humans. J Clin. Invest **86**:1211-1221.

219. **Der, S. D., A. Zhou, B. R. Williams, and R. H. Silverman**. 1998. Identification of genes differentially regulated by interferon alpha, beta, or gamma using oligonucleotide arrays. Proc. Natl. Acad. Sci. U. S. A **95**:15623-15628.

220. **Vanhems, P., B. Hirschel, A. N. Phillips, D. A. Cooper, J. Vizzard, J. Brassard, and L. Perrin**. 2000. Incubation time of acute human immunodeficiency virus (HIV) infection and duration of acute HIV infection are independent prognostic factors of progression to AIDS. J. Infect. Dis. **182**:334-337.

221. **Wallace, M. R., J. A. Nelson, J. A. McCutchan, T. Wolfson, and I. Grant**. 2001. Symptomatic HIV seroconverting illness is associated with more rapid neurological impairment. Sex Transm. Infect. **77**:199-201.

222. **Ji, P., S. Diederichs, W. Wang, S. Boing, R. Metzger, P. M. Schneider, N. Tidow, B. Brandt, H. Buerger, E. Bulk, M. Thomas, W. E. Berdel, H. Serve, and C. Muller-Tidow**. 2003. MALAT-1, a novel noncoding RNA, and thymosin beta4 predict metastasis and survival in early-stage non-small cell lung cancer. Oncogene **22**:8031-8041.

223. **Garden, G. A.** 2002. Microglia in human immunodeficiency virus-associated neurodegeneration. Glia **40**:240-251.

224. **Persidsky, Y.** 1999. Model systems for studies of leukocyte migration across the blood - brain barrier. J. Neurovirol. **5**:579-590.

225. **Brooke, S. M., J. R. McLaughlin, K. M. Cortopassi, and R. M. Sapolsky**. 2002. Effect of GP120 on glutathione peroxidase activity in cortical cultures and the interaction with steroid hormones. J. Neurochem. **81**:277-284.

226. **Walsh, K. A., J. F. Megyesi, J. X. Wilson, J. Crukley, V. E. Laubach, and R. R. Hammond**. 2004. Antioxidant protection from HIV-1 gp120-induced neuroglial toxicity. J Neuroinflammation. **1**:8.

227. **Haughey, N. J., R. G. Cutler, A. Tamara, J. C. McArthur, D. L. Vargas, C. A. Pardo, J. Turchan, A. Nath, and M. P. Mattson**. 2004. Perturbation of sphingolipid metabolism and ceramide production in HIV-dementia. Ann. Neurol. **55**:257-267.

228. **Heddi, A., P. Lestienne, D. C. Wallace, and G. Stepien**. 1993. Mitochondrial DNA expression in mitochondrial myopathies and coordinated expression of nuclear genes involved in ATP production. J. Biol. Chem. **268**:12156-12163.

229. **Murdock, D. G., B. E. Boone, L. A. Esposito, and D. C. Wallace**. 1999. Up-regulation of nuclear and mitochondrial genes in the skeletal muscle of mice lacking the heart/muscle isoform of the adenine nucleotide translocator. J. Biol. Chem. **274**:14429-14433.

230. **Cassarino, D. S. and J. P. Bennett, Jr.** 1999. An evaluation of the role of mitochondria in neurodegenerative diseases: mitochondrial mutations and oxidative pathology, protective nuclear responses, and cell death in neurodegeneration. Brain Res. Brain Res. Rev. **29**:1-25.

231. **Felderhoff-Mueser, U., M. Sifringer, S. Pesditschek, H. Kuckuck, A. Moysich, P. Bittigau, and C. Ikonomidou**. 2002. Pathways leading to apoptotic neurodegeneration following trauma to the developing rat brain. Neurobiol. Dis. **11**:231-245.

232. **Roumier, T., M. Castedo, J. L. Perfettini, K. Andreau, D. Metivier, N. Zamzami, and G. Kroemer**. 2003. Mitochondrion-dependent caspase activation by the HIV-1 envelope. Biochem. Pharmacol. **66**:1321-1329.

233. **Roggero, R., V. Robert-Hebmann, S. Harrington, J. Roland, L. Vergne, S. Jaleco, C. Devaux, and M. Biard-Piechaczyk**. 2001. Binding of human immunodeficiency virus type 1 gp120 to CXCR4 induces mitochondrial transmembrane depolarization and cytochrome c-mediated apoptosis independently of Fas signaling. J Virol. **75**:7637-7650.

234. **Nie, Z., B. N. Phenix, J. J. Lum, A. Alam, D. H. Lynch, B. Beckett, P. H. Krammer, R. P. Sekaly, and A. D. Badley**. 2002. HIV-1 protease processes procaspase 8 to cause

mitochondrial release of cytochrome c, caspase cleavage and nuclear fragmentation. Cell Death. Differ. **9**:1172-1184.

235. **Gu, Y., C. Wang, C. M. Roifman, and A. Cohen**. 2003. Role of MHC class I in immune surveillance of mitochondrial DNA integrity. J. Immunol. **170**:3603-3607.

236. **Iordanskiy, S., Y. Zhao, P. DiMarzio, I. Agostini, L. Dubrovsky, and M. Bukrinsky**. 2004. Heat-shock protein 70 exerts opposing effects on Vpr-dependent and Vpr-independent HIV-1 replication in macrophages. Blood **104**:1867-1872.

237. **Lim, M. C., S. M. Brooke, and R. M. Sapolsky**. 2003. gp120 neurotoxicity fails to induce heat shock defenses, while the over expression of hsp70 protects against gp120. Brain Res. Bull. **61**:183-188.